The Dissertation Committee for Litao Yang Certifies that this is the approved version of the following dissertation:

Coupling aptamer biosensors to signal amplification

Committee:

Andrew D. Ellington, Supervisor

George Georgiou, Co-Supervisor

David Hoffman

Vishy Iyer

Edwards Marcotte

Coupling aptamer biosensors to signal amplification

by

Litao Yang, B.S.; M.S.

Dissertation

Presented to the Faculty of the Graduate School of

The University of Texas at Austin

in Partial Fulfillment

of the Requirements

for the Degree of

Doctor of Philosophy

The University of Texas at Austin

May 2007

Dedication

For my family.

Acknowledgements

I'd like to thank my two great supervisors, Andy Ellington and George Georgiou, for their continuous encouragement, optimism, support and guidance. Without them, I could not have overcome obstacles to make accomplishments in my academia journey. I am grateful to my committee members, Vishwanath R. Iyer, David W. Hoffman and Edward M. Marcotte, for their helpful comments and suggestions.

I'd like to thank all former and current lab members for all of their help and friendship. I'd like to thank Amos Yan for always being like an elder sister assisting me whenever I had difficulties. I'd like to thank Matt Levy for teaching me Molecular Biology techniques, for sharing my scientific thoughts and providing research guidance. I'd like to thank Christine Fung, Jim Collett, Youme Gim, Sypriya Pai, Xi Chen, Li Zhou and Amrita Singh for their kindness and assistance. I'd like to thank Jamie Bacher for helping me learn protein evolution techniques and Eun Jeong Cho for collaborations on the chip-based RCA projects. I'd like to thank Brad Hall, Jessica Ebright and Ted Chu, for help and advices. I'd also like to thank Scott Kuersten, Xingwang Fang and Jian Gu from Ambion, Inc. for their supports and comments.

Particularly, I'd like to thank my daughter, Guanyi (Grace, Maomao), for bringing me happiness, making me a mature and more responsible person and encouraging me to

be more successful. I sincerely like to thank my husband, and my parents, for all their love, support and encouragement over the years.

Coupling aptamer biosensors to signal amplification

Publication No._____

Litao Yang, Ph.D.

The University of Texas at Austin, 2007

Supervisors: Andrew D. Ellington and George Georgiou

Nucleic acids amplification methods can be extremely useful for the identification and quantitation of nucleic acid analytes, but are more difficult to adapt to the detection of non-nucleic acid targets. To facilitate the development of nucleic acid amplification for small molecule and protein analytes, we have developed the use of aptazyme and conformation-switching aptamers to generate amplification signals upon interaction with their cognate analytes.

We have developed chip-based rolling circle amplification (RCA) for the detection of ATP utilizing a DNA aptazyme that could catalyze the ligation and circularization of a single-stranded DNA substrate upon ATP recognition. The method has demonstrated that aptazyme-coupled chip-based RCA could sensitively detect ATP and the reproducible signals can be easily read and acquired within a few minutes.

In addition to the design of aptazyme mediated ligation for the detection of small molecules, we have been interested in the adaptation of structure-switching aptamers to generate analyte-dependent ligations. We have developed a novel type of conformation-switching aptamer that can be circularized by T4 DNA ligase upon interaction with its

protein target, PDGF. Using this structure-switching aptamer real-time RCA can be used to quantitate PDGF down to low-nanomolar range, even against a background of cellular lysate. Our results also demonstrate that real-time RCA has advantages over chip-based RCA.

Furthermore, we have coupled conformation-switching aptamers with binding to an antisense oligonucleotide in a way that leads to ligation and the formation of a novel amplicon for real-time PCR. We have explored different strategies from four-piece to two-piece ligations. Our results show that the three-piece has sensitivity and simplicity over the four-piece ligation. However, both four-piece and three-piece ligations require ligation time as long as 8 hours, which is not practical for clinical diagnostics. Therefore, we have simplified the detection into a two-piece ligation, where the antisense sequence is attached to the aptamer and upon binding to protein analyte (PDGF or thrombin) the displaced antisense sequence is ligated to a substrate oligonucleotide. By real-time amplification (PCR) of the ligated product we find that the conformation-switching aptamers can sensitively and specifically detect thrombin or PDGF at picomolar level against a background of cellular lysate. The principal advantage of this method is that it can potentially be applied to a wide variety of analytes, thereby allowing the development of numerous amplificable aptamer biosensors.

Table of Contents

List of Tables

List of Figures

Chapter 1: Introduction

Nucleic acid technology is traditionally based on the recognitions of RNA or DNA via hybridization to complementary sequences. The discovery of naturally occurring catalytic RNA molecules (Kruger, Grabowski et al. 1982; Guerrier-Takada, Gardiner et al. 1983) and the development of *in vitro* selected ribozymes (Wilson and Szostak 1999; Schallmeiner, Oksanen et al. 2007) have demonstrated that nucleic acids are multitalented; capable of catalyzing various reactions. With these newly discovered functions, nucleic acids can be explored for new detection technologies, such as aptazyme and aptamer based detections for a variety of analytes.

Aptamers are single-stranded DNA and RNA binding elements selected *in vitro* by SELEX (systematic evolution of ligands by exponential enrichment) (Ellington and Szostak 1990; Tuerk and Gold 1990). Since their discovery about 17 years ago, aptamers have been selected against a variety of analytes, including inorganic ions, small organics, metabolites, peptides, proteins, and even whole viruses or cells (Proske, Blank et al. 2005; Yan, Bell et al. 2005; Bunka and Stockley 2006; Lee, Stovall et al. 2006). In addition, manmade catalytic nucleic acids (aptazymes) have been generated by conjugation of aptamer and natural ribozymes and by similar schemes used for aptamer selections (Joyce 2004).

ADVANTAGES OF APTAMERS AS BIOSENSORS

In vitro selected aptamers exhibit high affinity and specificity with their analytes as monoclonal antibodies do. For example, some anti-protein aptamers have K_d values in the low nanomolar range and can discriminate targets with very similar structures. Compared to monoclonal antibodies, aptamers can be easily synthesized and stored

without denaturation or degradation and it is relatively easy to incorporate a site-specific modification. Due to these characteristics, aptamers have become increasingly popular as biosensors for a wide range of analytical and diagnostic applications, broadly expanding the versatility of nucleic acid-based detection.

APPLICATION OF APTAMERS FOR SENSING

In the recent decade, many technologies and strategies have been explored to make aptamer biosensors simpler, faster, more sensitive and more generalizable.

As antibody substitutes for analyte capture

Because aptamers are selected as binding reagents, the use of aptamers as antibody substitutes for analyte capture are very straightforward. Like antibodies, aptamers have proved to be very useful in ELISA, western blots and affinity purification. In an ELISA-like application developed by Drolet and colleagues an analyte (human vascular endothelial growth factor; hVEGF) was captured by immobilized monoclonal anti-hVEGF antibodies (Drolet, Moon-McDermott et al. 1996). The detection limit (25 pg/mL) and specificity were equivalent to those of typical antibody mediated sandwich assays. Baldrich *et al.* could detect <1 nM thrombin using a similar experimental strategy (Baldrich, Restrepo et al. 2004), much more sensitive than a direct binding (K_d: ~200 nM) (Bock, Griffin et al. 1992). Liss *et al.* reported that aptamers as immobilized ligands in quartz crystal sensors could detect 0.5 nM of IgE and this was equivalent to antibodies immobilized on the same surface (Liss, Petersen et al. 2002). For western blot type applications, radiolabeled aptamers were used to detect different protein kinase C isozymes in filter binding assays where the bound species retained on the filter were

quantified after removing free aptamers by filtration (Conrad and Ellington 1996). The detection limits for IgE and thrombin were 46 pM and 40 nM, respectively, using fluorescently labeled aptamers in a capillary electrophoresis coupled with laser-induced fluorescence (CE-LIF) (German, Buchanan et al. 1998). Moreover, labeled aptamers were applied in cell sorting (Davis, Abrams et al. 1996; Davis, Lin et al. 1998), microbeads based assays (Rye and Nustad 2001; Yang, Li et al. 2003; Kirby, Cho et al. 2004), capillary electrochromatography (Kotia, Li et al. 2000; Rehder and McGown 2001), high-throughput screening assays (Green, Jellinek et al. 1996), fluorescence anisotropy (Potyrailo, Conrad et al. 1998; Fang, Cao et al. 2001; Yang, Fung et al. 2007) and affinity chromatography (Romig, Bell et al. 1999; Gustafsdottir, Nordengrahn et al. 2006).

In summary, nucleic acid aptamers have demonstrated both sensitivity and specificity in diagnostic assays akin to monoclonal antibodies (Jayasena 1999). However, the limitation of antibody-like assays is that washes and separations are usually needed to remove background from the excessive binders.

It has been known that aptamers recognize their analyte by forming 3-D shapes, and the binding conformations can be altered and manipulated by nucleic acid hybridizations. Therefore, it should be possible to construct a carefully engineered structure-switching aptamer used for detection without separating bound and unbound species, which can be performed directly in sample matrix without special and expensive instruments.

Optical structure-switching signaling aptamers

Optical (colorimetric or fluorometric) detections allow rapid and ideally real-time sample measurements. Fluorescent signaling aptamers have been extensively developed

based on the structure-switching strategies. As mentioned above, the recognition of analyte relies on both aptamer sequences and 3-D conformations, either the aptamers' stable structures or in many cases their analyte-induced conformations. The analyte induced conformational changes can be monitored by fluorescence or colorimetric changes. To get a better handle on the possible structure-switching models, it is necessary to present the typical strategies for engineering optical structure-switching aptamers.

Folding strategy

In the folding strategy, the aptamer is naturally denatured or contains no minimum free energy structure in the absence of analyte, and then upon binding the analyte a stable structure is formed. When the aptamer is fluorescently labeled, the structure switches can change the micro-environment of the fluorescent moiety thus the fluorescent signal.

For example, in the absence of thrombin the main conformation of the anti-thrombin aptamer is a random coil in solution. Thrombin binding assists the aptamer to fold into a quadruplex structure. Li *et al.* labeled the two termini of the anti-thrombin aptamer with two fluorescent dyes that form a FRET pair (Li, Fang et al. 2002). Upon adding thrombin, the aptamer forms into a quadruplex structure and the two fluorophores are brought into proximity to FRET (Figure 1-1A) leading to decreased (fluorescein-DABCYL pair) or increased (fluorescein-coumarin pair) fluorescence. Both methods resulted in similar apparent K_d values (5.20±0.49 nM vs 4.87±0.55 nM) and limits of detection (373±30 pM vs 429±63 pM). The analyte-induced conformational change can also be monitored using a dye that preferably intercalate into stacking bases. For example, Ho and Leclerc monitored the thrombin-aptamer binding with a polythiophene derivative (polymer 1), which exhibited different fluorescent colors when interacting with

unfolded and folded ssDNA (Ho and Leclerc 2004). The detection limit of this method was $2x10^{-15}$ mol (10 pM).

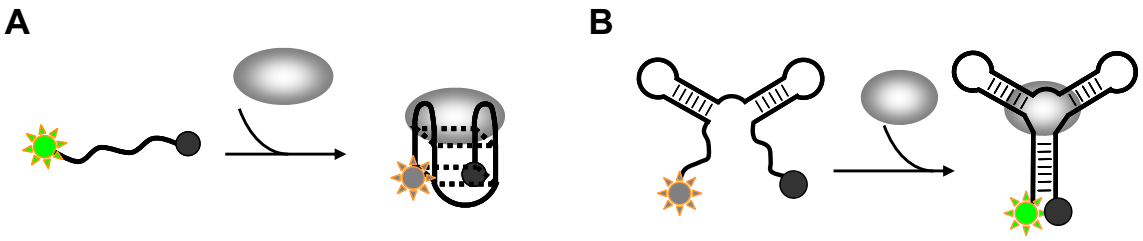

Figure 1-1. Folding strategy. (A) Coformational change of the anti-thrombin atpamer. The anti-thrombin aptamer is unfolded in the absence of thrombin. The fluorophore and quencher are brought together by forming a quadruplex structure in the presence of thrombin. (B) Conformational change of the anti-PDGF aptamer. The PDGF aptamer is truncated at both termini. In the absence of analyte (grey circle), the two ends are destabilized. Upon binding to analyte, the two ends hybridize bringing the fluorophore and quencher to proximity, resulting in fluorescence quenching.

Another approach is to design an unstable aptamer. In the absence of analyte, the aptamer stays at its unfolded form. When binding to the analyte, the folded structure of the aptamer becomes more stable, forcing terminal nucleic acid to hybridize. For example, the anti-PDGF aptamer was modified to be an open structure in the absence of PDGF but assumed its three-way junction structure when PDGF bound (Figure 1-1) (Fang, Sen et al. 2003). When the aptamer was labeled with a pair of fluorescent dyes, the folding leaded to fluorescence quenching. This 'folding' strategy was also applied to the detection of small molecule analyte such as cocaine (Stojanovic, de Prada et al. 2001). In addition, the bipartite anti-cocaine and anti-rATP aptamers can reassemble in the presence of their cognate analytes (Stojanovic, Prada et al. 2000). Such assays could detect PDGF as low as 110 pM PDGF (Fang, Sen et al. 2003) and small molecules at micromolars (Stojanovic, Prada et al. 2000; Stojanovic, de Prada et al. 2001).

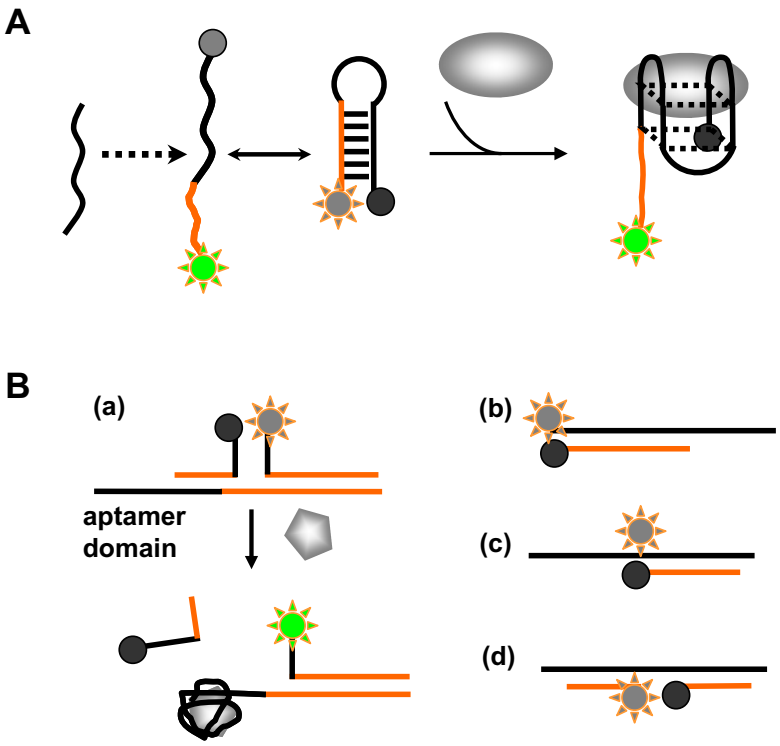

Figure 1-2. Re-folding strategy. Anstisense sequence (orange) works *in cis* (A) or *in trans* (B) with aptamer (black) to alter the binding conformation. Analyte (grey) binding causes the separation of the antisense-aptamer hybrid and leads to dequenching of the fluorophore.

Refolding strategy

The more popular engineering scheme for optical structure-switching aptamers is to convert from a stable structure to a different binding structure in the presence of analyte. In this strategy, the aptamer can be labeled with a fluorescent dye and the antisense oligonucleotide with a quencher (Figure 1-2). In the absence of analyte, the antisense strand hybridizes with the aptamer and thus quenches the fluorescence. When the analyte binds to the aptamer, the antisense oligonucleotide falls apart thus increasing fluorescence. Compared to the "folding" strategy, this unfolding strategy may not require

the knowledge of the secondary or tertiary structures of the selected or to be selected aptamers. In addition, this type of assay can be more sensitive because the fluorescence is quenched in the absence of analyte and thus the background signal is very low.

Using such approach an anti-thrombin aptamer beacon was created by adding a sequence complementary to a portion of the aptamer to form a nonbinding beacon structure in the absence of analyte (Hamaguchi, Ellington et al. 2001). The aptamer and antisense strand were labeled with fluorophore and quencher, respectively. Upon binding to thrombin the aptamer-antisense duplex separates resulting in increased fluorescence. The K_d value of a such designed beacon was 10 nM. Recently, we also generalized this strategy for the detections of other analyte such as IgE and PDGF in a chip based format (Soderberg, Gullberg et al. 2006).

Yamamoto *et al.* combined both "folding" and "refolding" strategies by modifying half of anti-HIV-1 aptamer into a hairpin beacon and the bipartite aptamer reassembled by Tat (Yamamoto, Baba et al. 2000). In the presence of Tat the beacon opens, which leads to fluorescent signals when the hairpin is labeled with a fluorophore and its quencher. In the presence of Tat the beacon is opened, resulted in a fluorescence signal. Li's group utilized a trans-acting antisense strand for a series of fluorescent structure-switching aptamer designs (Figure 1-2B), where two-piece and three-piece aptamer-antisense duplex were constructed for the detection of ATP and thrombin (Nutiu and Li 2003; Nutiu and Li 2004). The disassociation of the antisense strand induced by analyte binding was reflected by fluorescence increase. Such structure-switching aptamers could detect ATP and thrombin with K_d values of 600 μM and 400 nM. Moreover, trans-acting fluorescent structure-switching aptamer can also be created by *in vitro* selection (Nutiu and Li 2005).

Moreover, the "refolding" strategy has also proven adaptable to detection via either electrochemical couples (Xiao, Piorek et al. 2005) or nanoparticle signaling strategies (Levy, Cater et al. 2005; Liu and Lu 2005).

Assisted refolding strategy

Built on the "refolding" strategy, the analyte-dependent conformational change can be assisted by the formation of another duplex structure involving the displaced antisense strand. A typical example of "assisted refolding strategy" is the recently developed antiswitch, which can detect small molecules by controlling fluorescent protein expressions *in vivo* (Bayer and Smolke 2005) (Figure 1-3). The antiswitch (RNA) contains an aptamer domain and an antisense domain. The release of the antisense sequence and the ensuing hybridization to a target mRNA sends off signal. Both analyte and the 5'UTR of mRNA are required for the structure-switching. The aptamer domain binds the small molecule analyte and the antisense domain has a sequence complementary to the 5' end of mRNA to be regulated. For the "off-switch", the antisense domain interacts with the aptamer domain to fomr a hairpin in the absence of analyte. Upon binding to analyte, the hairpin structure opens up and the stem of the antisense domain becomes single stranded RNA, ready to hybridize to the target mRNA and blocks translation. For the "on-switch", the antisense domain is free to bind to target mRNA and suppress gene expression in the absence of analyte. Small molecule binding switches back to a hairpin formed by the aptamer domain and the antisense domain, thus releasing the target mRNA to rescue the gene expression.

In this dissertation, we take an approach similar to the "assisted refolding" strategy to detect proteins by ligation followed by real-time PCR. The displaced antisense strand binds a substrate oligonucleotide to be ready for subsequent ligation. In addition,

the antisense region is designed to form a short hairpin structure to enhance the ligation. Our design is the first example to adapt structure-switching aptamer for analyte-dependent ligation and amplification.

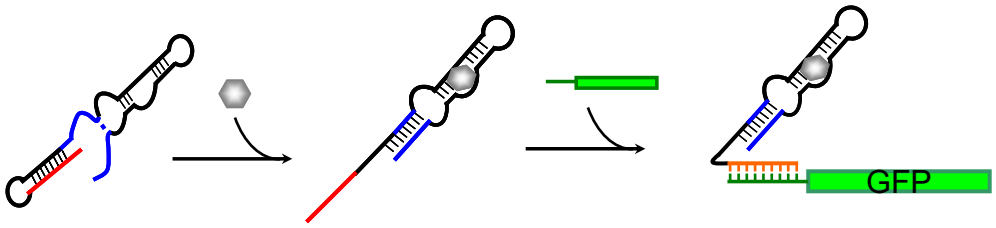

Figure 1-3. Assisted refolding strategy-antiswitch. In the absence of analyte, the antisense domain (red) folds into an "antisense stem". Analyte binding forces the antisense stem open. The displaced antisense domain therefore binds to its target transcript and turn the production of target gene (GFP) off.

In summary, fluorescent structure-switching aptamers have advantages such as versatile signaling, generalizable applications and easy of use. However, they are often not very sensitive for diagnostic applications and suffer from high background fluorescence caused by impurity of labeled dye, fluorescence quenching in real sample matrix and available signal of single labeled fluorophore. On the other hand, to have a high signal-to-noise ratio, the non-binding conformation should be very stable by strong hybridization between the aptamer and the antisense. This then requires more energy to switch to a binding conformation, and because part of the binding energy is transduced into the conformational change the apparent binding constant is increased (less apparent affinity). For example, the structure-switching aptamers developed by Nutiu and Li had K_d values of 60- and 2-fold reductions of those of the original aptamers (Nutiu and Li

2003). Future development may find ways to improve affinity reduction, and minimize background signals to increase detection sensitivity its dynamic range. With the applications of both rational design and in *vitro* selections, the affinity could be increased. Furthermore, the detection sensitivity may be greatly improved by coupling nucleic acid amplification techniques. The combination of amplification for aptamer based detection does not require sophisticated instruments and allows real-time assay with high sensitivity and specificity. Also, when rolling circle amplification (RCA) is used for amplification, this technology can be developed into a chip based biosensor.

Aptazyme

Analyte-dependent conformational changes can not only be transduced directly into optical signals, but into catalysis as well. Advantageous to antibodies, aptamers can be inserted into (deoxy)ribozymes to serve as allosteric binding sites. The construction of aptazymes takes advantage of the fact that many ribozymes contain stem-loop structures that are structurally conserved, but whose sequence can be changed. By introducing aptamers in place of these stem-loops, the analyte-dependent conformational changes that aptamers normally undergo can potentially be transmitted to the catalytic cores of ribozymes, influencing their catalytic activities. To date, various aptazymes capable of ligation or cleavage reactions have been either designed or *in vitro* selected (Table 1-1). They can be modulated by analytes such as small molecules, peptides, proteins and various metal ions (Koizumi, Soukup et al. 1999; Soukup and Breaker 1999; Robertson and Ellington 2001; Seetharaman, Zivarts et al. 2001; Robertson, Knudsen et al. 2004).

Like the fluorescent signaling aptamers, aptazymes can also transduce analyte recognition into optical signals. For instance, the activity of a hammerhead or hairpin aptazyme could be easily read by cleavage of a fluorescent substrate (Figure 1-4A).

In addition, same kind of ribozyme could be manipulated to detect different analytes, therefore these ribozymes can be arrayed onto a chip to detect multiple analytes simultaneously (Seetharaman, Zivarts et al. 2001; Hesselberth, Robertson et al. 2003). Our group has assayed combinations of aptazymes that detect small organics, peptides, and proteins in parallel (Figure 1-4B; Hesselberth, Robertson et al. 2003). The aptazyme substrates were labeled with biotin and the allosteric ribozymes were radioactive. Ligated products were retained in streptavidin coated 96-well plates, and unligated materials were washed away. The aptazyme ligases in the array could specifically and simultaneously detect their cognate analytes, and the limits of detection of the best aptazymes were in the nanomolar range.

An aptazyme has also been used in gold nanoparticle mediated colorimetric assays (Liu and Lu 2005). In this case, gold nanoparticles aggregate when the substrate oligonucleotide of the adenosine-dependent 8-17 deoxyribozyme binds to the DNA oligonucleotide conjugated on the nanoparticles. The nanoparticles turn into blue upon aggregation. In the presence of adenosine, the deoxyribozyme is activated and cleaves the substrate oligonucleotide. Therefore the nanoparticle aggregates dispel and the solution color changes to red. This method detects adenosine form 100 μM to 1 mM.

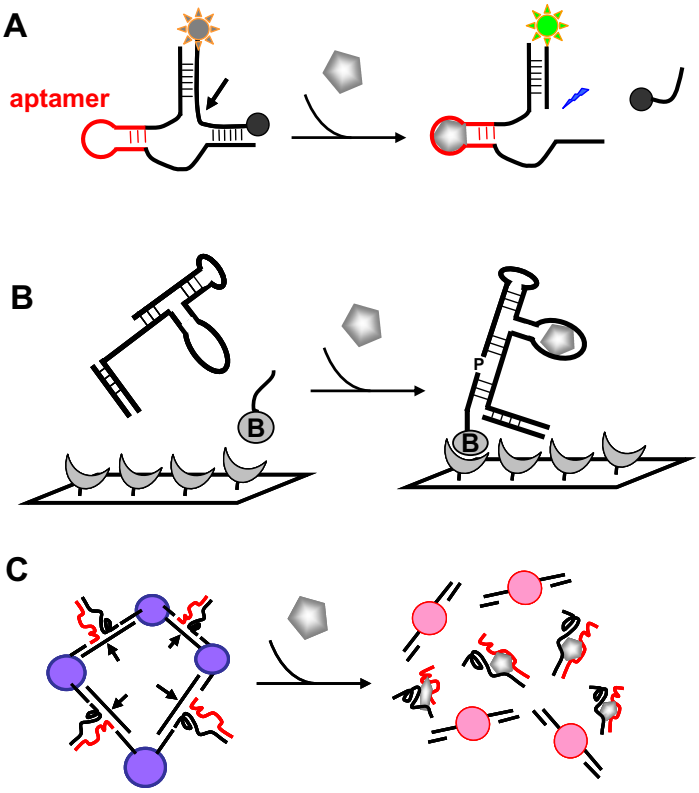

Figure 1-4. Mechanism of signaling aptayzme. (A) A typical cleavage fluorescent signaling aptazyme. Cleavage and subsequent dissociation of the substrate lead to the separation of a fluorophore from its quencher and increase in fluorescent intensity. (B) L1 ligase aptazyme array. Biotin-labeled substrate oligonucleotide and radiolabeled L1 ligase are used to detect a series of analytes. In the presence of their cognate analytes, aptayzme ligation products are immobilized on streptavidin-coated 96-well plates, producing a radioactive signal, while unligated aptazymes are washed away. (C) Colorimetric aptazyme assay. The substrate strands of the 8-17 DNAzyme hybridizes with both the enzyme and the DNA arms conjugated on gold nanoparticles. The cleavage activated by adenosine disperses nanoparticles from aggregates (blue circle) to individual particles (red circle).

However, aptayzmes usually have higher K_d values compared to the original aptamers due to the structure interference of the linked ribozyme. For instance, the K_d values for anti-protein aptamers are usually at the nanomolar level while a selected L1 ligase can detect proteins such as Cyt18 and lysozyme at micromolar level (1.5 μM and 1.3 μM, respectively) (Robertson and Ellington 2001). In another example, the K_d value

of the anti-therophylline aptamer is about 300 nM, while that of the anti-therophylline ligase is about 99 μM (Robertson and Ellington 2000). Therefore, this approach can only detect analytes at relatively high concentrations.

Table 1-1. Allosteric (deoxy)ribozymes generated by different strategies.

Analyte	Enzyme	Signaling Mechanism	Strategy	Reference
ATP, theophylline	Hammerhead ribozyme	Inhibition	Rational design	(Tang and Breaker 1997)
ATP, doxycycline, pefloxacin	Hammerhead ribozyme	Inhibition	*In vitro* selection	(Tang and Breaker 1997; Piganeau, Jenne et al. 2001; Piganeau, Thuillier et al. 2001)
FMN, theophylline	Hammerhead ribozyme	Activation	Rational design	(Araki, Okuno et al. 1998; Soukup and Breaker 1999)
cNMP, caffeine, aspartame, ADP, theophylline, 3-methylxanthine	Hammerhead ribozyme	Activation	*In vitro* selection	(Koizumi, Soukup et al. 1999; Soukup, Emilsson et al. 2000; Ferguson, Boomer et al. 2004)
FMN, theophylline ATP	Hammerhead ribozyme	Activation/ inhibition	Combination of rational design and *in vitro* selection	(Soukup and Breaker 1999)
FMN and theophylline	Hammerhead ribozyme	Cooperative activation	Rational design	(Jose, Soukup et al. 2001)
Oligonucleotides, tyrosyl tRNA synthetase (Cyt18), lysozyme, Rev ARM	L1 ligase	Activation	*In vitro* selection	(Robertson and Ellington 1999; Robertson and Ellington 2001)
ATP, theophylline, FMN	L1 ligase	Activation	Combination of rational design and *in vitro* selection	(Robertson and Ellington 2000)
ATP	Deoxyribozyme ligase	Activation	Rational design and *in vitro* selection	(Levy and Ellington 2002)
theophylline	Hepatitis delta virus (HDV) ribozyme	Activation	*In vitro* selection	(Kertsburg and Soukup 2002)
adenosine	RNA-cleaving 10-23 and 8-17 DNAzyme	Activation	Rational design	(Schweitzer, Roberts et al. 2002)
FMN	Hairpin ribozyme	Activation	Rational design	(Najafi-Shoushtari and Famulok 2005)

Coupling aptamer based detections to nucleic acid amplifications

Proximity (ligation) followed by real-time PCR or RCA

The combination of immunoassay techniques and nucleic acid amplification using antibodies labeled directly with nucleic acids, noted as ImmunoPCR, is very sensitive in detecting protein analytes (Adler 2005; Niemeyer, Adler et al. 2005; Barletta 2006), but have several distinct disadvantages relative to PCR for the detection of nucleic acids. It is difficult to reproducibly prepare antibody-DNA conjugates. Binding and amplification reactions must be performed under different reaction conditions, making it difficult to develop into a single-tube format; and both specifically and non-specifically bound probes can be amplified, potentially leading to high background signals.

In order to improve the detection sensitivity of immunoassay, various nucleic acid amplification technologies are coupled with aptamer based sensors for protein detections. Proximity ligation assay (PLA) has achieved a detection limit of 40 zeptomole (10^{-21} mol) which is equivalent to 1,000-fold improvement over the conventional ELISA (Fredriksson, Gullberg et al. 2002). In this assay, a pair of aptamers is brought into proximity by binding to PDGF-BB dimer (Figure 1-5A), allowing the extending ends of the two aptamer to hybridize to a splint oligoncucleotide. The ensuing ligation and PCR enables sensitive detection of the PDGF-BB dimer. Aptamer-PLA is also developed to sensitively detect live organisms, such as 100 *B.anthracis* and 10 *B.subtilis* spores, and down to 1 *B.cereus* spore (Pai, Ellington et al. 2005).

In another assay, Di Giusto *et al.* utilized a pair of aptamers recognizing different epitopes of thrombin (Di Giusto, Wlassoff et al. 2005). One of the aptamer serves as a primer and the other circular one serves as a template (Figure 1-5B). Thrombin binding brings the two aptamers in proximity and triggers the RCA and the amplified product can

be monitored in real time. The detection limit for thrombin is about 30 pM, 3-fold lower than the K_d value of the anti-thrombin aptamer.

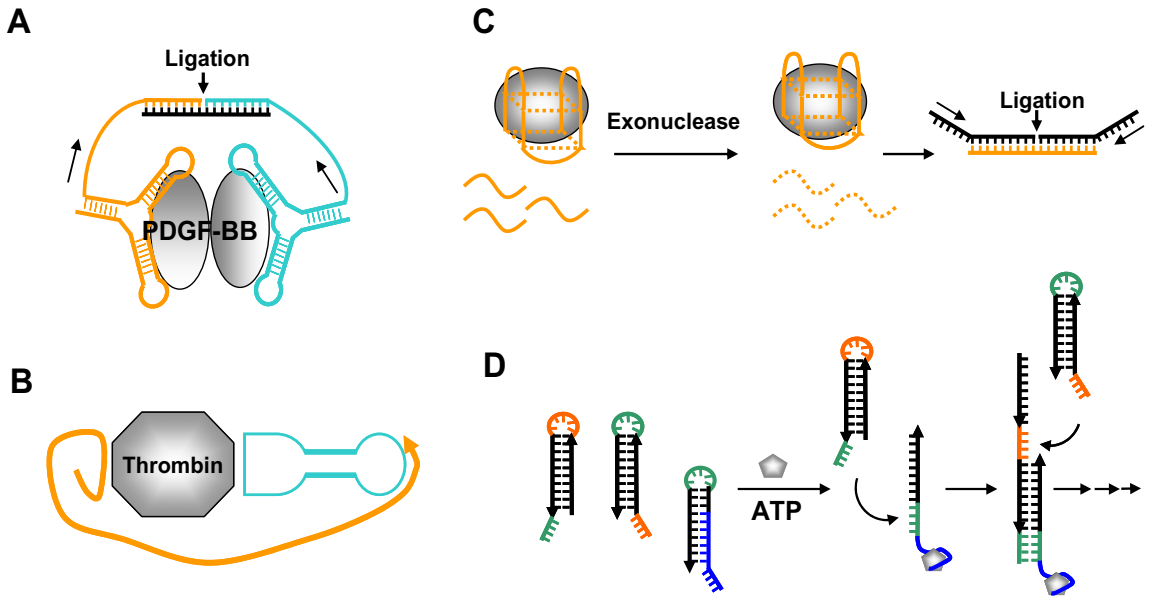

Figure 1-5. Coupling aptamer recognition to nucleic acid amplification. (A) Proximity ligation followed by real-time PCR. (B) Proximity extension of anti-thrombin aptamer. (C) Exonuclease protection followed by real-time PCR. (D) Analyte binding induced HCR.

However, proximity based ligation requires multimeric analyte or multiple binding sites on the analyte for the binding of two different aptamers, thus difficult to expand to be universally used for any analyte detection.

Exonuclease protection assay followed by real-time PCR

Exonuclease protection assay is very similar to nucleic protein assay, where analyte binds an aptamer to protect it from nuclease degradation. The undegraded aptamers serve as templates for ligation followed by real-time PCR for detection. Wang

et al. could detect several hundred thrombin molecules by real-time PCR of exonuclease I digested thrombin/aptamer mixture (Wang, Li et al. 2005) (Figure 1-5C). This method has sensitivity similar to that of PLA. Theoretically, this method should also be applicable for other analyte detections. However, no further example has been reported. The limitation of this assay is that the incomplete degradation of the excessive free aptamer probes, which could lead to false positive or over-estimation of the analytes.

Hybridization Chain Reaction (HCR)

HCR is an enzyme-free amplification method alternative to PCR for the rapid detection of specific analyte (Dirks and Pierce 2004) (Figure 1-5D). An anti-ATP aptamer was used to block the initiator strand *in cis* by hybridization. ATP binding exposes the initiator strand, which triggers a cascade of hybridization between two hairpin species to "polymerize" into a nicked double helix.

RESEARCH OUTLINE

Ligase-based analyses have many attractive features such as high specificity from pairwise hybridization to targets and high sensitivity due to amplificable products. In addition, assays could be differentiated by inserting a DNA tag during amplification. Therefore, our research focuses on the studies of the possibility of gaining in sensitivity by signal amplification; and the possibility of using simple antisense methods to generally couple aptamers to ligation and signal amplification.

Previous studies have shown that the structure-switching aptamer can be coupled with fluorescent signaling and it is generalizable for both small molecule and protein analyte detections. However, it is not known whether the structure-switching aptamers can be adapted to ligation and amplification. On the other hand, since modified aptamers

or aptazymes usually have lowered affinity with analyte, it would be significant if amplification could improve the sensitivity of the detections.

Coupling amplification with aptazyme based detection

As we described above, aptazymes usually have limited sensitivities which may be improved by product amplification. We have modified an ATP dependent aptazyme mediated ligation so that circularized product can be amplified by RCA (Chapter 2; Cho, Yang, et al., 2004). Using this strategy, we have successfully detected ATP in both solution and also with a chip based assays. The chip based RCA can detect as low as 1 μM ATP. Such detection limit is lower than the K_d value of the original aptamer (6 μM) (Huizenga and Szostak, 1995) while binding constants for the unmodified ATP dependent ligase are 10 mM and 10 μM (Levy and Ellington 2002).

Coupling amplification with structure-switching aptamer based detection

Because nucleic acid secondary structure can be readily 'programmed' (Nutiu and Li 2003; Bayer and Smolke 2005), we propose to couple conformation-switching aptamers using an antisense strategy in a way that leads to ligation and the formation of an amplicon for real-time RCA or PCR. We have applied these methods to the well-known anti-protein aptamers. Our designs differ from the antiswitch strategies with a hairpin stem inserted in the displacing sequences. We find that such designed conformation-switching aptamers can detect protein analytes sensitively and specifically both in solution and in cell lysate.

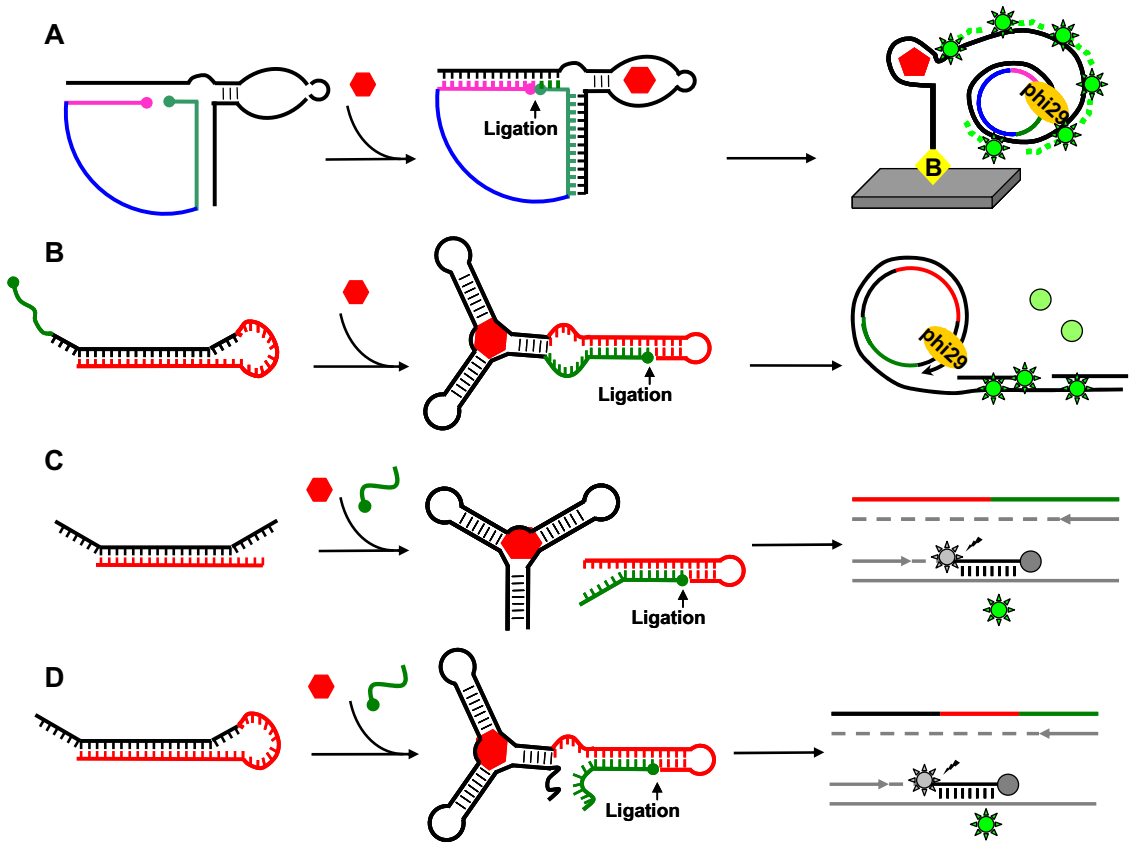

Figure 1-6. Research outline: analyte-activated ligation followed by amplification. Analyte is represented in red. Aptamer or aptamer domain is labeled in black. (A) Aptazyme ligase mediated ligation followed by chip based RCA. In the presence of analyte, the padlock probe is ligated into a circle by the aptazyme ligase. The ligase also serves as a primer for amplification of the circular probe. (B, C, D) Structure-switching aptamer-mediated ligation followed by real-time amplifications. These structure-switching aptamers are designed based on an antisense strategy. An antisense sequence (red) binding to the aptamer disrupts the binding conformation. In the presence of protein analyte, the displaced antisense strand forms into a short hairpin which subsequently binds to a substrate strand for ligation. The ligated product is amplified by either real time RCA (B) or real-time PCR (C and D).

Chapter 2 describes the combination of chip-based RCA with ATP dependent aptazyme circularization. The potential of using other aptazyme for ligation and RCA is also discussed. Chapter 3 illustrates a protein dependent aptamer circularization followed by real-time RCA for the detection of protein analyte. Chapter 4 describes coupling

structure-switching aptamer with four- and three-piece ligations followed by real-time PCR for the detection of protein analyte, which also serves the guidance for the assay designed in Chapters 3 and 5. Chapter 5 reports the further improvement of structure-switching aptamer coupled with ligation and real-time PCR. The final assay of two-piece ligation and real-time PCR is capable of detecting proteins in general with high sensitivity and ease of use.

Chapter 2: Using a deoxyribozyme ligase and rolling circle amplification to detect ATP

INTRODUCTION

Since the Breaker group initially joined an aptamer with a nucleic acid enzyme to generate the allosteric ribozyme, the so called aptazyme (Tang and Breaker 1997), RNA or DNA aptamers have been adopted for allosteric ribozymes or deoxyribozymes (Yang and Ellington 2006). The resultant aptazymes have two domains: the aptamer binding domain and an enzymatic domain. The aptamer binding domain changes its conformation upon binding to its cognate analyte so as to switch on or turn off the activity of the catalytic domain. Majority of the generated aptazymes are those capable of either cleavage or ligation. Such aptazymes have been rationally designed or *in vitro* selected to detect analytes such as ATP, FMN, theophylline, peptide and protein analytes. Aptazyme-based chip arrays have also been performed to detect multiple analytes (Seetharaman, Zivarts et al. 2001; Hesselberth, Robertson et al. 2003). The unique property of the aptazyme ligase is that they can convert the recognition of analytes into the production of amplicons, which would allow rapid and robust detections using amplification techniques.

Rolling circle amplification (RCA) was first observed in bacteriophage replication. And it was found that single-stranded circular DNA can also serve as a RCA template for DNA polymerase to generate numerous concatemerized product (Daubendiek and Kool 1997). Moreover, Eric Kool's lab has generated small circular substrates with 26-74 nucleotides (nt) in lengths, which can serve as efficient RCA templates for several DNA polymerase enzymes *in vitro* (Kool 1996). In RCA, a small nucleic acid circle hybridizes to a primer, which is in turn extended around the circle,

ultimately displacing the original primer and continuing to produce long nucleic acid product. Phi29 DNA polymerase which is highly processive is often used in RCA. It has exceptional strand displacement ability and it can also maintain the polymerization reaction for as least 12 hours (Baner, Nilsson et al. 1998).

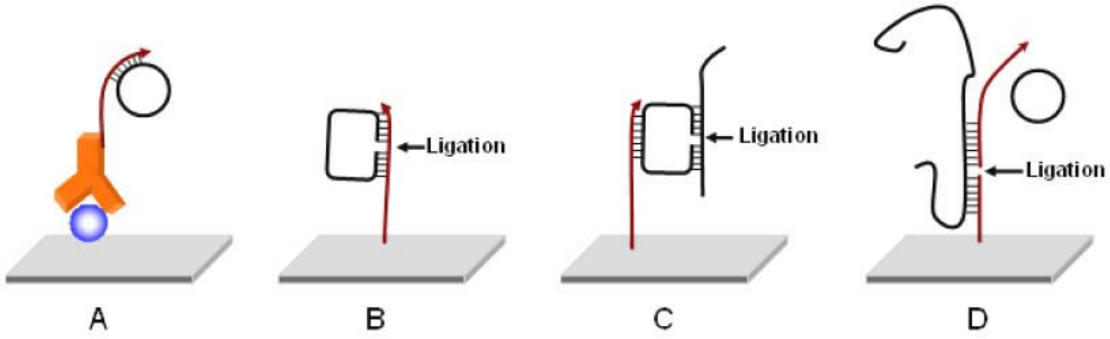

Figure 2-1. Schematic representation of surface RCA for protein and nucleic acid detections. (A) An RCA primer is tagged on an antibody, which binds to a protein immobilized on the surface. Unbound antibodies are washed away. Bound antibodies are detected by extension of the primers around the circular probes. (B) Nucleic acid target is immobilized on a surface. Both the 5' and 3' termini of the padlock probe are complementary to the target. DNA ligase circularizes the padlock probe and the target DNA serves as a primer for RCA. (C) The RCA primer is immobilized on the surface. In the presence of target nucleic acid, the padlock probe is circularized, and the immobilized primer is extended by the polymerase in a RCA reaction. (D) Immobilization of the primer dependent on ligation. In the presence of nucleic acid target, the primer used for RCA is ligated to the oligonucleotide attached on the surface. Therefore, RCA product is deposited on the surface.

RCA has been used for detection of both DNA and RNA either in solution (Faruqi, Hosono et al. 2001; Zhang, Zhang et al. 2001; Rector, Tachezy et al. 2004) or *in situ* (Zhou, Calciano et al. 2001) and the latter has been accomplished at single cell level (Christian, Pattee et al. 2001). RCA has been an especially useful process for surface-

based signal amplification because RCA products are deposited and remain localized at the surface spot. In addition, the isothermal conditions are easily operated on chips. Chip-based RCA has been developed for both nucleic acid and protein detections (Lizardi, Huang et al. 1998; Hatch, Sano et al. 1999; Schweitzer, Wiltshire et al. 2000; Nallur, Luo et al. 2001; Schweitzer, Roberts et al. 2002; Zhou, Bouwman et al. 2004; Soderberg, Gullberg et al. 2006). By far, RCA protein chips (Figure 2-1A) have been profiled to hundreds of proteins and extensively used for diagnostics, high throughput screening, expression proteomic applications and clinical biomarker discovery (Kingsmore and Patel 2003). Moreover, it has also been demonstrated that RCA can effectively screen mutant nucleic acid targets using a solid-phase format under different strategies (Figure 2-2B, C, D) (Lizardi, Huang et al. 1998; Hatch, Sano et al. 1999). However, only few chip-based RCA has been reported for the detection of small molecules.

Currently, the cleavage or ligation reactions catalyzed by aptazymes are usually detected by gel assays or fluorescent assays which are not very sensitive. On the other hand, aptazymes usually have decreased detection limits compared to the selected aptamers probably because increased free energy required to drive a conformational transition in the catalytic core of the aptazyme. Therefore, it would be extremely useful to harness aptazymes for amplification of a nascent binding and ligation signal. On the other hand, RCA is 20 ^{o}C -37 ^{o}C, which makes the adaptation of aptamer based sensing to chip-based RCA desirable. Based on these points above, we propose to couple chip-based RCA with aptazyme mediated analyte-activated ligations.

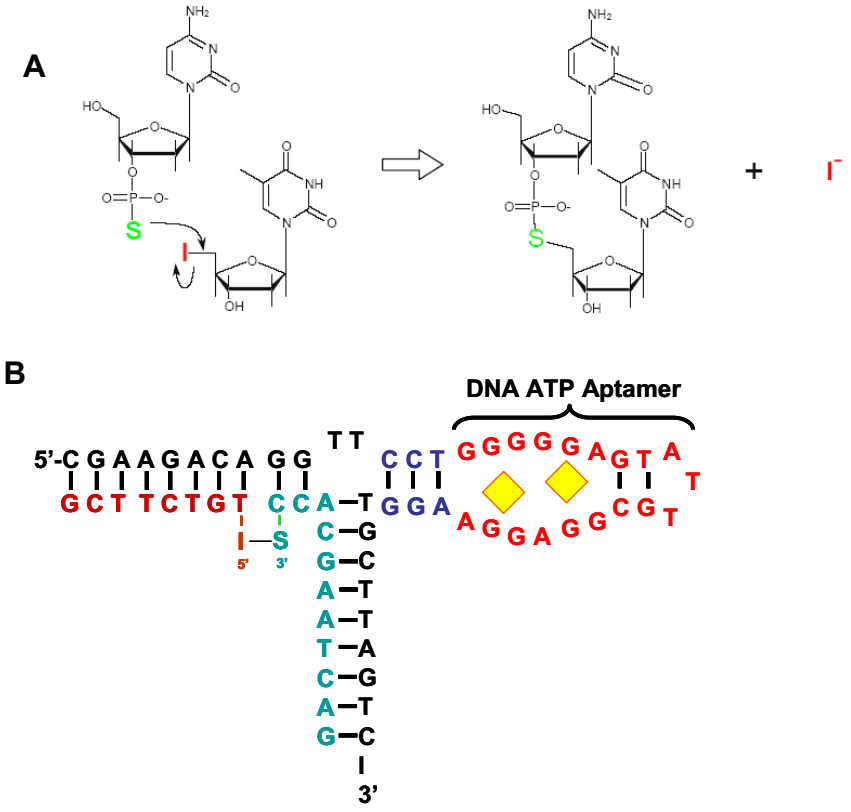

Finger 2-2. The ATP-dependent ligation by deoxyribozyme ligase. (A) The iodinophosphorothiote-reaction producing the linkage between two linear substrates (from Dr. Matthew Levy's dissertation (Levy 2003)). (B) ATP-dependent ligase together with substrate oligonucleotide (Levy and Ellington 2002). This aptazyme has 250-fold activation upon ATP recognition.

To address this goal, we carried out modification of an ATP dependent deoxyribozyme ligation, which was previously created in our lab by appending the anti-ATP aptamer to a selected deoxyribozyme ligase (Levy and Ellington 2002). This deoxyribozyme ligase catalyzes the autoligation of a 3'-phophorothiate onto a 5-iodine residue, and ligation activity is activated up to 250-fold in the presence of 10 mM ATP (Figure 2-2). We designed the substrate of this aptazyme into a padlock probe that could

be ligated into a circle in the presence of ATP. Since the 3' end of the aptazyme anneals to the padlock probe, the immobilized aptazyme also serves as a primer for chip-based RCA.

RESULTS AND DISCUSSION

Design of the padlock probe

In order to generate circular ligation products, we modified the substrates for ligation. The original ATP-dependent aptazyme ligase was created by appending the anti-ATP aptamer to a selected deoxyribozyme (Figure 2-2B). In the presence of ATP, the 5' and 3' ends of the two substrate oligonucleotides are juxtaposed, and joined by a phosphorothiate-iodine linkage (Figure 2-2A). To generate circular ligation product, a linker sequence was introduced to connect the two substrate strands resulting in a padlock probe. As an initial test, we designed four padlock probes with different linker lengths as shown in Figure 2-3. The linker CT rich region was chosen to prevent any secondary structure that might interfere with ligase binding site. Some G and A bases in the linkers were to form a short hairpin with some of the C and T bases; thus bringing one end close to the other and stabilize the structure of the linker. The secondary structure of the redesigned padlock probe was confirmed by MFOLD (http://www.bioinfo.rpi.edu/applications/mfold/old/dna). The lengths of these four padlock probes were 43, 56, 58 and 63 nt, respectively. We tested the ligation activities of the aptazyme using these probes in the absence or presence of 10 mM ATP. Ligation signals were generated by all of these above substrates as soon as 5 min in the presence of ATP but not in the absence. Even when incubated up to 1 h, these aptazymes demonstrated strong ATP preference, and ligation product with ATP was significantly

more than that without ATP. However, if the incubation time was longer than 2 hr, the background ligation level accumulated significantly (Figure 2-4). After 2 h ligation incubation, the 63 nt padlock probe (Sub.63) demonstrated the highest signal-to-noise ratio among all the designed padlock probes. Therefore, we chose Sub.63 to carry out the following ligation and amplification assays.

A

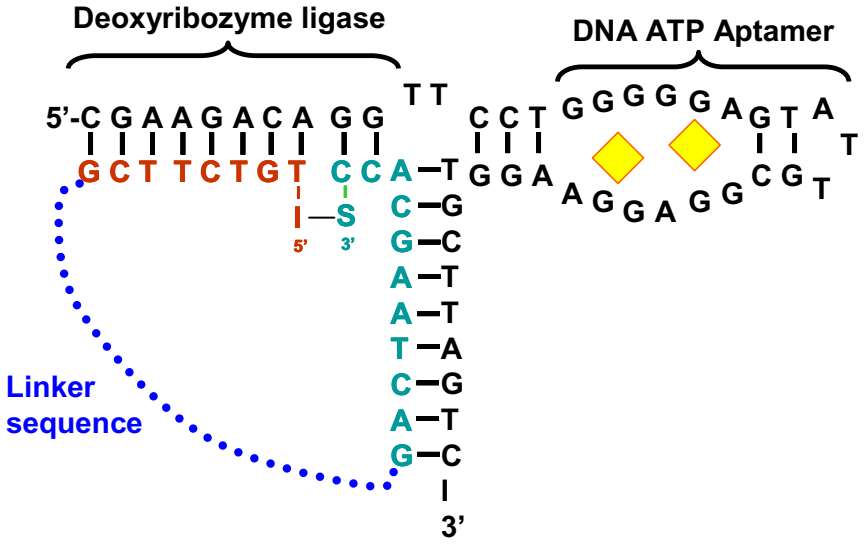

B

Padlock probe	Linker sequence
Sub.43	5'-TCCTCCCATGCTGCTGCTGTACTA
Sub.56	5'-CCTTCTTGTTTCCTTTCCTTGAAACTTCCTTCTTCTC
Sub.58	5'-CCTTCTTGTTTCCTTTCCTTGAAACTTCTTCCTTCTTTC
Sub.63	5'-CCTTCTTGTTTCCTTTCCTTGAAACTTCTTCCTTTCTTTCTTTC

Figure 2-3. Designed padlock probes were derived from the two linear substrates of the ATP-dependent aptazyme. (A) A padlock probe was created by connecting the substrate recognition sites (brown and green) via a linker strand (blue). Therefore the ligated product by aptazyme (black) is a circular probe. (B) Linker sequences of the designed padlock probes.

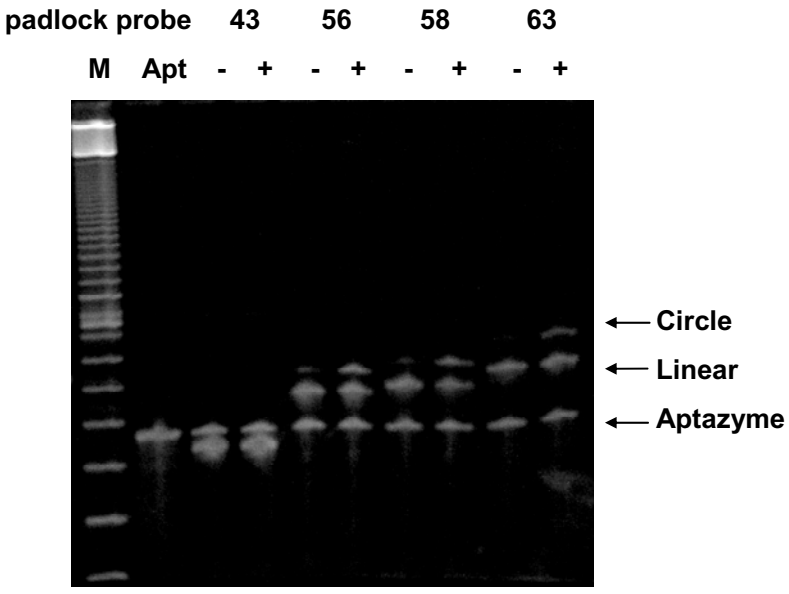

Figure 2-4. Ligation assays using designed padlock probes. Ligations were carried out in the presence or absence of 10 mM ATP for 2 h. Ligated and unligated padlock probes (Sub.43, Sub.56, Sub.58 and Sub.63) were separated by 8 % PAGE. M represents a 10 bp DNA ladder. Apt stands for reactions containing only aptamers.

Optimization of ligation in solution

To find out monovalent cation's effect on ligation activation, we performed assays with 500 mM NaCl. This concentration of NaCl was also present in the deoxyribozyme ligase selection buffer (Levy and Ellington, 2002). Since our final goal is to carry out chip-based RCA, in order to determine the affect of NaCl on chip-based assays both biotinylated and unmodified aptazymes were assayed for ATP activated ligations. In these assays, Sub.63 and the aptazyme were mixed at 25 ^{o}C and ligation was carried out either in the presence or in the absence of 10 mM ATP. Aliquots of the terminated ligation reactions were taken after different incubation time. Ligated and unligated probes were separated using a denaturing 8 % polyacrylamide gel and

visualized by SYBR Gold staining. The results are presented in Figure 2-5. Both assays with and without NaCl demonstrated ATP activation. At 30 min ligation, for both biotinylated and unmodified aptazymes the extent of ATP activation in the presence of NaCl was comparable to that obtained without NaCl. However, when ligation time was extended to 60 min, NaCl caused the increase of background ligation of biotinylated aptazyme while the unmodified aptazyme behaved in the same way both in the presence and absence of NaCl (Figure 2-5).

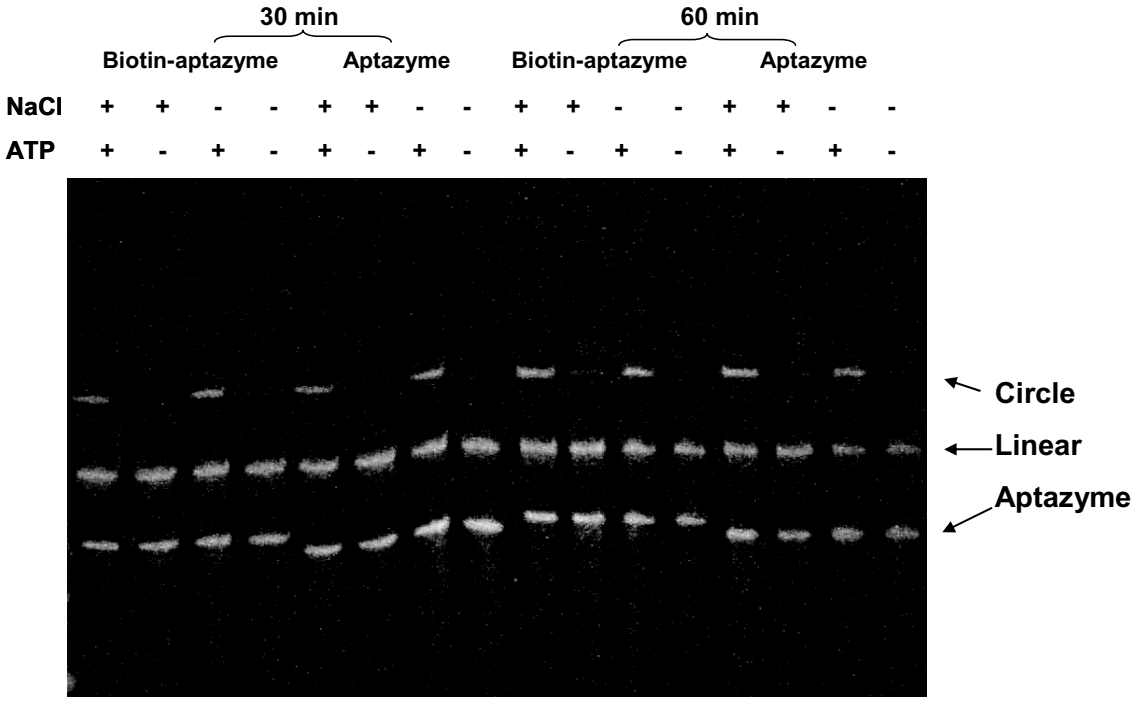

Figure 2-5. The effect of NaCl on ligation. Ligations with or without 10mM ATP were carried out using biotin-labeled and unmodified aptazymes with padlock probe Sub.63 in the presence or absence of 500 mM NaCl. Ligations were determinated at 30 min and 60 min.

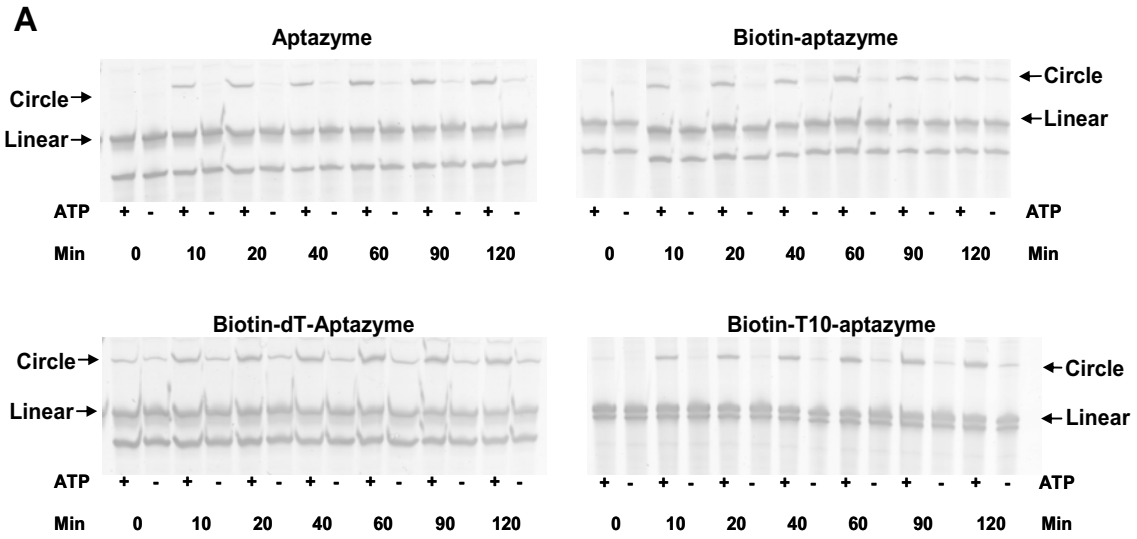
A
Aptazyme
Biotin-aptazyme
Circle
Linear
ATP
Min
0 10 20 40 60 90 120
Biotin-dT-Aptazyme
Biotin-T10-aptazyme

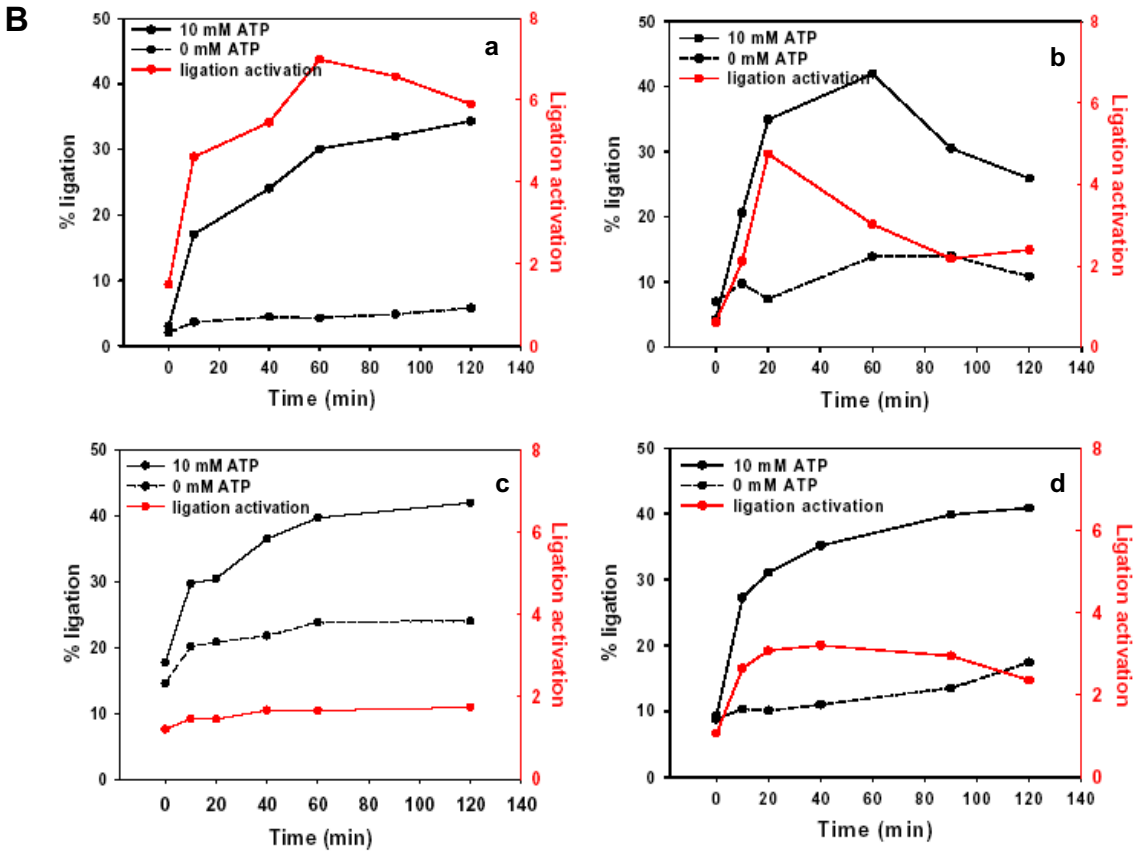
B
10 mM ATP
0 mM ATP
ligation activation
% ligation
Ligation activation
Time (min)
a
b
c
d

Figure 2-6. Time course monitoring of ligation activation for labeled and unlabeled aptazymes in solution. (A) PAGE images of ligation activities. (B) Kinetic analyses of aptazymes (a), biotinlabeled aptazyme (b), biotin-dT-labeled aptazyme (c), and biotin-T10-labeled aptazyme (d), respectively. Black lines represent % ligation in the presence of ATP, black dotted lines represent % ligation in the absence of ATP, and red line represents ligation activity (ratio of % ligation in the presence of ATP vs % ligation in the absence of ATP).

Previous studies have reported that the immobilization of aptamers and aptazymes onto solid substrates altered their target-binding and kinetic characteristics (Seetharaman, Zivarts et al. 2001; Kirby, Cho et al. 2004); therefore, it was possible this would occur for the deoxyribozyme ligase as well. In concerning of the applicability of chip-based RCA, additional biotinylated aptamers with different liners (dT and T10) were also constructed in order to tether the aptazymes to chip surfaces. These linkers locate at the 5' ends that would extend them away from the surface. Unmodified, biotin-, biotin-dT and biotin-T10 labeled aptazymes were assayed with the Sub.63. Using the NaCl-free ligation buffer, ligation signals were monitored as a function of time (Figure 2-6). All four aptazymes showed strong ATP preferences over the whole time course. The biotin-aptazymes demonstrated a slightly higher extent of ligation (40-42 %) compared with unmodified aptazymes (34 %) in the presence of ATP, but they also showed a significant increase in background ligation in the absence of ATP (14-24 % of ligation for biotin-labeled aptazymes vs 6 % ligation for unmodified aptazyme). As a result, the ligation activation (ratio of percent ligation in the presence of ATP vs percent ligation in the absence of ATP) for the biotin-labeled aptazymes was between 1.7 and 4.7, whereas the ligation activation for the unmodified aptazyme was 7.0. Interestingly, the catalytic activity of

biotin-labeled aptayzmes decreased by about 32-64 % by adding linkers such as dT and T10.

However, the ligation activation levels observed here are much lower than that (~250-fold) of the unmodified ATP dependent aptazyme (Levy and Ellington, 2002). The increased background ligation may be explained by the shortened distance between the two substrate binding sites. The change from intermolecular to intramolecular distance would facilitate the hybridization between the aptazyme and the padlock probe.

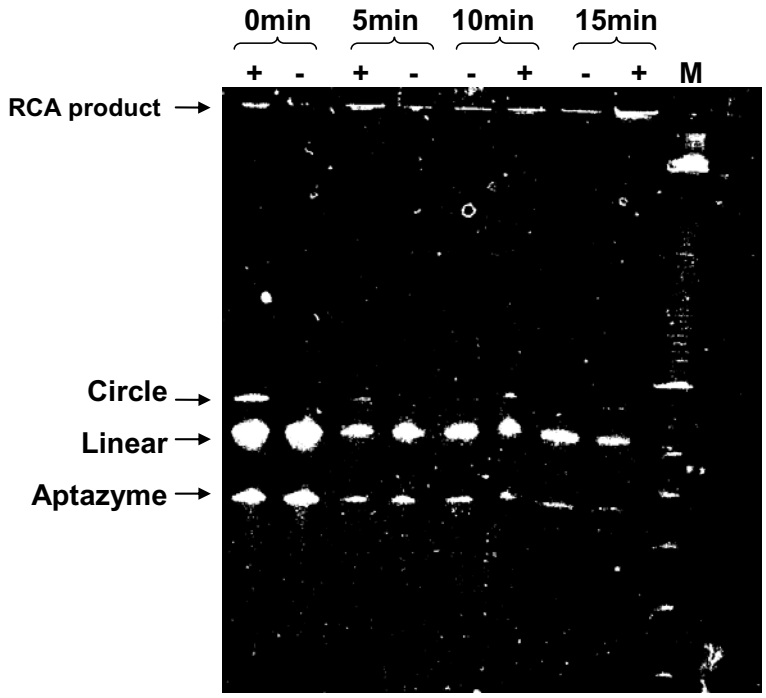

Figure 2-7. Amplification of ATP-dependent ligation activities using fluorescent dCTP. Ligation was carried out for 1 h followed by RCA for various time periods (0, 5, 10 and 15 min, respectively). (+) and (-) represent the presence and absence of 10 mM ATP, respectively. RCA product, circularized padlock probe, unligated padlock probe and aptazyme were separated by an 8 % PAGE gel. M represents a 10-bp DNA ladder.

RCA using fluorescent dCTP

The advantage of direct incorporation of fluorescent dNTPs in an RCA product is that the product could be directly visible in gel and surface assays and would not require future staining or labeling. Therefore, we tested the feasibility of RCA using fluorescent dCTP. Because the 3' end of the aptazyme was completely complementary to the substrates, we simply used the aptazyme as an RCA primer for amplification.

Ligation was carried out for 1 h. Aliquots of the terminated ligation mixture were transferred into an RCA reaction containing 10 mM dCTP, 0.15 mM F-dCTP (F=Alexa Fluor 488-7-OBEA) and 0.25 mM each of the other dNTPs. RCA was performed at 37 ^{o}C for 5, 10 and 15 min and stopped by heating at 65 ^{o}C for 3min. Amplified product was assayed by gel electrophoresis without any additional staining. However, the fluorescence amplification signals in the gel image (Figure 2-7) were much weaker than those obtained by amplification using unlabeled dNTPs and staining with SYBR Gold (Figure 2-8). This may indicate that amplification using fluorescent dCTP was not as efficient as that using regular dCTP. Furthermore, this may suggest that F-dCTP was not compatible with phi29 polymerase. Due to the reduced amplification caused by F-dCTP, all the following RCA reactions were carried out using unlabeled dNTP. Therefore, RCA product in solution were examined by PAGE stained by SYBR Gold, and RCA on surface was visualized by hybridization with Cy3-labeled probe oligonucleotides.

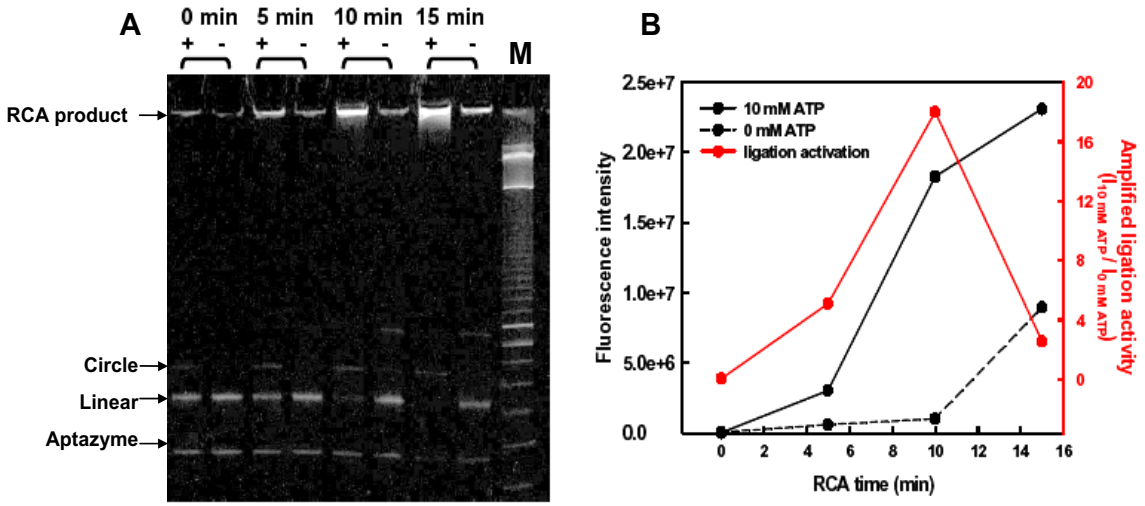

Figure 2-8. Unlabeled aptazyme-mediated ATP-dependent ligation followed by RCA in solution. (A) Analysis of RCA product by gel electrophoresis. (+) and (-) represent the presence and absence of 10 mM ATP, respectively. Ligations were carried out for 1h, followed by RCA for various time periods (0, 5, 10 and 15 min). RCA product, circularized padlock probe, unligated padlock probe and aptazyme are indicated. M is a 10 bp DNA ladder. (B) Quantitative analysis of RCA product as a function of RCA time. Black lines represent % ligation in the presence of ATP, black dotted lines represent % ligation in the absence of ATP, and red lines represent amplified ligation activity (ratio of % ligation in the presence of ATP vs % ligation in the absence of ATP).

RCA in solution

The aliquots of ligations using unlabeled aptazymes were taken after 1 h, ligated products were directly amplified without further purification by using the phi29 DNA polymerase at 37 ^{o}C, and the amplification mixtures were separated by gel electrophoresis (Figure 2-8). The signal due to RCA increased approximately 1500-fold after 10 min of amplification. The signal in the presence of ATP was about 19-fold higher than in the absence of ATP. Biotin-labeled aptazyme was also tested with the 5 min

ligation product used for RCA at 10, 20 and 30 min (Figure 2-9). Again, the activation was about 33-fold by ATP, which was much lower than previously reported (250-fold, Levy and Ellington, 2002), likely because the amplification provided by RCA overrepresented the background ligation reaction. Even without optimization of the ligation and RCA reactions, the positive signal was clearly detectable when compared to the negative control. Additionally, these results suggested the potential for analyte quantitation in a multiplexed format.

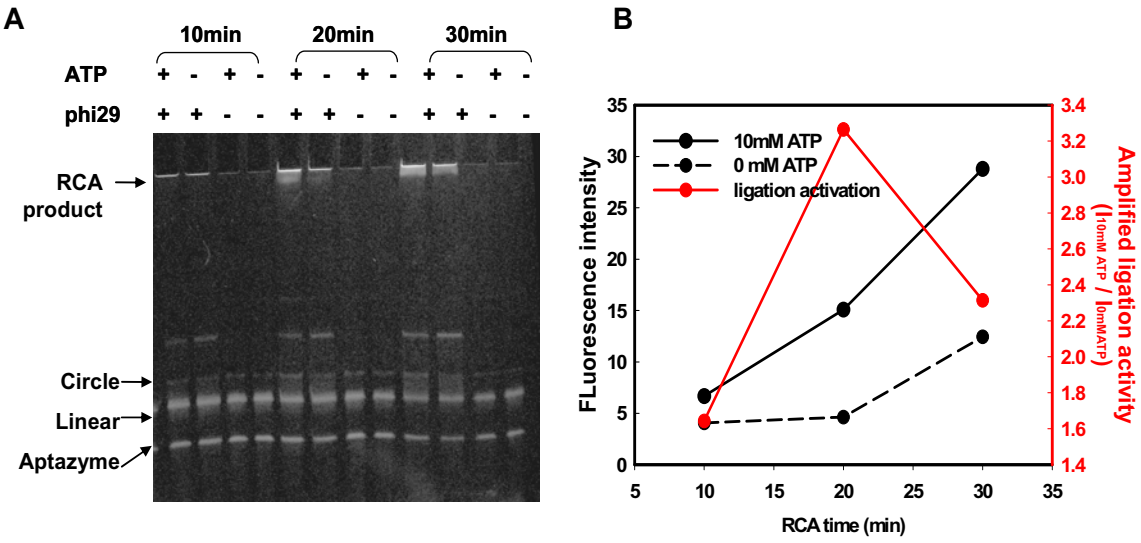

Figure 2-9. Biotin-labeled aptazyme-mediated ATP-dependent ligation followed by RCA in solution. (A) Gel images of RCA activities. Ligation and RCA were carried out using biotin-labeled aptazyme as descibed in Figure 2-7. RCA was carried out for 10 min, 20 min and 30 min, respectively. (B) Quantitative analysis of RCA product as a function of RCA time.

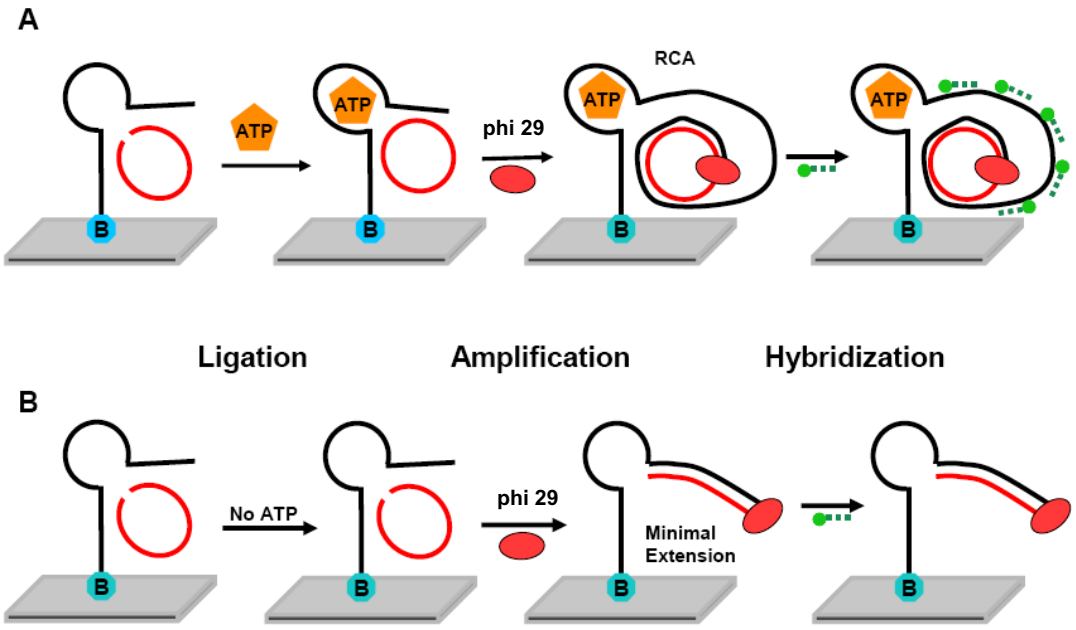

Figure 2-10. Schematic drawing of aptamer-mediated chip-based RCA. The biotin-aptazymes are immobilized on streptavidin-coated glass slides. Ligations are carried out in the presence (A) and absence (B) of ATP. RCA is initiated from the 3' end of the aptazyme, and the extended aptazymes are visualized by hybridization with Cy3-labeled complementary oligonucleotides (green circle). Aptazymes bound to circularized padlock probes generate long concatemers RCA product (A) and aptazymes bound to linear padlock probes get minimal extension (B).

Chip-based RCA assay

This novel assay strategy could be readily applied to a chip array format (Figure 2-10). As a chip-based immunoRCA assay, the amplified product would be localized within the spots on arrays. Aside from its better applicability, the chip array has other advantages: we had noticed that the background in solution RCA was high, probably due to the fact that ligation could not be stopped prior to RCA. Because an array assay would allow washing and removal of the unligated padlock probe and the analyte, ATP, presumably generating lower background compared with solution assays.

Next, we prepared chip arrays by printing biotin-labeled aptazymes. Printed aptazymes were incubated at room temperature for 1 h under high humidity (60-80 %) to allow better binding of streptavidin and biotin and then exposed to either 10 mM or 0 mM ATP. Initially, we tried 1 μM aptazyme for printing; however, the amplification signal was so strong that fluorescence quenched in the center of the spots (data not shown). Instead, using 0.1 μM aptazyme printing, no signal saturation was found while the fluorescence was still high enough. Additionally, reducing padlock probe concentration resulted in decreased ATP activation (ATP+/- signal ratio). As a result of optimization in chip-based assays, the same padlock probe concentration and one tenth of the aptazyme concentration were used as compared with these concentrations in solution.

After 10-90 min ligation, slides were washed with ligation buffer (50 mM Tris-Cl buffer, pH 7.4, and 50 mM $MgCl_2$) containing 0.05 % Tween 20. Ligated products were amplified by RCA at 37 °C for 5 min, and the slides were again washed twice with SSC buffer containing 0.05 % Tween 20. Finally, amplified products were detected by hybridization with 0.5 μM complementary, fluorescent oligonucleotide probes at 37 °C for 30 min. Fluorescent spots were visualized using an Axon Instruments (Union City, CA) 4000B confocal microarray scanner. The fluorescence intensity at excitation of 532 nm was analyzed using GenePix 4.1 software (Axon Lavoratory). Figure 2-11 showes the fluorescence images of biotin-modified aptazyme spots when they were subjected to various ligation times. A 60 min ligation followed by 5 min RCA demonstrated the highest activation (~62-fold) upon ATP recognition.

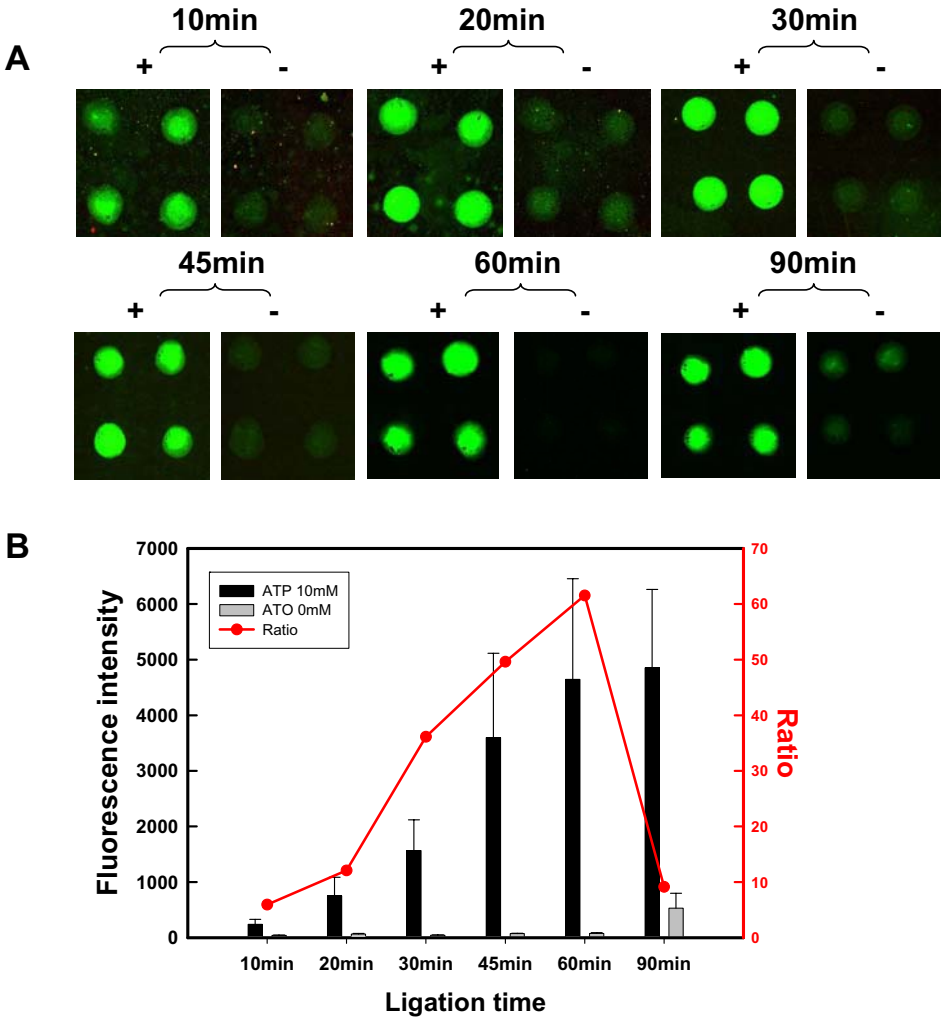

Figure 2-11. Effects of varied ligation timeperiods on amplification signals in chip-based assays. (A) Fluorescent images of amplified ATP activation. Ligations were carried out in the presence or absence of 10 mM ATP for different time periods and then followed by 5 min RCA. Amplifications were visualized by hybridization with Cy3-labeled complementary probes. (B) Analysis of fluorescence intensity and ATP activation of those shown in (A).

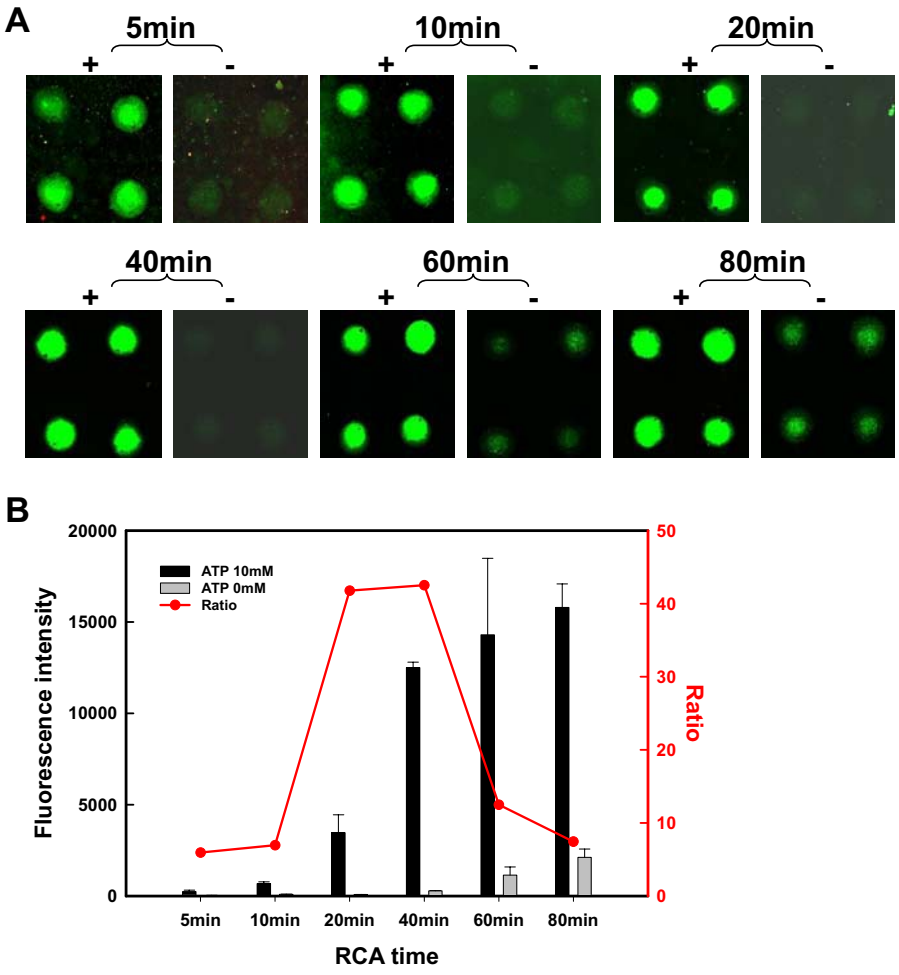

Figure 2-12. Effects of varied RCA timeperiods on amplification signals in chip-based assays. (A) Fluorescent images of amplified ATP activation. Ligations were carried out in the presence or absence of 10 mM ATP for 10 min, and then followed by RCA for different time periods. (B) Quantitation of fluorescence intensity and ATP activation.

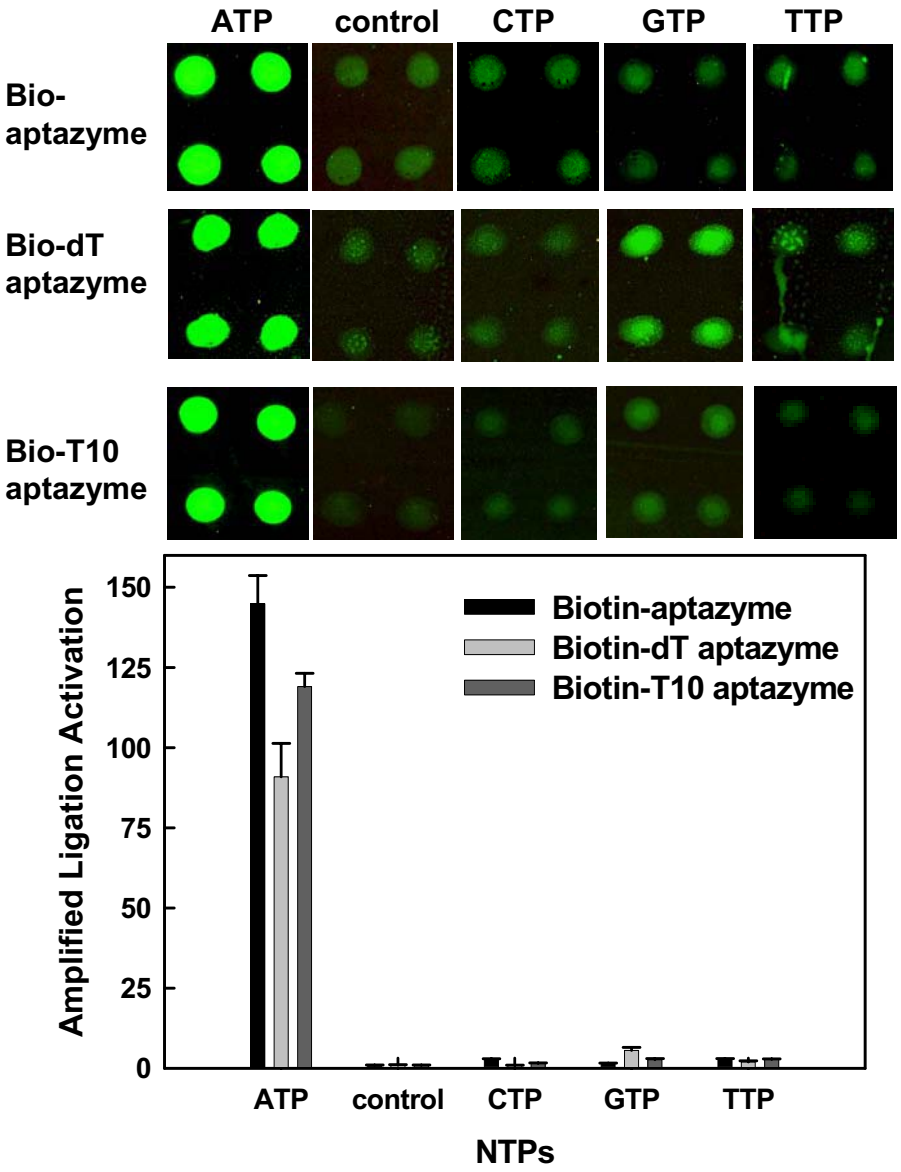

Figure 2-13. Detection specificity of chip-based RCA. (A) Fluorescence images of amplified ligation activities using biotin-lableled aptazymes with various linkers on chip arrays showing the specificities over various nucleotides. (B) Amplified ligation activity measured in the presence of NTPs (10 mM ATP, UTP, GTP and CTP) and in the absence of NTPs (denoted as control) for biotin-modified aptazymes with various linkers: no linker, dT, and T10.

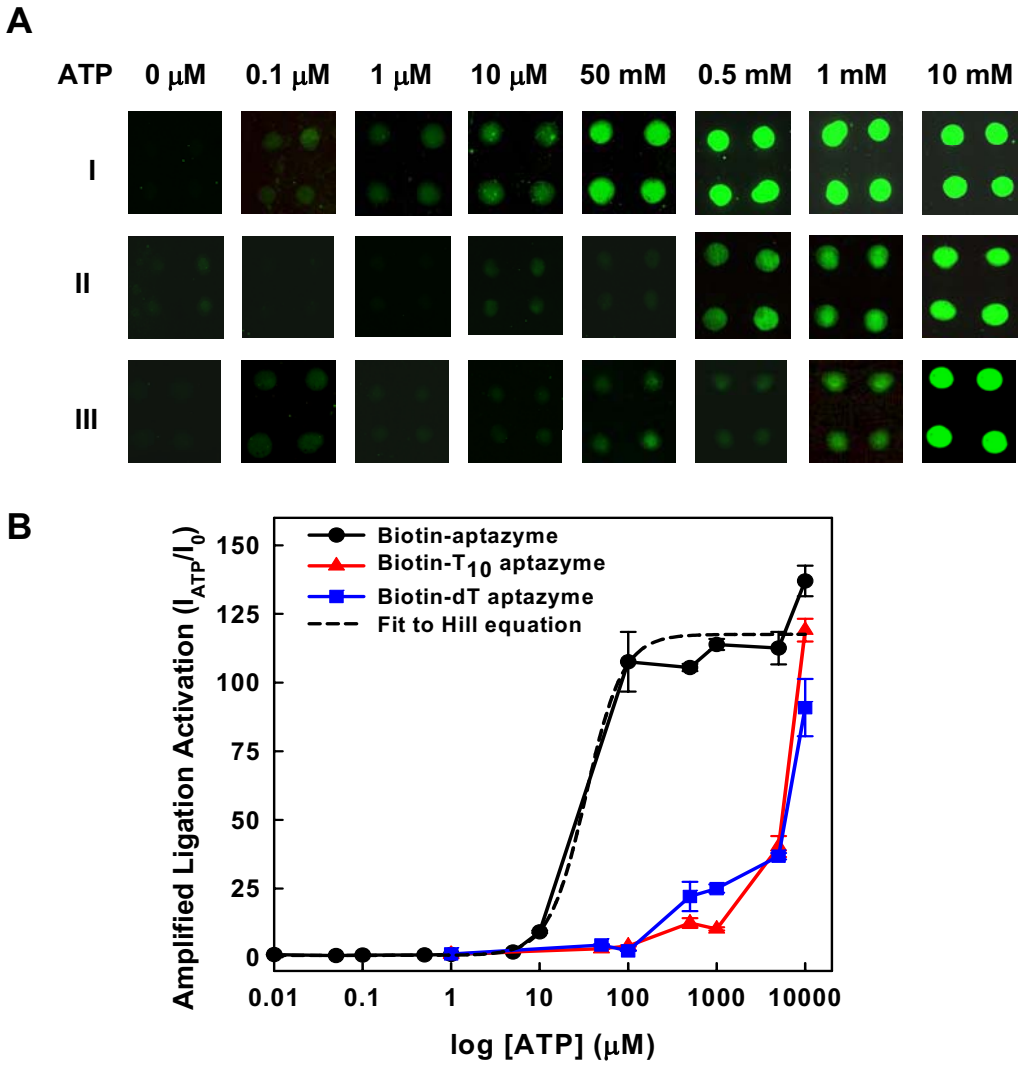

Figure 2-14. ATP-sensing performance on a chip array. (A) Fluorescence images of biotin-aptazyme (I), biotin-dT-aptazyme (II) and biotin-T10-aptazyme (III) spots on a chip array at various ATP concentrations. (B) Amplified ligation activity as a function of ATP concentration for biotin-modified aptazymes with various linkers: no linker, dT, and T10. The dotted line represents the best fit to the Hill equation (SigmaPlot, SPSS, Chicago, IL).

Similarly, ligation was carried out for 10 min followed by RCA for 5-80 min (Figure 2-12). Though high activation (~45-fold) was seen with 20-40 min RCA, this value was still below the activation achieved by 60 min ligation coupled with 5 min RCA (~62-fold). So the final optimal conditions for chip-based RCA were 60 min ligation followed by 5 min RCA.

Using the optimized conditions, amplified ATP activation was examined by printing biotin-modified aptazymes with and without linkers. Printed aptazymes were processed as described previously and then exposed to either 10 mM ATP, UTP, CTP, or GTP. After 1 h ligation, slides were washed with ligation buffer to remove unbound NTPs and unligated padlock probes. Ligated padlock probes were amplified by phi29 polymerase at 37 °C for 5 min. After termination of RCA by washing out RCA reagents, amplified products were detected by hybridization with 0.5 μM complementary, fluorescent oligonucleotide probes at 37 °C for 30 min. Figure 2-13A shows the fluorescence images of biotin-modified aptazyme spots when they were subjected to various nucleotides. Even though the images were taken at relatively low excitation power (PMT power of 400V at λ_{ex} 532 nm), bright signals due to signal amplification using RCA (~13-fold) could readily be seen.

Figure 2-13B summarizes the amplified ligation activities for three biotin-modified aptazymes with various linkers. In general, the aptazyme without a linker showed higher activation than aptazymes containing linkers, as was the case in solution. However, all aptazymes exhibited more than 100-fold activation in the presence of ATP and showed no or very weak activation (<5 %) above background by other NTPs. The improved responsivity on the surface relative to that in solution could be attributed in part to the fact that unreacted, linear substrate could be washed away prior to initiating RCA and was therefore unable to react further during the amplification step. These results

demonstrate that aptazyme-catalyzed effector-dependent ligation coupled with RCA can differentiate between structurally similar molecules such as UTP, CTP, and GTP on a sensor platform with a preparation time of an hour and a development time of only a few minutes.

Finally, to determine if a combination of aptazyme-catalyzed ligation and RCA could be used to quantitate analytes in the chip array format, response curves were obtained by measuring the fluorescence intensity of RCA products as a function of ATP concentration. Responses were measured for all three ATP responsive deoxyribozyme ligase aptazymes with different linker sequences. Figure 2-14A shows the scanned images of fluorescently-labeled aptazyme-catalyzed circularization and RCA reactions as a function of ATP concentration. The biotinylated aptazyme without any linker again yielded the best responsivity (Figure 2-14B). As previously reported, the anti-ATP aptamer has two ATP binding sites, which seem to function cooperatively (Levy and Ellington, 2002; Jhaveri, Kirby, et al., 2000). Therefore, the sharpness of the sigmoidial response curve is not surprising. The calculated Hill coefficient for the biotin-labeled aptazyme was 2.1± 0.56. While as little as 1 μM ATP could be reproducibly detected by the deoxryibozyme ligase, a large response was produced over a relatively narrow concentration range (from 10 to 100 μM). The deoxyribozyme essentially serves as a "switch" that activates amplification only at a threshold concentration of ATP. Selected aptazymes that we and others have reported have lower background rates of ligation and thus might give better limits of detection. In addition, the fact that the assay takes places directly on a chip surface in the presence of a very small amount of aptazyme (ca. 300 amol) may make it possible to prevent the dilution of cellular metabolites into large volumes, as is the case for many conventional, enzyme-based assays.

CONCLUSIONS

We have described a novel analytical approach in which analytes are transduced into amplicons, in this case circular probes that could be readily amplified by rolling circle amplification. The utility of this strategy has been demonstrated for the sensitive detection of ATP. Aptazyme-coupled RCA was adapted to a sensor platform that could be easily read and multiplexed, and reproducible signals were acquired within a few minutes.

FUTURE PLANS

As we described previously, many aptazymes have been created to be modulated by analytes. However, among them only a few are deoxyribozymes. In order to use more aptazymes to couple with nucleic acid amplification, the future directions might be the development of more DNA aptazymes by either rational design or *in vitro* selection and the use of RNA aptazyme for this purpose. The development of the former may directly generate amplicons. However, the latter may need different strategies for the purpose of amplification.

For RNA aptazyme ligases, the most direct way is to use real-time RT-PCR for the detection of analyte-dependent ligations. For example, the L1 ligase could ligate itself to another RNA oligonucleotide upon interaction with either small molecule or proteins. Therefore, real-time RT-PCR should be able to detect the ligations caused by analyte binding.

Besides generating ligation product in the presence of analyte, production of a primer could be another configuration for coupling aptazyme activity to RCA. Recently, Jonstrup *et al.* have reported that detection of miRNA using RCA (Jonstrup, Koch et al. 2006). In this instance, the padlock probes anneal to the miRNA and are subsequently

ligated by DNA ligase. MiRNA then serves as a primer for RCA. This result demonstrated the feasibility to use RNA as primers for RCA. Therefore, similar strategy as Figure 2-1D might be suitable for chip-based RCA using the RNA aptazyme such as L1 ligase. The substrate oligonucleotide of L1 ligase can be immobilized on microarray slides and the 3' sequence of L1 ligase can serve as a primer for RCA. In the presence of analyte, L1 ligase is ligated to the substrate strand and retained on surface. With additional circular template and polymerase, the ligated species can be amplified. However, the unligated species must be removed by washing prior to amplification.

RNA aptazyme capable of analyte-dependent cleavage can also be modified to generate a primer for amplification. For example, the 5' end of substrate strand of the allosteric hammerhead ribozyme can be immobilized and the other end can be modified with a 3' terminator base such as ddC to block amplification. So when there is analyte dependent cleavage, the substrate is cleaved and the new 3' terminal can hybridize to a circular DNA for amplification.

With the development of multiple configurations of coupling aptazyme activity with signal amplification, more aptayme biosensors could be generated and should be especially useful for the detection of both small molecules and proteins.

ACKNOWLEDGEMENT

The work described in Chapter 2 was done by collaboration with Dr. Eun Jeong Cho. I prepared ligation and RCA mixtures and Dr. Cho performed aptazyme printing. Ligation and RCA assays as well as data analyses were done by both of us.

MATERIALS AND METHODS

Oligonucleotides

The designed padlock probes were synthesized in our laboratory on an Expedite 8909DNA synthesizer (PE Biosystems, Foster City, CA) via standard phosphoramidite chemistry using synthesis reagents purchased from Glen Research (Sterling, Virginia). The sequences of the padlock probes are shown in Figure 2-3. They all contain 5'-iodine and 3'-phosphorothioate. The 3' phosphorothioates were synthesized on 3' phosphate-CPG by replacing the normal oxidizing reagent with the sulfurizing reagent thiosulfonate. The 5' I-dT of synthesized oligonucleotides were deprotected in NH_4OH at room temperature for 24 h followed by purification by denaturing polyacrylamide gel in the presence of 7 M urea prior to use.

The following oligonucleotides were purchased from IDT (Coralville, IA).

Aptazymes with different modifications at the 5' end, including aptazyme, biotin-aptazyme, biotin-dT-aptazyme and biotin-T10-aptazyme, have the same sequences (5'-CGAAGACAGGTTCCTGGGGGAGTATTGCGGAGGAAGGTGC). F-probe (fluorescent oligonucleotide probe: 5'-Cy3-GTTTTCGCCTTCTTGTTTCC-3') contains complementary sequence to the RCA product.

Ligation assay in solution.

Ligation reactions were carried out at room temperature in a 20μL reaction volume. 15 μL pre-ligation mixture containing 0.5 μM aptazyme/biotin-aptazyme/biotin-dT-aptazyme/biotin-T10-aptazyme, 50 mM Tris-HCl (PH. 7.4), 50 mM $MgCl_2$, 0.5 M NaCl was heated at 70 ^oC for 3 min. Then 1 μL of 20 μM padlock probe, 2 μL of 20 μM DTT, 2 μL of 100 mM ATP or H_2O was added to the pre-ligation mixture. Ligtation

reactions were incubated at room temperature for different time periods and then terminated by addition of 95 % formamide gel-loading buffer. Ligated (circular) and unligated (linear) padlock probes were separated by denaturing 8-10 % acrylamide gels containing 7 M urea followed by SYBR-Gold (Molecular Probe, Eugene, OR) staining at room temperature for 5 min. The fluorescent bands were visualized either by a UV illuminator or a fluorescent scanner (Biorad, Hercules, CA). The fluorescence intensity of DNA bands was quantitated using ImageQuant 5.2 software (Molecular Dynamics, Sunnyvale, CA).

RCA in solution

RCA reactions were prepared by mixing aliquots of 4 μL of the ligation mixture, 2 μL of 10x phi29 buffer (400 mM Tris-HCl, 500 mM KCl, 100 mM $MgCl_2$, 50 mM $(NH4)_2SO_4$, 40 mM DTT), 2 μL of 10x dNTP (2.5 mM), 3 μL of phi29 polymerase (10 ng/μL) (Epicenture, Madison, WI) and 10 μL H_2O. Reactions were performed at 37 ^oC for 5-120 min and stopped by heating in 47.5 % formamide gel-loading buffer at 65 ^oC for 10 min. Electrophoresis analysis of RCA was carried out by either 8 % or 10 % denatured polyacrylamide gels, which were then stained with SYBR Gold, and the bands were quantitated.

Ligation reactions on streptavidin coated glass slides

The streptavidin-coated microarray slides were purchased from Pierce Biotechnology (Rockford, IL). Pre-ligation mixture containing 0.1 μM either biotin-aptazyme, biotin-T10-aptazyme or biotin-dT-aptazyme were denatured at 70 ^oC for 3 min and cooled to room temperature prior to printing. Then glycerol was added to these

aptazymes to obtain 5 % final concentration. Aptazymes were printed using a manual arrayer (V&P Scientific, Inc., San Diego, CA) within a 60-80 % humidity chamber. The slides were incubated in the same chamber at room temperature for 1 h after printing to allow biotinylated moieties of the aptazymes to be bound to the streptavidin coating on the slides. Then the printed areas were enclosed within a CoverWell incubation chamber with self-adhesive rubber gasket for 4 wells (Schleicher and Schuell, Keene, NH). 1 mL of ligation buffer containing 0.05 % Tween 20 was pipetted into each chamber through access ports that were sealed to remove unbound aptazymes. Ligation was carried out using 70 μL substrate mixture (1.0 μM padlock probe, 50 mM Tris-HCl, 50 mM $MgCl_2$, 0.5 mM DTT) with different ATP concentrations (0-10 mM) for individual chambers. Ligation reaction was stopped by washing the chamber using 1x ligation buffer plus 0.05 % Tween-20.

RCA reactions on streptavidin coated glass slides

RCA was carried out using 70 μL RCA buffer (40 mM Tris-HCl (pH 7.5), 50 mM KCl, 10 mM $MgCl_2$, 5 mM $(NH_4)_2SO_4$, 4 mM DTT, 0.25 mM dNTP, 0.2 mg/μL BSA) with 2 ng/μL phi29 polymerase in each chamber. The reactions were incubated at 37 ^oC for 5-120 min and then terminated by washing the chamber with 2x SSC (300 mM sodium chloride and 30 mM sodium citrate) containing 0.05 % Tween 20. Then 70 μL hybridization buffer (2x SSC with 0.05 % Tween-20) containing 0.5 μM Cy3-probes were applied to each chamber for hybridization with the RCA product at 37 ^oC for 30 min. Finally, covers of the chambers were peeled away and the slides were washed twice using 2x SSC/0.05 % Tween-20 for 10 min, twice with 1x SSC/0.05 Tween-20 for 10 min, and once with 0.5x SSC for 20 min. The slides were dried by centrifuging at 600 rpm at 25 ^oC for 5 min. Slides were scanned on an Axon Instruments (Union City, CA)

4000B confocal microarray scanner. The photomultiplier tube (PMT) voltage for 532 nm (CY3) and 635 nm (CY5) were 400 and 650 volts, respectively. The fluorescence intensities at excitation of 532 nm were analyzed using GenePix 4.1 software (Axon Lavoratory).

Chapter 3: Real-time rolling circle amplification (RCA) for protein detection

INTRODUCTION

Real-time PCR is now the method of choice for many diagnostic applications (Barletta 2006; Espy, Uhl et al. 2006; Watzinger, Ebner et al. 2006). However, it is difficult to adapt real-time amplification to the detection of protein (rather than nucleic acid) analytes.

RCA is instead being adapted to the detection of proteins (Schweitzer, Wiltshire et al. 2000; Schweitzer, Roberts et al. 2002; Zhou, Bouwman et al. 2004; Di Giusto, Wlassoff et al. 2005; Soderberg, Gullberg et al. 2006). In RCA, a small nucleic acid circle hybridizes to a primer, which is in turn extended around the circle, ultimately displacing the original primer and continuing to produce long concatameric nucleic acid products. The nucleic acid products can be detected by a variety of methods, including hybridization of fluorescent oligonucleotide probes. Interestingly, the concatamers are so massive that they can accumulate and be detected as discrete single molecules on surfaces (Lizardi, Huang et al. 1998; Schweitzer, Wiltshire et al. 2000; Nallur, Luo et al. 2001; Schweitzer, Roberts et al. 2002; Zhou, Bouwman et al. 2004; Cho, Yang et al. 2005).

It has recently proven possible to carry out real-time RCA reactions using strategies similar to those for real-time PCR detection, such as detection of newly synthesized products with molecular beacons, cleavable probes, or SYBR Green (Nilsson, Gullberg et al. 2002; Harvey, Lee et al. 2004; Smolina, Demidov et al. 2004; Di Giusto, Wlassoff et al. 2005; Yi, Zhang et al. 2006). Because of the advantages inherent in using real-time methods to quantitate amplification reactions, it would be extremely

advantageous to be able to adapt RCA for the detection of proteins to real-time methods. However, it is not immediately obvious how this might be done, given that real-time reactions are not routinely carried out on surfaces and that the capture of circular templates by protein ligands must be separated in time from RCA itself.

The most current method for RCA detection of proteins typically involves linking an oligonucleotide to an antibody, binding the conjugate to an immobilized protein target, washing away unbound antibodies, and carrying out RCA for detection of the bound conjugates. In chip-based methods, a sandwich assay is typically used, and several secondary antibodies may be added prior to RCA. These methods are time-consuming, expensive, cumbersome, and far from real-time.

We propose to combine real-time RCA with protein detections using aptamers. A real-time RCA assay for the detection of protein analytes would not only be fast and quantitative but could also potentially be carried out in heterogeneous solutions without having to wash away unbound affinity reagents or DNA templates. In order to combine these two techniques, we will catalyze the formation of circular RCA templates by protein analytes rather than by hybridizing nucleic acid analytes. The vehicle for the protein-dependent formation of circular templates will be structure-switching nucleic acid aptamers. Aptamers are single-stranded DNA and RNA molecules selected *in vitro* from random sequence libraries. Aptamers have been selected against a variety of analytes, including inorganic ions, small organics, metabolites, peptides, proteins, and even whole viruses or cells (Proske, Blank et al. 2005; Yan, Bell et al. 2005; Bunka and Stockley 2006; Lee, Stovall et al. 2006). Aptamers typically assume defined, compact secondary and tertiary structures and demonstrate high affinities (K_d values in the nanomolar range) and selectivities for their targets.

Aptamers often undergo conformation changes upon binding to their targets, and these conformational changes can be further magnified by engineering. Structure-switching aptamers are typically created by manipulating the secondary structure of an aptamer, so that two conformations can be assumed, one in the absence of the cognate analyte and a different one in the presence of the analyte. For example, Tan's group modified an PDGF aptamer beacon so that it was unfolded in the absence of PDGF but assumed its secondary and tertiary structure in its presence (Fang, Sen et al. 2003; Vicens, Sen et al. 2005). Labels appended to the aptamer led to fluorescence quenching in the presence of PDGF. This "folding" strategy can be generalized to the detection of small molecule analytes, such as cocaine (Stojanovic, de Prada et al. 2001). A variation on this theme is to add sequences *in cis* or *in trans* to an aptamer to stabilize an alternative secondary structure and then have the aptamer refold in the presence of analyte, again with a change in fluorescent signal (Yamamoto, Baba et al. 2000; Hamaguchi, Ellington et al. 2001; Bayer and Smolke 2005). The use of antisense DNA oligonculeotides *in trans* has proven to be a particularly facile strategy for generating so called aptamer beacons (Nutiu and Li 2003; Nutiu and Li 2004; Nutiu, Yu et al. 2004). Indeed, this "refolding" strategy has proven adaptable to detection via either electrochemical couples (Xiao, Piorek et al. 2005) or nanoparticle signaling strategies (Levy, Cater et al. 2005; Liu and Lu 2005). Quarternary structural changes (adjacent binding of two different aptamers) have also been exploited for signaling (Heyduk and Heyduk 2005).

We believe that analyte-mediated conformational changes in aptamers can also be transduced to powerful nucleic acid amplification and detection methods. Analyte-mediated protection of an aptamer from exonuclease digestion preceded oligonucleotide ligation and PCR and could be used for the detection of a few hundred thrombin

molecules (Wang, Li et al. 2005). Proximity methods in which two aptamers bind adjacent to one another and are ligated have been harnessed to both RCA and PCR amplification technologies (Fredriksson, Gullberg et al. 2002; Di Giusto, Wlassoff et al. 2005), and zeptomole amounts of PDGF were detected (Fredriksson, Gullberg et al. 2002). It is noteworthy, though, that these methods were not for the most part adapted to real-time detection.

One of the simplest and most robust methods for generating conformation-switching aptamers is to utilize an antisense sequence either in *cis* or *trans* to disrupt aptamer structure and function (Hamaguchi, Ellington et al. 2001; Nutiu and Li 2003; Bayer and Smolke 2005). Based on our design of the structure-switching aptamer in chapter 4, we have now engineered a structure-switching aptamer that upon interaction with its analyte (PDGF) can be circularized and the product detected by real-time RCA. This method can potentially be adapted to multiple aptamers, and the real-time nature of the amplification reduces background and improves detection significantly.

RESULTS AND DISCUSSION

Designs for analyte-dependent aptamer circularization

Previously, we have shown that analyte-dependent aptazyme catalyzed ligation of can be used in conjunction with rolling circle amplification for the sensitive detection and quantitation of small molecules such as ATP (Cho, Yang et al. 2005). However, this method was inherently limited by the fact that to date very few aptazyme ligases have been designed or selected. In contrast, large numbers of aptamers have been selected (see, for example, the Aptamer Database http://aptamer.icmb.utexas.edu). In order to adapt aptamer recognition of analytes to real-time amplification methods such as RCA

we used protein enzyme catalyzed ligation (rather than a ribozyme-mediated ligation) and designed conformation-switching aptamer beacons that could be circularized (Figure 3-1).

This design was based on the three-piece system we developed in Chapter 4, where the antisense sequences were in *trans* with the aptamers. To create a padlock probe, both the antisense sequence and the substrate sequence were attached to either end of the anti-PDGF aptamer (Figure 3-1). In the presence of PDGF, the 13 nucleotide antisense sequence would form ligation junction with the 5' end of the aptamer, resulting in aptamer circularidization by T4 DNA ligase. With additional RCA reagents, the amplification of PDGF-dependent ligation could be monitored in real time.

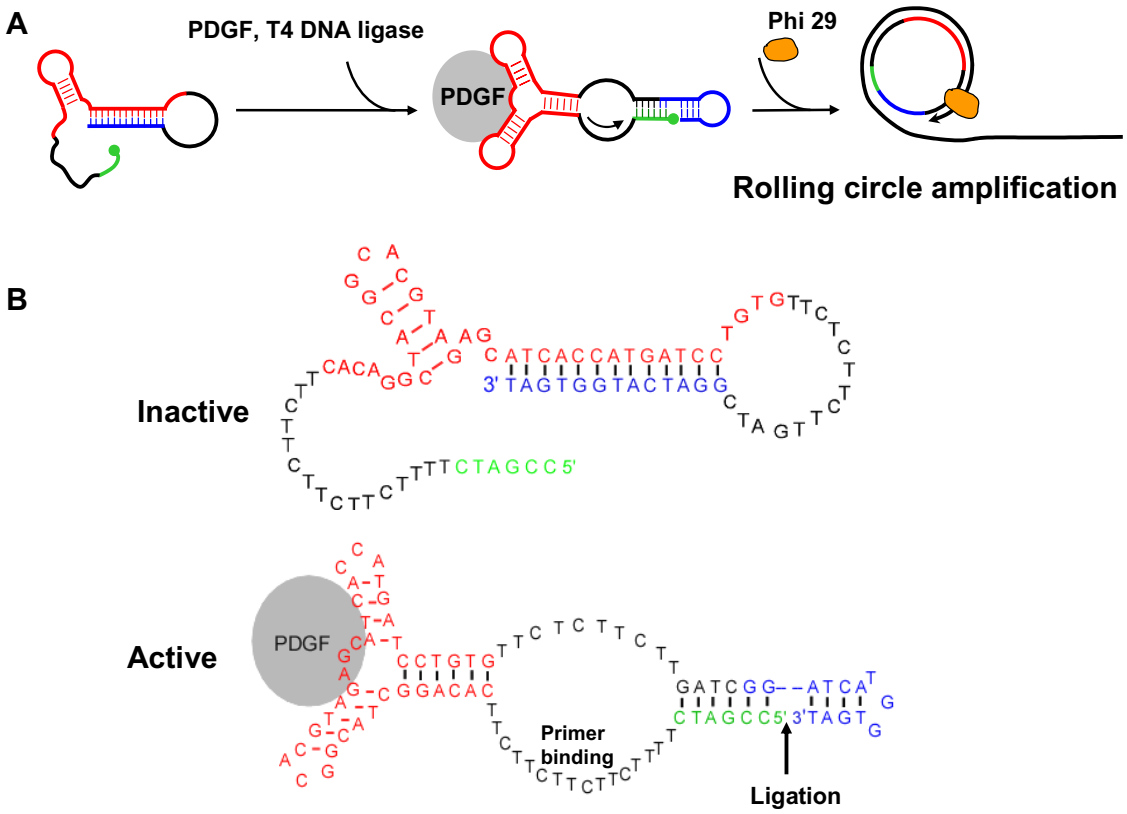

Figure 3-1. Design for PDGF-activated circularization. (A) General design principles. The lengths of different DNA segments in the aptamer are not drawn to scale in the three steps illustrated. The original aptamer is shown in red. Blue sequence is added to the 3'-end of the aptamer in order to promote the formation of a duplex structure and denature the aptamer. Green sequence is added to the 5'-end of the aptamer; there is also a 5'-phosphate. In the presence of a protein analyte such as PDGF, the 3'-extension (blue) is displaced and hybridizes with the 5'-end to form a ligation junction. This conformational change is assisted by the formation of a short hairpin structure involving the 3'-extension. Following ligation with T4 DNA ligase, the circularized aptamer can serve as a template for RCA. (B) Sequence and secondary structure of the designed anti-PDGF, conformation-switching aptamer N5C0. The 5'- and 3'-extensions are attached to the two termini of the aptamer via additional linker regions (black).

In the binding conformer, the 3' sequence extension should be displaced from the aptamer and form a short hairpin structure (Figure 1, blue). The 6 nt substrate sequence in the previous three-piece ligation was added to the aptamer via another linker (Figure

1B, green) and could potentially pair with this hairpin structure to form a ligation junction (Figure 1B) for the aptamer termini that could be closed with T4 DNA ligase. Ligation of the adjacent ends leads to the circularization of the aptamer.

The two linker regions were very important for feasibility of ligation because the participation of two proteins (the analyte and the DNA ligase) in the ligation reaction meant that the analyte-binding domain of the aptamer had to be well-separated from the ligation junction. In addition, the linker should not interfere with either substrate or antisense sequence binding. As the designed three-piece analyte dependent ligations, the protein-dependent circularization of the engineered anti-PDGF aptamer is mechanistically similar to other signal transduction strategies that have been developed for aptamers (Rajendran and Ellington 2002; Cho, Rajendran et al. 2005; Yang and Ellington 2006). Such as displacement of an antisense oligonucleotide upon re-folding, as pioneered by Li's group (Nutiu and Li 2003; Nutiu and Li 2004) and the antiswitch strategy adopted by Bayer and Smolke (Bayer and Smolke 2005). For example, our strategy is similar to some aptamer beacon strategies that have previously been developed. In general, aptamer beacons can be categorized as either undergoing ligand-dependent folding from an unfolded state or ligand-dependent refolding from a folded state. Presumably, both apatmer and antisense sequences together on a single strand there should be less conformational heterogeneity in the starting population, and this may in turn reduce background. Our designs are different from the antiswitch strategies by building a hairpin stem into the displaced sequences. Since this hairpin is essential for the formation of a ligation junction, the sequence and the length of the hairpin stem can also potentially be rationally manipulated in order to further poise the aptamer between binding and non-binding conformations. Also base numbers and sequences at the other side of the ligation junction would be optimized to improve the detection.

Observation of analyte-mediated aptamer circularization

To confirm that circularization occurs, ligation products were separated on a denaturing gel. There was significantly more circular product in the presence of PDGF-BB than in its absence (Figure 3-2, lanes 2 and 4). In addition, the aptamer was treated with or without PDGF and T4 DNA ligase followed by exonuclease VII digestion. Unligated, single-stranded, aptamers should be digested, while the rearranged, circularized conformers should not be digested (Figure 3-2, lanes 3 and 4). As expected, the circular, ligated aptamer is seen in the presence of PDGF and remains following exonuclease digestion. Finally, digested ligation mixture was amplified by RCA. There was significantly more amplified product in the presence of PDGF than in its absence (Figure 3-2, lane 5 and 6).

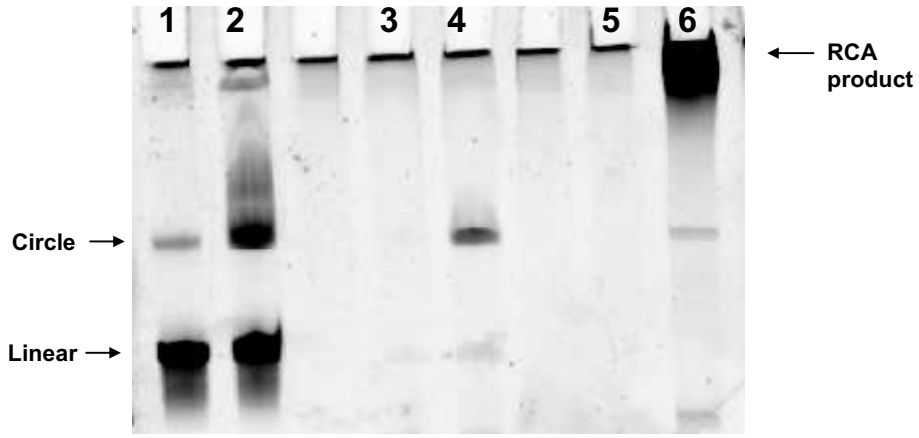

Figure 3-2. Circularization and amplification of N5C0. Ligation reactions were carried out in the presence (Lanes 2, 4, 6) and absence of PDGF (Lanes 1, 3, 5) at room temperature for 16 h, and treated with exonuclease VII (Lanes 3, 4) for 1h. Exonuclease VII digested samples were amplified by RCA at 37 ^{o}C for 1 h. Samples were separated on a denaturing 8 % polyarylamide gel and stained with SYBR Gold. M represents 10 bp DNA ladder. Arrows show the linear and circularized aptamers.

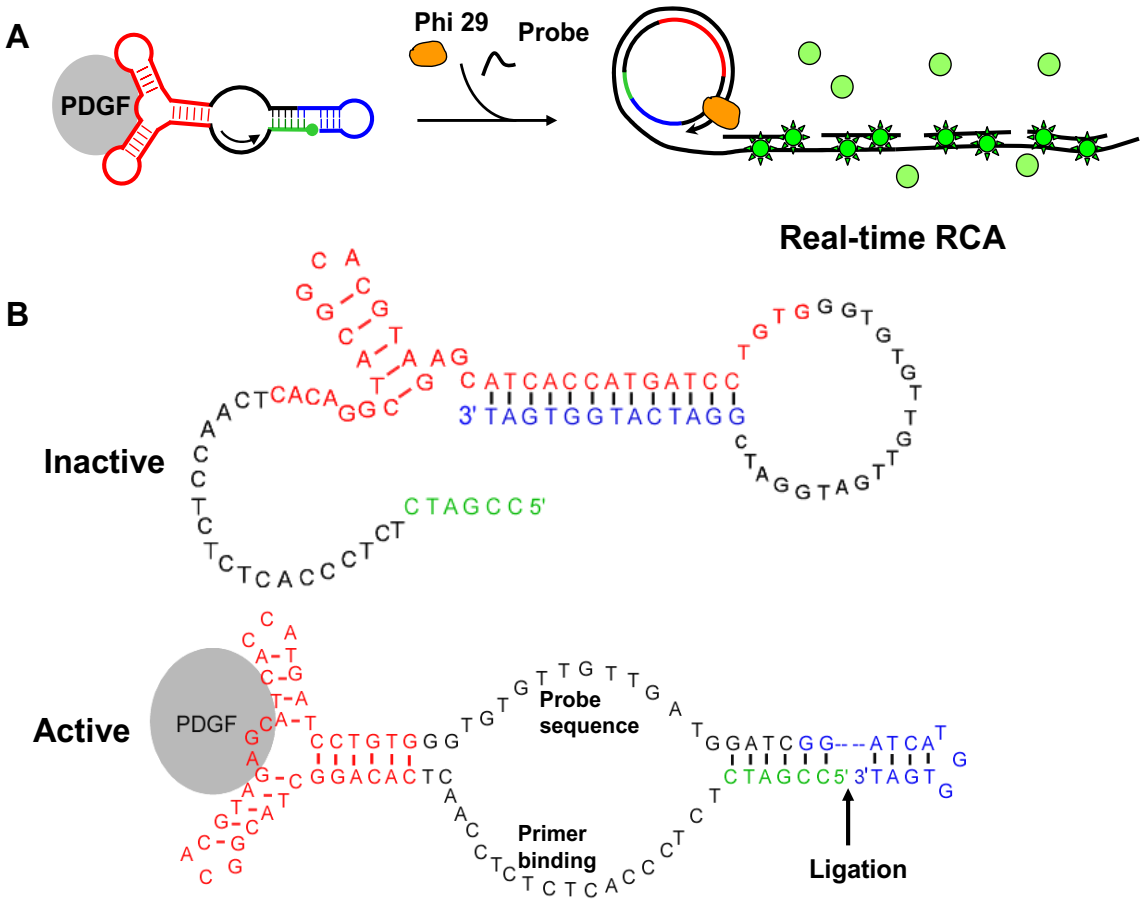

Figure 3-3. Design for a new construct N5C1 by optimization of the two linkers of the N5C0. (A) General design principles for real-time SYBR Green detection based on Figure 3-1. In RCA, probes form duplexes with the amplification product. SYBR Green binds to the double stranded regions and generates fluorescence. (B) Sequence and secondary structure of the designed anti-PDGF, conformation-switching aptamer N5C1. Additional linker regions between the aptamer and the 5' and 3' extensions serve as primer binding site and probe sequence for RCA.

Introducing a probe sequence for real-time amplification

Initially, we designed construct N5C0 and carried out real-time RCA detected by SYBR Green. However, the real-time RCA signals were very weak and hard to quantitate (data not shown). This was probably due to few double stranded regions formed by the amplified product at 37 ^{o}C. Therefore, we introduced probe oligonucleotides to bind to the RCA product to form duplex for SYBR Green sensing.

This design takes the advantage of the linker regions. We designed a new construct N5C1, whose linker regions are suitable for primer and probe binding for real-time RCA. The design of the linker regions was based on the following concerns: these regions should not have any secondary structure while contain certain number of GC bases for stable primer and probe binding. The secondary structure was conformed by Mfold (http://www.bioinfo.rpi.edu/applications/mfold/old/dna) and the Tm values of the linker regions were kept above 40 ^{o}C, which should above the amplification temperature (37 ^{o}C). These designs were also assessed computationally. The energies of the conformational equilibrium between the non-binding, duplex DNA conformer and the three way junction binding-competent conformer were roughly predicted by specifying those structures in. The free energy of folding of the non-binding conformation was predicted to be -19.2 kcal/mol, while the free energy of folding of the binding conformation was predicted to be -14.1 kcal/mol. The free energy of protein binding was estimated to be -13.7 kcal/mol based on the reported K_d value (Green, Jellinek et al. 1996). Therefore, given the typical caveats that apply to secondary structure prediction in nucleic acids (failure to assess pseudoknots and tertiary structural interactions; assessment of individual structures rather than structural ensembles) the energy of protein-binding should be more than sufficient to substantially alter the conformational equilibrium.

To confirm that circularization occurs, ligation products were separated on a denaturing gel. There was significantly more circular product in the presence of PDGF-BB than in its absence (Figure 3-4, lanes 1 and 2). In addition, the aptamer was treated in either the absence or presence of PDGF and T4 DNA ligase followed by exonuclease VII digestion. Unligated, single-stranded, aptamers should be digested, while the rearranged, circularized conformers should not be digested (Figure 3-4, lanes 3 and 4). In fact, a circular, ligated aptamer is seen in the presence of PDGF and remains following exonuclease digestion.

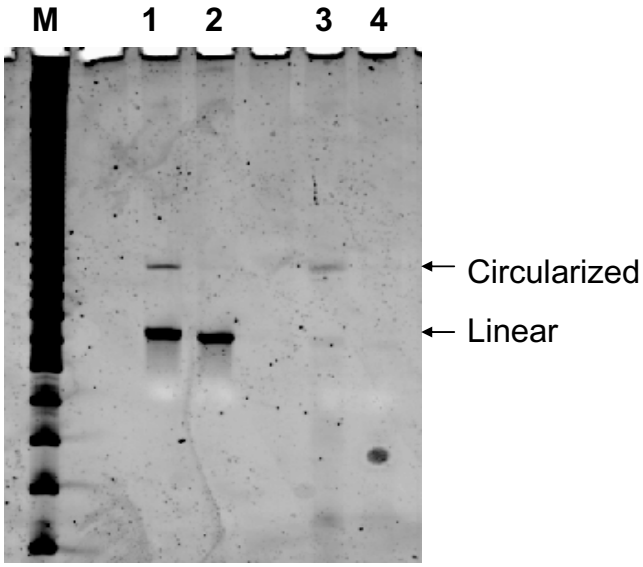

Figure 3-4. Circularization of the conformation-switching aptamer N5C1. Ligation reactions were carried out in the presence (Lanes 1, 3) and absence of PDGF (Lanes 2, 4), and treated with exonuclease VII (Lanes 3, 4). Samples were separated on a denaturing 8 % polyacrylamide gel and stained with SYBR Gold. M represents 10 bp DNA ladder. Arrows show the linear and circularized aptamers.

Real-time amplification of analyte-mediated aptamer circularization

In order to determine whether the observed, analyte-mediated circularization could be detected by RCA, we again used gel assays to examine the amplification product. Following ligation, RCA was carried out within one hour. The amplification products were very high molecular weight DNA that could not enter a denaturing polyacrylamide gel (data not shown).

To initiate RCA, aliquots of terminated ligation reactions were mixed with RCA primers that bound within an unstructured portion of the 5' extension (Figure 3-3). In order to amplify and quantitate circularized products in real time, a probe oligonucleotide that was identical to an unstructured portion of the 3' extension (Figure 3-3) was also included in the reaction. The probe could bind to the RCA product and the double-stranded DNA could in turn be detected with SYBR Green. In order to improve assay reproducibility the T4 gene 32 protein was included. This single-stranded DNA binding protein has previously been used in a variety of RCA assays to help melt double-stranded structures that can block polymerization (Lizardi, Huang et al. 1998; Qi, Bakht et al. 2001).

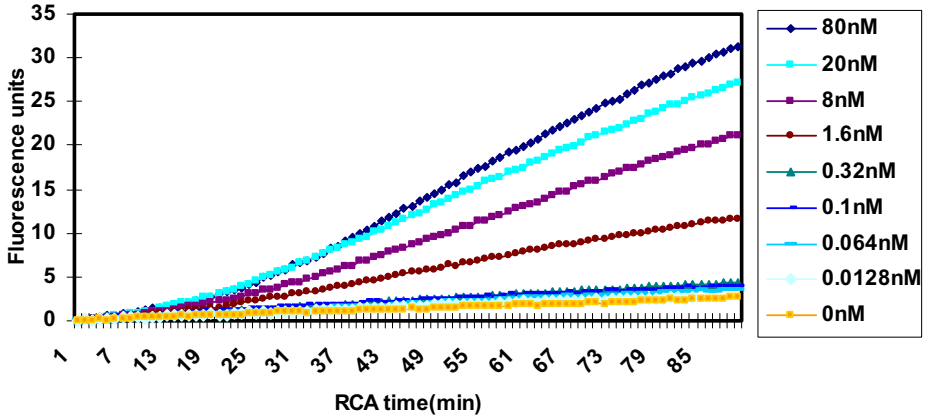

Figure 3-5. Real-time RCA detection of PDGF. Arbitrary fluorescence units were collected based on SYBR Green intercalation into concatamer-probe duplexes and collection via a HT7900 real-time PCR instrument (ABI) at a variety of protein concentrations.

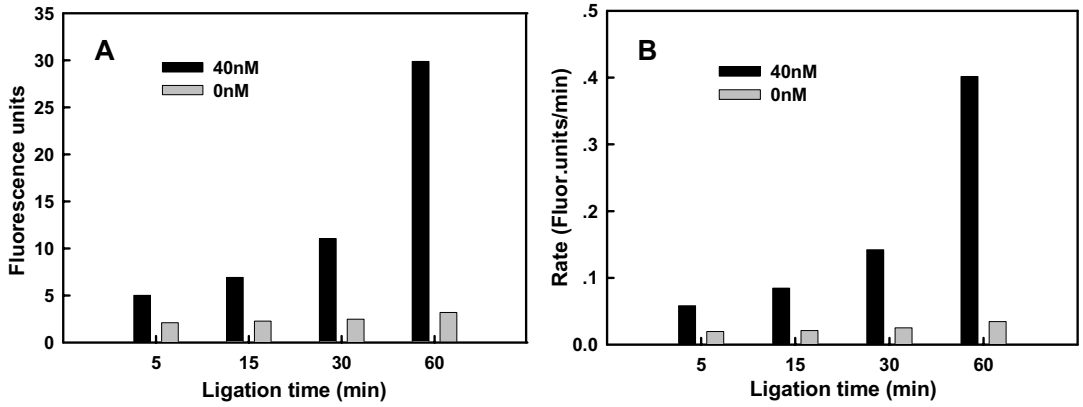

Figure 3-6. Detection as a function of ligation time. Ligation reactions were carried out in the presence (black bars) or absence (grey bars) of 40 nM PDGF-BB and then detected via real-time RCA. Signals were determined either based on (A) fluorescence endpoint values after 90 min, or (B) amplification rates (obtained from the linear regressions of data collected from 20-90 min, see Figure 3-5).

Ligation reactions containing 40 nM PDGF-BB were initially carried out within 60 min, and real-time RCA was then monitored over 90 min (Figure 3-6). The addition of probe was necessary to see robust fluorescent signals (data not shown). In order to keep protein concentrations uniform and to avoid loss of analyte, PDGF-BB was diluted into BSA that was at a final concentration of 0.004 % in this and all other experiments. Initial results with 40 nM PDGF-BB revealed protein-dependent signals at all of the ligation timepoints assayed (Figure 3-6). However, a maximal signal-to-background ratio was achieved after ligation reactions had proceeded for one hour. It is noteworthy that background signal did not seem to accumulate over time. Indeed, the fact that reproducible signals could be observed at ligation timepoints as short as 5 minutes bodes well for the further development of high-throughput diagnostic assays. Nonetheless, for the purposes of methods development all additional experiments were carried out using a one hour ligation time.

Using these standard assay procedures, RCA signals were monitored as a function of time at a variety of protein concentrations (Figure 3-5). PDGF-BB concentration as low as 1.6 nM could be readily detected. The RCA reaction was roughly linear over time and because of this it proved possible to generate standard curves for detection (Figure 3-7). Irrespective of whether the end point (90 min) of the RCA (Figure 3-7A) or the rate of accumulation of product (Figure 3-7B; obtained from the linear regressions of data collected from 20-90 min, see Figure 3-5) was used, the assay demonstrated good responsivity between low concentration of PDGF-BB and 80 nM PDGF-BB. The black line in these dose-dependent curves represents the best fit using 3-parameter Hill equations (SigmaPlot, SPSS).

The detection limits (1.6 nM) observed in our assay were similar to those observed with other detection methods involving the anti-PDGF aptamer, including an

aptamer beacon developed by Tan's group (Fang, Sen et al. 2003; Vicens, Sen et al. 2005), fluorescence anisotropy (Fang, Cao et al. 2001), a colorimetric determination technique using aptamer-modified gold nanoparticles (Huang, Huang et al. 2005), a luminescence detection strategy (Jiang, Fang et al. 2004), and an exciton detection strategy (Yang, Jockusch et al. 2005). The similarity between the detection limits is not surprising, since in each instance detection is ultimately limited by the binding affinity (Green, Jellinek et al. 1996) of the aptamer itself. As even higher affinity aptamers are developed, it seems possible that the amplification methods that we have developed here may yield even lower detection limits, as our conformation-switching aptamers are not labeled and hence there is no initial background fluorescence.

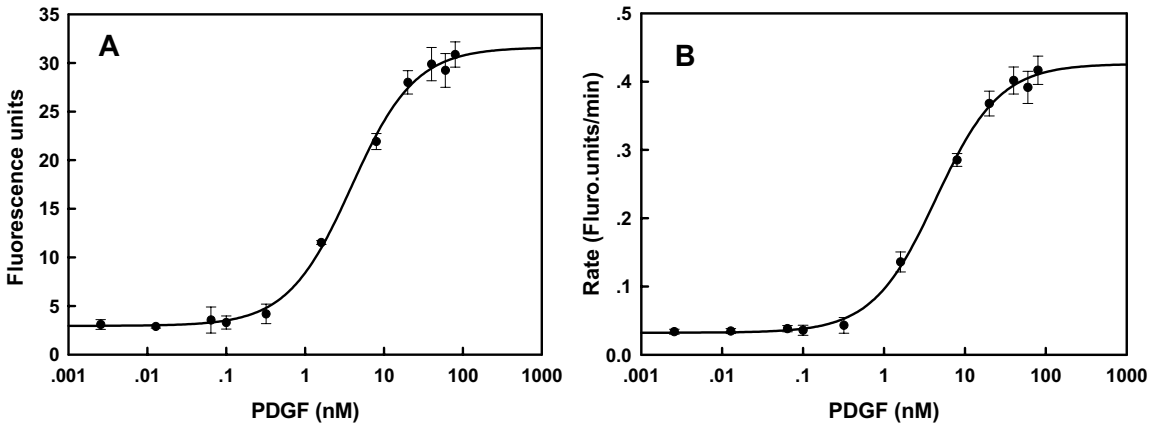

Figure 3-7. Dose-response curves for real-time RCA. Signal was determined as a function of protein concentration based on either (A) fluorescence endpoint values after 90 min, or (B) amplification rates. The black lines represent the best fit to the Hill equation: $y = y_0 + ax^b / \left(c^b + x^b\right)$ using SigmaPlot (SPSS, Chicago, IL).

Indeed, our results were extremely encouraging for the generality of the method, since it can be expected that at least some of the binding energy of the original aptamer was transduced into conformational change in the engineered aptamer, and thus the K_d value of the engineered aptamer was likely higher than 0.1 nM. Previous attempts to engineer conformational changes in aptamers have shown reductions in binding affinity. For example, conformation-switching aptamer beacons for thrombin and ATP showed apparent decreases in affinities for thrombin and ATP of 2- and 60-fold, respectively (Nutiu and Li 2003). It is precisely because binding energy is of necessity transduced into conformational change and potentially reduced sensitivity that we believe it is important to couple conformation-switching aptamers to signal amplification methods.

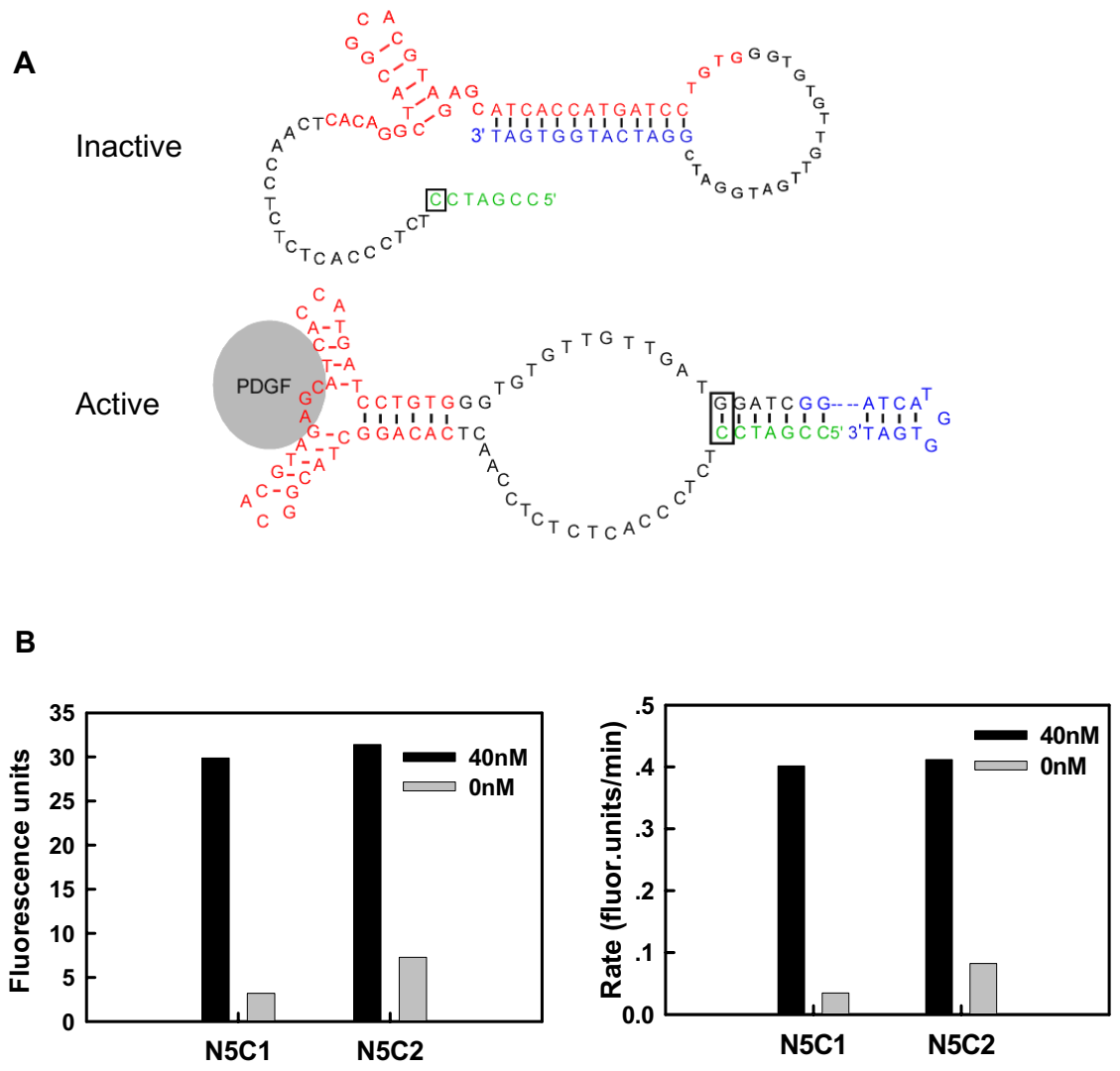

Figure 3-8. Altering signal by altering aptamer sequence. (A) Design of NC52. Based on N5C1 (Figure 3-3B) we made N5C2, which has one more basepair at the 5' end of the ligation junction (boxed). (B) RCA assay of NC52. Signal was determined as in Figure 3-6 for either the parental aptamer (N5C1) or another designed construct (N5C2).

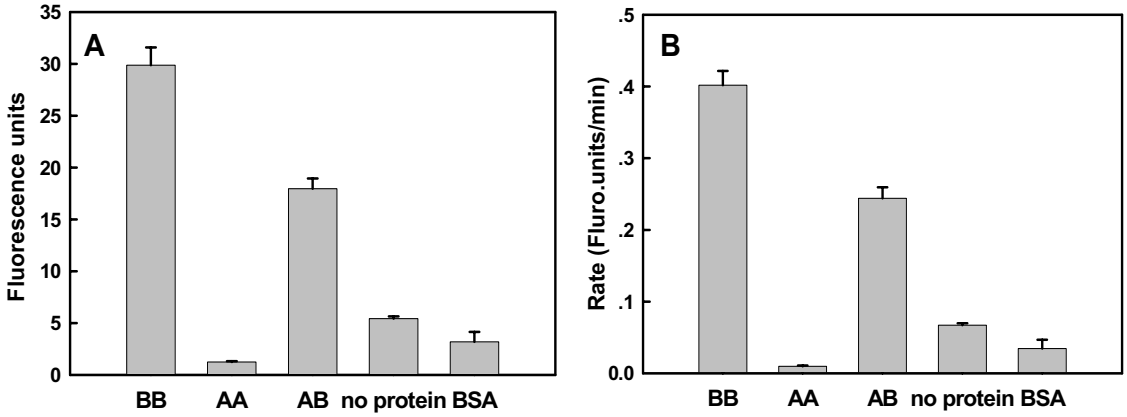

Figure 3-9. Specificity of response. Reactions were carried out and analyzed as in Figure 3-6, except that either 40 nM PDGF-AA, -AB, or -BB were used. In addition, negative controls were carried out in the absence of protein or in the presence of BSA (0.004 %).

While it is significant that our designed construct could detect nanomolar levels of protein in a simple RCA assay format, additional changes in the sequence of the engineered aptamer may lead to improved responsivities and sensitivities. While we attempted to ensure that the primer and probe binding sites were largely unstructured, further destabilization of any nascent intramolecular secondary structures should further encourage the initiation of RCA and the accumulation of signal. More importantly, manipulating the number and type of basepairs in the unbound, inactive and/or bound, active conformers should differentially influence the free energies of folding for these states, and hence should influence the relative levels of background and protein-dependent circularization and signal that are observed. As an initial test of this hypothesis, we added a single basepair to the active conformer (aptamer N5C2; Figure 3-8A). While the overall design still worked and yielded a PDGF-dependent real-time RCA signal, the background observed was higher, and the overall level of activation for N5C2

was roughly half that determined in parallel with N5C1 (4.3 (endpoint) and 5 (rate) for N5C2, versus 9.3 (endpoint) and 12 (rate) for N5C1) (Figure 3-8B). These results suggest that it should be possible to further optimize the performance of engineered aptamers for analyte-mediated circularization and RCA, and we are currently attempting to determine how designed sequences, computational structure predictions, and signaling function correlate with one another. These efforts will be enhanced by the fact that the antisense sequences in our design can fold into a hairpin stem. By manipulating the sequence and length of this hairpin, we should be able to better poise the conformation-switching aptamer between binding and non-binding conformations. Selection experiments can also be carried out to identify optimum sequences for folding transitions and RCA, and may further increase the sensitivity of the assay.

The specificity of the designed aptamer biosensor was assayed using different dimeric isoforms of PDGF: PDGF-AB and AA (Figure 3-9). Signals were seen with both PDGF-BB and PDGF-AB, but not with PDGF-AA, as was expected given that the aptamer was originally selected to bind to the B-chain. The signal with PDGF-BB was greater than the signal with PDGF-AB, as has previously been observed by others (Fang, Cao et al. 2001; Fang, Sen et al. 2003; Yang, Jockusch et al. 2005; Zhou, Jiang et al. 2006). Interestingly, the addition of either PDGF-AA or BSA slightly suppressed the background signal observed in the absence of protein, possibly by competing with DNA ligase for non-specific binding to the aptamer.

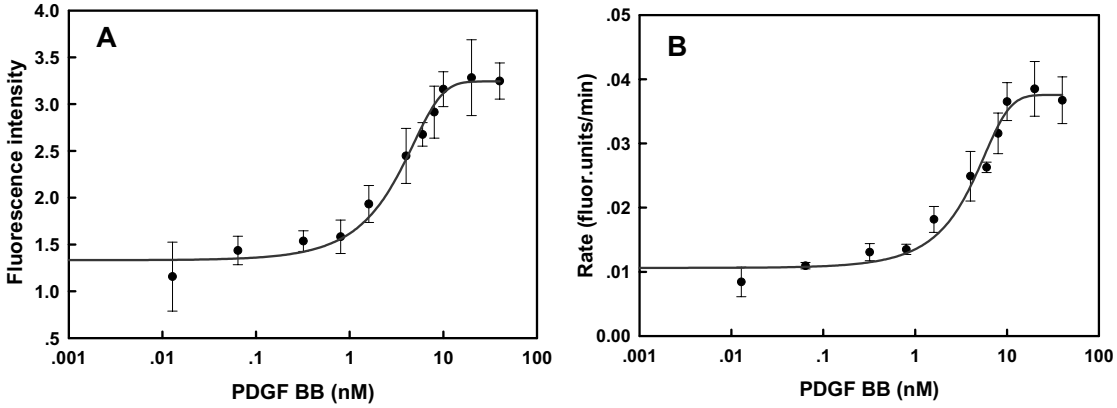

Figure 3-10. PDGF detection against a background of cell lysate. Signal was determined as in Figure 3-7, except that ligation reactions were carried out in 10 µg/mL human 293T fibroblast cell lysate. Signal was determined as a function of protein concentration based on either (A) fluorescence endpoint values after 90 min, or (B) amplification rates. The black lines represent the best fit to the Sigmoid equation: $y = a/\left(1 + e^{-(x/b - z_0/b)}\right)$ using SigmaPlot.

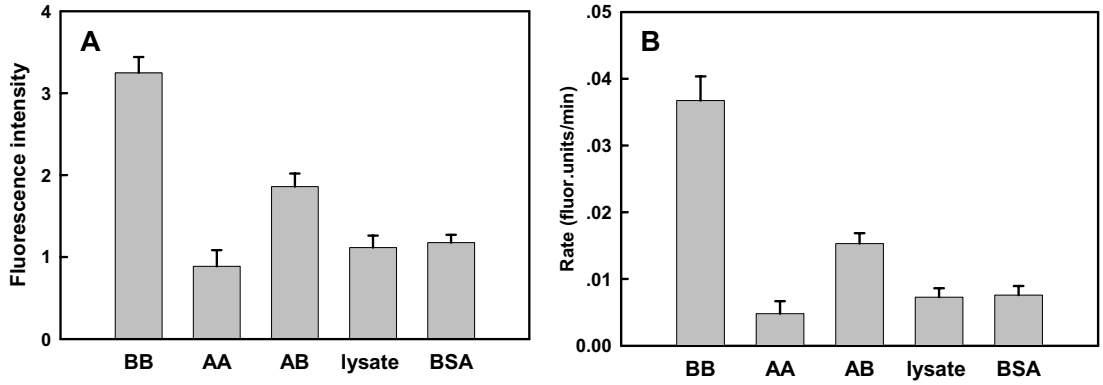

Figure 3-11. Specificity of response in a background of cell lysate. Reactions were carried out and analyzed as in Figures 3-6 and 3-9. Negative controls included lysate with no additions ('lysate') or lysate + 0.004 % BSA ('BSA').

Real-time RCA detection of PDGF against a background of cell lysate

Real-time RCA experiments were repeated in a manner similar to that described above, except that PDGF at different concentrations was doped into human 293T fibroblast cell lysate (final total protein concentration of 10 μg/mL). As before, the total sample reaction time prior to amplification was only 1.5 hours, and real-time amplification was monitored over 90 minutes. As shown in Figure 3-10, even though the reaction mix now contained multiple proteins and nucleic acids the structure-switching aptamer coupled with real-time RCA once again yielded dose-response curves for PDGF-BB that were qualitatively similar to those previously observed (Figure 3-7). The rate of amplification was lower than in the absence of lysate, which may be explained by the presence of interfering degradative enzymes, enzyme inhibitors, or contaminating nucleic acids. Further optimization of the reaction for clinical samples should further improve responsivity. Nonetheless, very little response was observed in the absence of introduced PDGF, consistent with the lack of this cytokine inside of cells (as opposed to in serum), and PDGF concentrations as low as 1.6 nM could still be detected though the lysate proteins were in 1,000-fold (w/w) excess. These results were especially remarkable given that the mixture spent 90 minutes prior to real-time RCA in the presence of active nucleases. Once again, the assay showed very high specificity for the PDGF-BB and -AB dimers as opposed to PDGF-AA or other unrelated proteins (Figure 3-11). PDGF levels in human serum have been found to be 14.4-24.8 ng/mL, which is equivalent to subnanomolar concentrations (Singh, Chaikin et al. 1982; Bowen-Pope, Malpass et al. 1984). The sensitivities observed with our method are very similar to these physiological levels. In addition, PDGF levels have been reported to be elevated in many diseased tissues (Green, Jellinek et al. 1996). Therefore, with further optimization our detection method may prove to be feasible for PDGF detection in clinical samples.

Chip-based RCA assay

We have previously used aptazymes and chip-based RCA to detect ATP in Chapter 2 (Cho, Yang et al. 2005). It should also be possible to use conformation-switching aptamers in a similar manner. The RCA primer was conjugated to biotin either via a C3 spacer phosphoramidite or a dT residue at its 5' end (Figure 3-12). The modified primers were immobilized on streptavidin-coated glass slides. A mixture of analyte-mediated ligated circles and components of a RCA reaction (polymerase, dNTPs) was incubated with the primer array for 30 min at 37^{o} C. The concatamer products were then hybridized with a Cy3-labeled probe.

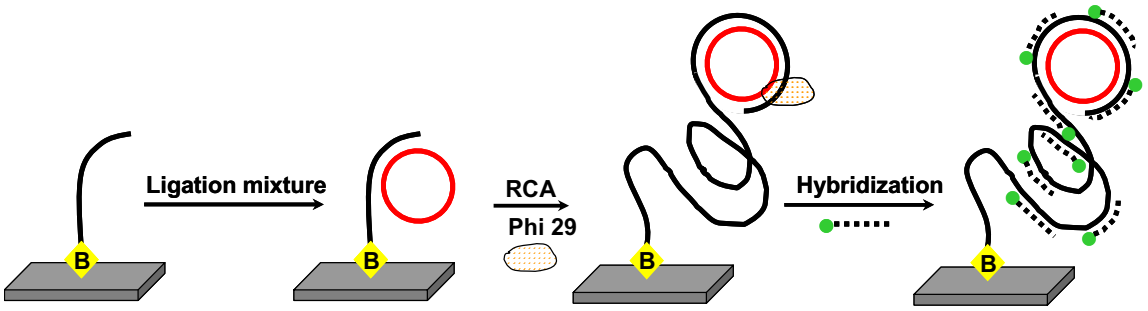

Figure 3-12. PDGF-mediated RCA on a chip array. A primer labeled with biotin at its 5' end was immobilized on a streptavidin-coated glass slide. Terminated ligation reactions containing circularized aptamers (red) and RCA reagents were applied to the chip, and RCA was initiated from the 3' end of the immobilized primer. Elongated concatamers were visualized by hybridization with Cy3-labeled oligonucleotide probes (green).

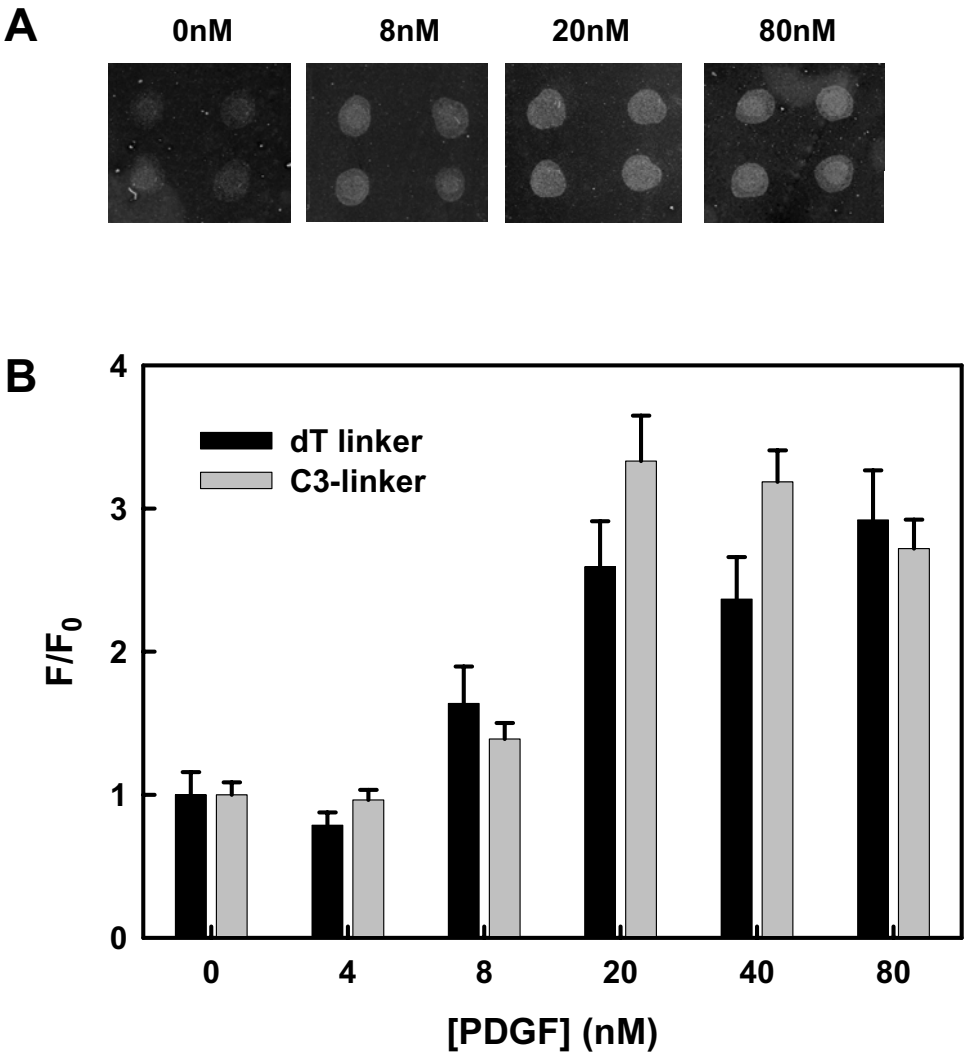

Figure 3-13. Detection of PDGF via RCA on a chip array. (A) Fluorescence images acquired with an Axon Instruments 4000B confocal microarray scanner in the presence of 0, 8, 20, and 80 nM PDGF-BB. (B) Amplified signal at a series of PDGF concentrations using primers with either a biotin-C3-linker or primers with a biotin-dT-linker.

The detection of PDGF-BB in three replicate experiments is shown in Figure 11. While there is some background that prevents detection at the lowest concentration assayed (4 nM), analyte-dependent amplification can be readily observed on the chip at 8 nM (Figure 3-13A), and signal saturates at higher (> 20 nM) PDGF concentrations (Figure 3-13B). There was no significant difference between results obtained with the two types of linkers. Signal saturation may have been due to either the completed production of DNA concatamers or to fluorescence self-quenching of the saturated spots. The combination of high background and signal saturation in the end point assay limited sensitivity relative to the real-time assay (compare with Figure 3-5), and further emphasizes the current superiority of real-time assays for protein detection.

Nonetheless, it should eventually be possible to use structure-switching aptamers or aptazymes and chip-based RCA assays for quantitation. Chip-based RCA assays have previously been used to quantitate both DNA and protein molecules (Nallur, Luo et al. 2001; Schweitzer, Roberts et al. 2002). An immunoRCA assay reported by Schweitzer *et al.* yielded a dose-response curve over a greater range of IgE concentrations than a corresponding ELISA assay; the sensitivity of detection was two orders of magnitude greater (Schweitzer, Wiltshire et al. 2000). ImmunoRCA can also be used to profile the expression of many different proteins from cell lysates in a high-throughput manner, although purified proteins had to be used as quantitation standards (Schweitzer, Roberts et al. 2002). However, in general there are relatively few examples of quantitative, chip-based RCA (Nallur, Luo et al. 2001; Schweitzer, Roberts et al. 2002) and chip-based RCA does not have sensitivites as good as those of ELISA assays (Kingsmore and Patel 2003). The reasons are likely similar to those we have cited above, that in chip-based methods background accumulation of RCA products can be quite high.

Overall, in order to fully develop quantitative RCA methods it may be much better to use real-time rather than chip-based methods. However, it is generally difficult to develop immunoRCA methods that can be analyzed in real time, largely because unbound antibodies must be removed prior to amplification. Conformation-switching aptamers and aptazymes that can form circular templates upon addition of protein analytes are one of the few methods that may be compatible with performing real-time protein detection with RCA. Similarly, Di Giusto *et al.* have developed a proximity method in which a circular template and a primer are brought together by a protein intermediary (thrombin) (Di Giusto, Wlassoff et al. 2005). However, this method requires the identification of affinity reagents that bind to two different epitopes on a protein surface, similar to a sandwich assay. While the real-time RCA assay reported here is somewhat less sensitive (0.4 nM versus 0.03 nM), the conformation switching aptamers recognize only a single epitope. Moreover, binding, ligation, and amplification can potentially all occur in the same reaction mixture, and one-step real-time RCA reactions may be possible.

CONCLUSIONS

While conformation-switching aptamers have previously been used as biosensors, the methods that have previously been pursued were not in general of use for adapting aptamers to real-time nucleic acid amplification methods. Therefore, we designed a conformation-switching aptamer that could assume a circular conformation in the presence of a protein analyte, PDGF, and subsequently ligated with T4 DNA ligase. This allowed the specific detection of PDGF by real-time RCA, at concentrations down to 1 nM or better. Detection did not suffer from the addition of other proteins or even cell lysate. While the conformation-switching aptamer could also be adapted to surfaces, it

proved difficult to quantitate RCA on a chip, further emphasizing the importance of real-time amplification methods for sensitive analyte quantitation. While nucleic acid and other affinity reagents have previously been adapted to real-time methods using proximity methods (i.e., the proximity ligation assay, PLA) these methods all require two different aptamers or other affinity reagents. In contrast, almost any single aptamer can be adapted to the conformation-switching, circularizing format described, and this demonstration should therefore facilitate a more general use of real-time nucleic acid amplification methods for the detection of proteins.

FUTURE PLANS

Future plans of analyte-dependent aptamer circularization followed by real-time RCA could focus on both improvement of current detections and applications for other analyte detections.

Though our method could sensitively detect PDGF both in solution and cell lysate, the detection could be further improved by both rational design and *in vitro* selections. The linker regions connecting ligation junction and the aptamer, lengths and sequences in the ligation junction, and number and bases in the antisense sequences could all be optimized. Using computational design, folding energies of the inactive, non-binding conformer and the active, binding conformer could be calculated. Therefore, the analyte-dependent ligation activities of designed constructs could be predicted. However, rational design may not be able to perfectly predict the behavior of any sequences and structures. Therefore, in combination of *in vitro* selection, the generation of better constructs could be more possible.

On the other hand, our method should be generalizable to other analyte detections. DNA aptamers for both small molecule and protein detections could be adapted to our

methods. For example, aptamers for the detections of thrombin (Bock, Griffin et al. 1992), IgE (Wiegand, Williams et al. 1996) and ricin (Tang, Xie et al. 2006) could be adapted. However, for protein detections, the lengths of the linker regions separating aptamer binding and ligation junction need to optimize and aptamers of such lengths may not be synthesized. Therefore, ligating two ssDNAs may be a good way to generate the full length the padlock aptamer. In contrast, for the adaption of small molecule binding aptamer such as the anti-cocaine aptamer (Stojanovic, de Prada et al. 2001), the length of the aptamer may not be a big issue.

In all, both optimization and generalizability of this strategy are worthy being explored in the future.

MATERIALS AND METHODS

Materials

The following oligonucleotides were purchased from IDT (Coralville, IA). The circularizing aptamers N5C0, N5C1 and N5C2 (sequences shown in Figure 3-1, 3-3 and 3-8) had phosphates at their 5'-ends. The primer, biotin-dT-primer, and biotin-C3-primer for RCA all shared the same sequence (5'-AGTTGGAGAGAGTGGGAG). The sequence of both real-time and 5'-Cy3-labeled RCA probes was 5'-GGTGTGTTGTTGATG. PDGF-BB, -AA, and -AB were purchased from R&D Systems (Minneapolis, MN). The PDGF proteins were reconstituted in 4 mM HCL with 0.2 % BSA (Invitrogen, Carlsbad, CA), as suggested by the supplier.

Ligation assays

Preligation mixtures (46.5 μL) contained 40 nM N5C1, 137 mM NaCl, 10.1 mM Na_2HPO_4, 1.8 mM KH_2PO4, pH 7.4, 2.7 mM KCl, 10 mM Tris-Cl, pH 7.4, and 2.5 mM $MgCl_2$. The reaction mixture was incubated with PDGF-BB for 30 min, and then 1.5 μL of 25 mM ATP and 1 μL of T4 DNA ligase (2 units/ μL, Epicentre, Madison, WI) were added separately. Ligation proceeded for various times at room temperature (see Figure 2-6) and were terminated by heating at 95 °C for 15 min. Ligated and unligated species were separated on denaturing (7 M urea) 8 % polyacrylamide gels and stained with SYBR Gold (Molecular Probes, Eugene, OR).

To carry out assays in lysate, $1x10^7$ human 293T fibroblast cells (ATCC, Manassas, VA) were collected. Cells were treated with 4 mL of M-PER mammalian protein extraction reagent (Pierce Biotechnology, Rockford, IL) and shaken at room temperature for 10 min. After centrifugation at 10,000 rpm at 4 °C for 25 min, pellets containing cell membranes and hydrophobic membrane proteins were removed, and the supernatant consisting of intracellular proteins and nucleic acids was collected and frozen at -80 °C. Total protein in lysate aliquots was quantitated using a bicinchoninic acid total protein assay kit (Pierce Biotechnology). The final concentration of lysate proteins in each 50-μL ligation reaction mixture was 10 μg/mL, and PDGF at different concentrations was added the lysates. PDGF samples were always in 0.004 % BSA; irrespective of PDGF concentration, BSA was always in excess. Ligation reactions were then carried out as described above.

Real-time RCA measurements

The primer and probe for RCA were denatured at 95 °C and then cooled to room temperature. The primer (final concentration 0.3 μM) and probe (final concentration 1.3

μM) were added to the RCA reaction mixture containing 1x phi29 reaction buffer (40 mM Tris-HCl pH 7.5, 50 mM KCl, 10 mM $MgCl_2$, 5 mM $(NH4)_2SO_4$, and 4 mM DTT), 416 μM dNTPs (Epicentre), 1.5 μL of SYBR Green I (1: 2000 dilution of a 10,000x solution as described by the manufacturer; Cambrex, Rockland, MI), 3 units of phi 29 DNA polymerase (Epicentre) and 66.7 ng/μL T4 gene-32 protein (Ambion, Austin, TX), all in a 30- μL total volume. Finally, 4 μL of each terminated ligation mixture was added right before starting the real-time RCA reaction. Real-time RCA was carried out in a 96-well PCR plate (Applied Biosystems (ABI), Foster City, CA) covered with optical strip caps (ABI) at 37 °C for 90 min. Fluorescence accumulation was monitored in the green channel in an HT7900 real-time PCR instrument (ABI).

RCA on a chip

Primers were immobilized on glass slides for RCA assays. A solution of 500 nM biotin-C3-primer or biotindT-primer in Tris buffer (50 mM Tris-HCl, pH 7.4) containing 5 % glycerol was heat denatured at 70 ^oC for 3 min and then cooled to room temperature before printing. The primers were printed onto streptavidin-coated glass slides (Pierce Biotechnology) using a manual arrayer (V&P Scientific, Inc., San Diego, CA) as previously published in Cho *et al*. (Cho, Yang, et al., 2004). The slides were incubated within a humidity chamber for 1 h after printing to allow conjugation of biotinylated oligonucleotides to streptavidin. The printed area was enclosed within a CoverWell incubation chamber (Schleicher and Schuell, Keene, NH), and 1 mL of Tris buffer containing 0.05 % (v/v) Tween 20 was pipetted into each chamber through access ports. Each chamber was then incubated with 70 μL of RCA mixture (40 mM Tris-HCl pH 7.5, 50 mM KCl, 10 mM $MgCl_2$, 5 mM $(NH_4)_2SO_4$, 4 mM DTT, and 10 μL of terminated

ligation mixture) at 37 °C for 30 min. The RCA reaction was terminated by washing the chamber with 1 mL of 2x SSC (300 mM sodium chloride and 30 mM sodium citrate, pH 7.4) buffer containing 0.05 % Tween 20. Cy3-labeled probe in 2x SSC with 0.05 % Tween 20 was hybridized to RCA products at 37 °C for 30 min. Slides were washed twice with 2x SSC with 0.05 % Tween 20 solution, twice with 1x SSC with 0.05 % Tween 20 solution, and once with 0.5x SSC. Slides were dried by immediate centrifugation and scanned on an Axon Instruments (Union City, CA) 4000B confocal microarray scanner. Images were analyzed using GenePix 4.1 software (Axon Instruments).

Chapter 4: Detection of protein analyte using aptamer mediated three- and four-piece ligation systems followed by real-time PCR

INTRODUCTION

ImmunoPCR methods can be used for the sensitive detection of protein analytes (Adler 2005; Niemeyer, Adler et al. 2005; Barletta 2006), but have several distinct disadvantages relative to PCR for the detection of nucleic acids. It is difficult to reproducibly prepare antibody-DNA conjugates, binding and amplification reactions must be separated in time, preventing the development of real-time formats; and both specifically and non-specifically bound probes can be amplified, potentially leading to high background signals.

In order to better couple protein detection with nucleic acid amplification, nucleic acid binding species (aptamers) have been adapted to a variety of amplification assays, including exonuclease-protection mediated ligation followed by PCR (Wang, Li et al. 2005); and proximity extension by rolling circle amplification (RCA) (Di Giusto, Wlassoff et al. 2005; Soderberg, Gullberg et al. 2006). Aptamers have also been used for the generation of allosteric ribozymes (aptazymes) that have similarly been coupled to amplification reactions (Robertson and Ellington 2001; Cho, Yang et al. 2005).

Proximity ligation assay (PLA) is the focus of current PCR based detection. In this case, oligonucleotide probes are attached to the binders (either aptamer or antibody) (Fredriksson, Gullberg et al. 2002; Gullberg, Gustafsdottir et al. 2004; Gustafsdottir, Schallmeiner et al. 2005; Gustafsdottir, Nordengrahn et al. 2006; Schallmeiner, Oksanen et al. 2007). The probes are brought adjacently by at least two epitopes binding to the antibodies or aptamers on the analyte. Fredriksson *et al.* (2002) could detect zeptomole

PDGF through proximity DNA ligation followed by PCR. PLA has also been carried out for oligonucleotide circularization followed by RCA (Soderberg, Gullberg et al. 2006).

However, proximity based ligation requires multi-meric analyte or at least two binders recognizing different epitops on the analyte. Such disadvantage limits the generazliability of this assay. Therefore, a generalizable method capable of sensitive and specific detection needs to be developed.

We and others have previously reported that aptamers can be engineered so as to transduce the binding energy of ligands into changes in aptamer conformations. The resultant analyte dependent folding of aptamers have been used to optically signal the presence of ligands in solution (Stojanovic, Prada et al. 2000; Yamamoto, Baba et al. 2000; Hamaguchi, Ellington et al. 2001; Stojanovic, de Prada et al. 2001; Li, Fang et al. 2002). For example, an anti-thrombin aptamer that formed a quadruplex structure was extended so that it folded into a non-binding, stem-loop structure. A fluoropore and a quencher were placed at the termini of the non-binding stem-loop. Upon the addition of thrombin, the original quadruplex structure was stabilized, splitting apart the fluorophore and quencher, and yielding a fluorescent signal (Hamaguchi, Ellington et al. 2001). Thrombin could be detected in the nanomolar range, and no fluorescent signal was generated in with other, non-cognate proteases.

The key feature of structure-switching aptamer technology (Nutiu and Li 2003; Bayer and Smolke 2005) is that it is generalizable to any kind of aptamers without knowing the aptamers' secondary or tertiary structures. The main strategy is to use antisense oligonucleotide either *in trans* or *in cis* to form a duplex with the aptamer and oligonucleotide displacement occurs when analyte binding. When the aptamer and antisense oligonucleotide are fluorescently labeled, oligonucleotide displacement results in separation of the fluorophore and quencher (Nutiu and Li 2003) (Figure 4-1). In

another case, the displaced antisense oligonucleotide controls target expression by hybridization with the 5' UTR of the mRNA (Bayer and Smolke 2005). Similarly, structure-switching aptamers have also been adapted to electronic (Xiao, Piorek et al. 2005) and nanoparticle sensors (Levy, Cater et al. 2005; Liu and Lu 2005).

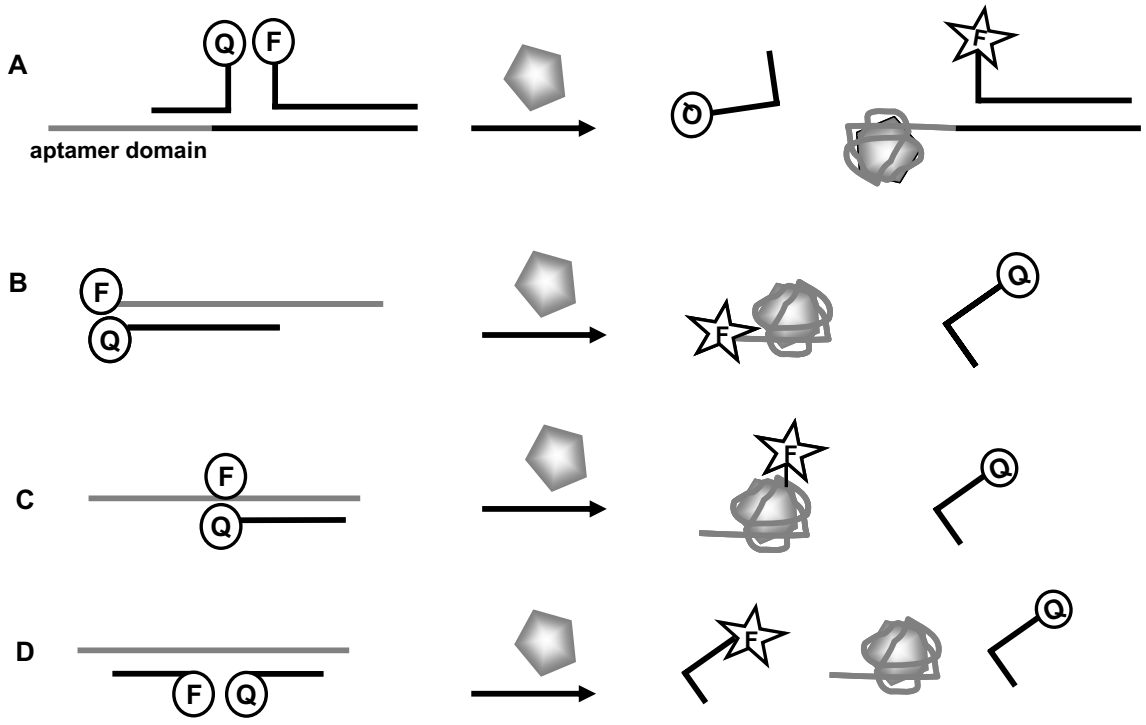

Figure 4-1. Mechanism of antisense-mediated, structure-switching aptamers. Tripartite (A, D) and bipartite (B, C) quenched systems are designed based on aptamer and antisense sequences. Upon ligand binding, the equilibrium between the aptamer and the complementary antisense strand is shifted, and the complex is disrupted, resulting in dequenching of either a terminal or internal incorporated fluorophore.

By far, no approach has been developed to adapt structure-switching aptamers to PCR amplification. Probably it is not obvious how to generate amplicons. A variety of configurations for coupling aptamer conformational changes to PCR can be envisioned,

but the most likely would be either to have aptamer conformational changes lead to the production of a template for PCR or a primer for PCR. The production of a PCR template would likely lead to greater sensitivity of detection, since conformational transduction to produce even a single template should lead to amplification, while multiple primers would have to change conformation in order to support an amplification reaction. However, a PCR template that was only amplified in one conformation would also likely lead to an inherently high background signal, since conformational equilibration even in the absence of analyte would lead to at least some template being available at all times, especially during thermal cycling and in the presence of a DNA polymerase that could read through restrictive conformations.

Therefore, we decided to reduce background by requiring a ligation step to produce competent templates for PCR amplification. As we mentioned above, structure-switching aptamers usually involves oligonucleotide displacement. So the switch between double stranded and single stranded nucleic acid would allow the design of the ligation junction. In this way, the ligation reaction can be separately optimized to reduce background and no further ligation should occur during thermal cycling. Most importantly, the ligation reaction can be directly coupled with a real-time PCR without additional wash or other steps.

Inspired by the antisense strategy developed by Nutiu and Li (Figure 4-1; Nutiu and Li, 2003), we now propose to adapt such strategy to generate analyte-dependent product for real-time PCR. In the presence of analyte, the antisense oligonucleotide is displaced by analyte binding and changes into a signal stranded DNA, which will be used to construct the ligation junction. In our previous experience, we found that the ligation junction and the protein analyte binding site should be well separated to prevent steric hindrance (data not shown). To separate ligation junction and aptamer binding site,

similar to those designed by Nutiu and Li, we decide to have aptamer and antisense oligoncucleotide on separate molecules. Moreover, additional substrate oligonucleotides need to be designed to complete the ligation junction. Because the structure-switching aptamers usually have reduced affinities with their cognate analytes (Nutiu and Li, 2003), it will be important to determine if amplification could improve the sensitivity. In addition, our method will explore the possibility of using simple antisense methods to generally couple aptamers to ligation and signal amplification.

We have applied these methods to the anti-PDGF aptamers in part because of the detailed knowledge that is already available regarding its binding characteristics and structures, but also to more readily compare our results with other biosensor paradigms that have previously been advanced. We find that the three-piece ligation could sensitively and specifically detect PDGF, however long ligation time (8 hours) is required.

RESULTS AND DISCUSSION

Rational of the design

Previously, it has been shown oligonucleotide displacement coupled with fluorescence assay can be used for ATP and thrombin detection (Nutiu and Li 2003). However, fluorescence-based assays are not sensitive enough and have limitations such as enhanced background caused by impurity of dye-labeling, fluorescence quenching by improper environment and low detection signal due to single fluorophore labeling. Therefore, sensitivity and efficiency of the assay may be increased by creating aptamer biosensors that utilize nucleic acid amplification techniques. In order to adapt aptamer recognition of analytes to real-time PCR, we have designed an anti-PDGF aptamer

(Green, Jellinek et al. 1996) for protein dependent ligation based on an antisense strategy (Nutiu and Li 2003). First, we designed short oligonucleotides to test the feasibility of the PDGF activated aptamer ligation. Then, we optimized these oligonucleotide sequences for the purpose of real-time PCR. Finally, we developed ligation and real-time PCR assays and explored the specificity and sensitivity of the detections.

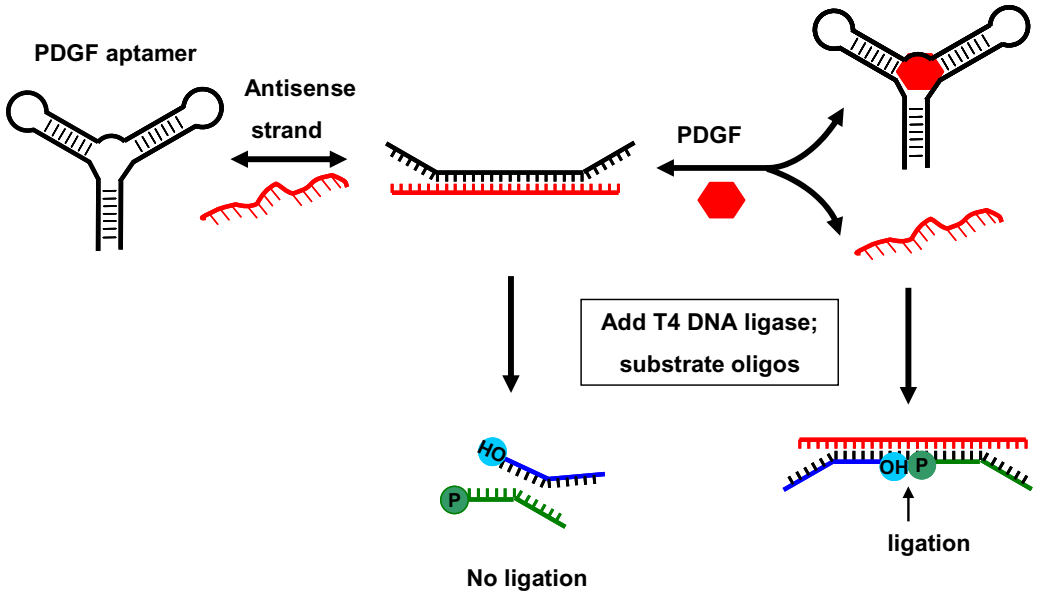

Figure 4-2. Schematic drawing of the strategy of four-piece ligation for analyte (PDGF) detection. In the absence of analyte, aptamer (black) forms a duplex structure with the antisense strand (red). Analyte binding displaces the antisense strand, which can serve as a template for two substrate oligonucleotides (blue and green) to be ligated by T4 DNA ligase.

T4 DNA ligase is usually the choice for specific ligation because its template dependent characteristics. It seals the nicks in double-stranded nucleic acids but can not ligate single-stranded nucleic acids. Therefore, the ligation junction was constructed by two oligonucleotide substrates hybridizing to a splint. As shown in Figure 4-1, in the presence of analyte the displaced antisense oligonucleotide is in free status in solution. Thus, the antisense oligonucleotide should be suitable to build the ligation junction.

However, the antisense strand could serve as either a ligation substrate or a splint. At this time point, we also concerned about the lengths of the antisense oligonucleotides. Previously, for ATP and thrombin detections, the duplex regions formed by the aptamers and the antisense strands were about 10-12 bp in lengths (Nutiu and Li 2003). The reason for such lengths is because in the absence of analyte the duplex needs to be stable under the assay temperatures (22-37 ^{o}C). In conjunction with ligation we proposed that the Tm values of the ligation junctions should be lower than those of the aptamer-antisense duplexes. Therefore, the lengths of the antisense sequences designed here might be even longer than those Nutiu and Li designed. On the other hand, we wanted to keep the minimal length of the ligation junction; for example, 6 basepairs at each side. So if the displaced strand is one of the substrates in the ligation junction, it is still possible that such antisense strand can bind to both ligation substrate and the aptamer simuteously. As a result, the background ligation level is high. Therefore, it would be better if the antisense strand serves as a splint for two substrate oligonucleotides (Figure 4-2).

Table 4-1. Oligonucleotides used in ligation assays.

Oligos	Sequences
aptamer	5'-CACAGGCTACGGCACGTAGAGCATCACCATGATCCTGTGGGTGTG-3'
11p	5'-TTTGATCGGATCATGGTG-3'
12p	5'-TTTGATCGGATCATGGTGA-3'
13p	5'-TTTGATCGGATCATGGTGAT-3'
14p	5'-TTTGATCGGATCATGGTGATG-3'
15p	5'-TTTGATCGGATCATGGTGATGC-3'
3'SUB	5'-TTTTTTTTCATGAT-3'
5'SUB	5'-pCCGATCTTTTTTTTT-3'

Based on these above concerns, complementary sequences to the anti-PDGF aptamer were designed to disrupt the binding conformation of the aptamer (Table 4-1, underlined sequences). These sequences start from the same 5' ends and have different lengths at their 3' ends. Also same sequences were added to the 5' ends of the antisense oligonucleotides to complete the templates for ligations (oligonucleotides: 11p-15p in Table 4-1). Two substrate oligonucleotides (5' SUB and 3' SUB) were also designed to form six basepairs at each side of the ligation junction, respectively (Figure 4-2). The Tm of the ligation duplex is 38.3 ^{o}C, which is lower than the Tm of the antisense duplex formed by 12p-15p with the aptamer (Tm= 40.1-48.7 ^{o}C). So in the absence of PDGF, the aptamer-antisense duplex should be more stable than the antisense-substrate duplex. Analyte binding promotes the formation of aptamer-analyte duplex and the release of the antisense strand to bind to substrates for ligation. However, if the antisense is one base shorter (underlined sequence of 11p) its Tm (37.0 ^{o}C) is lower than that of the splint. Therefore, 12p, 13p, 14p and 15p were chosen for further ligation assays (Figure 4-3).

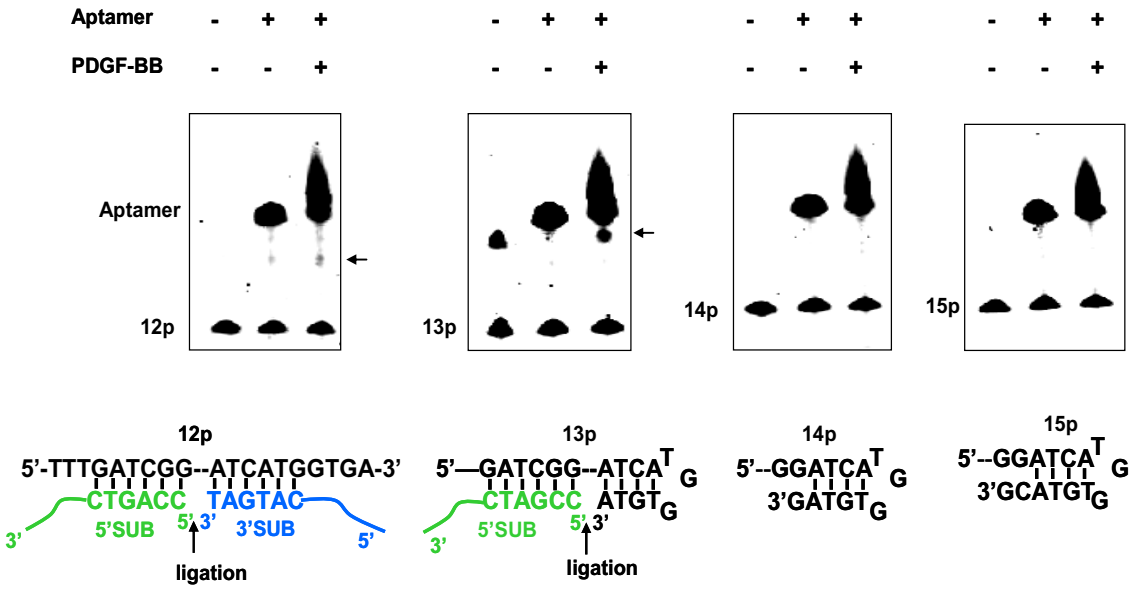

Figure 4-3. PDGF-activated ligation activities using short oligonucleotides. Ligations in the presence or absence of PDGF are carried out using 12p, 13p, 14p and 15p as splints, respectively. Also controls with only antisense strand and substrate oligonucleotides are used to monitor ligation ability. The predicted secondary structures are shown under the gel pictures. 12p serves as a splint for the ligation of two substrate oligonucleotides (5'SUB and 3'SUB). 13p forms half of the ligation junction and binds to 5'SUB. The short hairpins formed by 14p and 15p are unable to open up to bind to the substrate oligonucleotides. Arrows indicate the ligation product.

The proposed four-piece ligation system contains the anti-PDGF aptamer, antisense strand (12p-15p) and two substrate oligonucleotides (3'SUB and 5'SUB) (Figure 4-2). Before ligation, aptamers and the antisense strands were denatured together, followed by incubation with or without PDGF. Then substrate oligonucleotides, ATP and T4 DNA ligase were introduced in the pre-ligation mixture. In addition, ligation mixture without aptamer was prepared as a control. As shown in Figure 4-3 after incubation at 25 ^{o}C overnight, ligation signals were observed from reactions using 12p or 13p. In addition,

stronger ligation signals were seen in the presence of PDGF than those in the absence. Furthermore, controls without aptamer demonstrated the ligation product of the same size. However, assays using splints such as 14p and 15p did not show any ligation activity no matter PDGF was present or not, even for the controls without aptamer. It is very interesting that the ligation product using 13p was bigger than that of 12p, though they should be of the same size. By analyzing the secondary structure of these "splint" oligonucleotides, we found that 12p-15p may all form stable short hairpin structures, which were not expected because hairpin stem as short as four basepairs was not considered to be so stable previously. The short hairpins formed by 14p and 15p might be too stable to open up (Figure 4-3), therefore it is hard for them to hybridize with the substrates. The same thing occured for 13p, however, the hairpin formed by 13p may incidentally serve as half of the ligation junction (Figure 4-3). Consequently, 13p might be ligated to 5'SUB, resulting in bigger size ligation product than that obtained using 12p. On the contrary, the hairpin with three basepairs formed by 12p might be less stable, so 12p could serve as a template for the ligation of 3'SUB and 5'SUB.

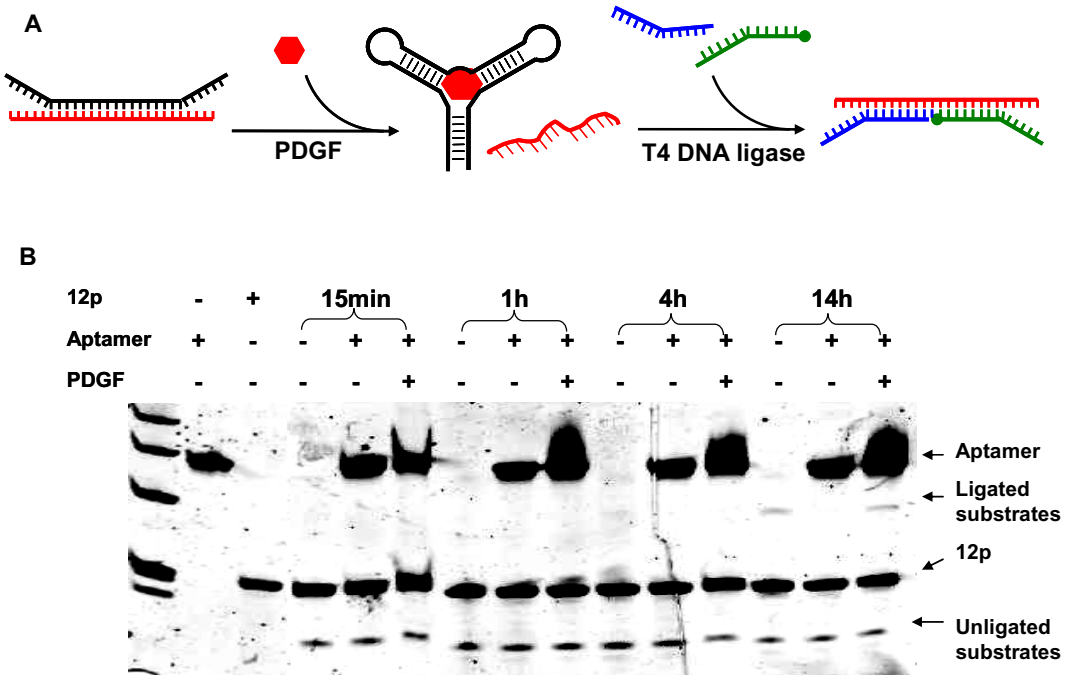

Figure 4-4. Time-course assay for the four-piece ligations using 12p. (A) Proposed ligation mechanism. (B) Ligation signals after incubation at 25 ^{o}C overnight. Ligated and unligated substrates are indicated. The ligated product (29 mer) in the presence of PDGF is of the same size as that of the control which does not contain aptamer and PDGF.

To test these hypotheses, we repeated time course assays using 12p and 13p mediated ligations (Figure 4-4 and Figure 4-5). It took overnight incubation to detect the ligation signals mediated by 12p. In the presence of PDGF, the size of the ligated product was again about 29 mer, indicating that it was the ligation product of 3'SUB and 5'SUB. In addition, in the absence of PDGF, no ligation activities were observed even after overnight incubation (Figure 4-4). These results suggested that PDGF induced the separation of 12p and the aptamer and the released 12p bound to both substrate oligonucleotides (3'SUB and 5'SUB) for ligation.

For ligations using 13p, we found that the 3' substrate strand (3'SUB) was not required (Figure 4-5). In addition, the size of the ligation product was about 35 mer, which should be the total length of 13p and 5'SUB. Also its ligation rate was faster than that using 12p because PDGF-activated ligation was seen as soon as 4 hours. The faster ligation rate using 13p is probably due to the ease of association of two strands instead of three strands.

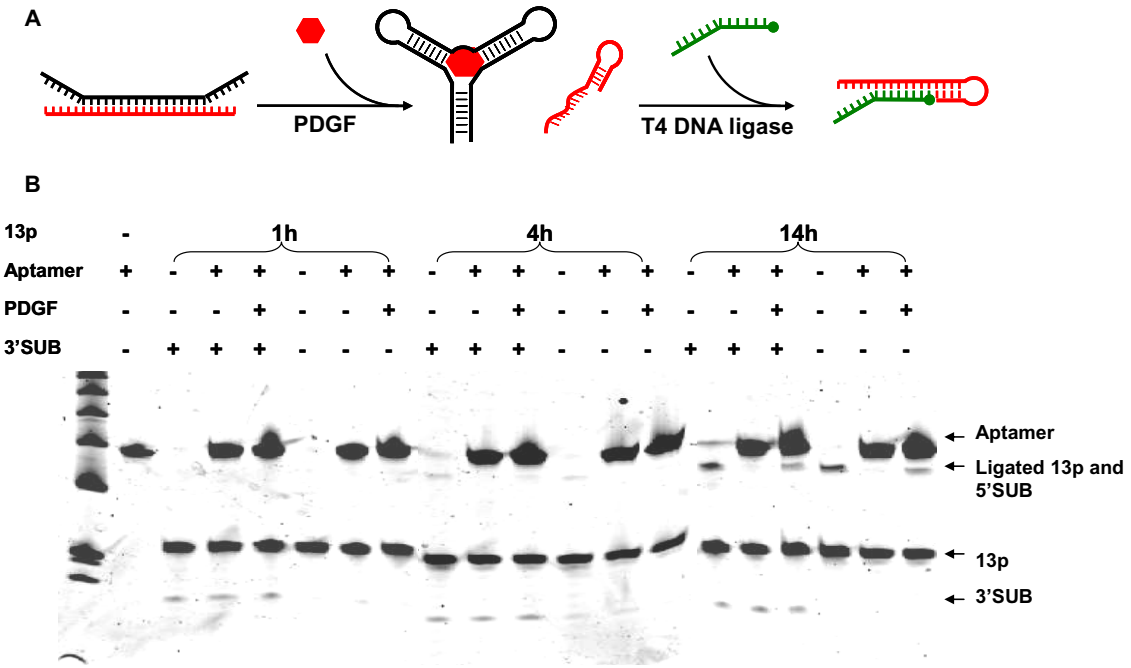

Figure 4-5. Confirmation of the three-piece ligation system. (A) Proposed ligation mechanism. (B) Time course ligation assays using 13p, aptamer and substrate oligonucleotides. Similar ligations were carried out as those described in Figure 3-3 except additional controls without the 3' substrate strand (3'SUB). The ligated product (35 mer) in the presence of PDGF is of the same size of the control which does not contain aptamer and PDGF. In addition, ligation is independent on the presence of 3' SUB, supporting that the ligation product is composed of 13p and 5'SUB.

Optimization of the oligonucleotide sequences for real-time PCR

Therefore, we obtained two ligation strategies: four-piece (12p, aptamer, 3'SUB and 5'SUB) and three-piece (13p, aptamer and 5'SUB). However, the ligated oligonucleoties were too short to generate optimal primer and probe sequences for real-time PCR. In order to add primer and probe sequences to the ligated products, we extended those oligonucleotide sequences (Table 4-2). Therefore, two new substrates (SUB2 and N. SUB2) were created from 5'SUB and they contain either regular Taqman probe or MGB probe sequence. 13ntT1 and 13ntT3 are derived from 13p. SUB1 is the longer version of 3'SUB. Because SUB2 and N. SUB2 have identical regions, same reverse primers were used for all the ligations (Table 4-2). Alternative oligonucleotides were of the same usage; therefore, we were able to test the ligation and amplification abilities using oligonucleotides with different but similar sequences. Because these redesigned oligonucleotides were longer than those initially tested, they were more likely to have secondary structures that might interfere with either substrate or antisense binding.

Table 4-2. Oligonucleotides used in both ligation and real-time PCR.

Oligos	Sequences	Note
12p	5'-TTTGATCGGATCATGGTGA -3'	12nt complementary with aptamer
13ntT1	5'-GTGTAGCCTTTCTCGATCGGATCATGGTGAT-3'	Derived from 13p
13ntT3	5'-TGGTAAGCCTTTCTCGATCGGATCATGGTGAT-3'	Derived from 13p
SUB1	5'-GAATCCAGTTCAAGCCTTCACAGCCTTCCTATTCATGAT-3'	3' side ligation substrate using 12p as a splint
SUB2	5'-pCCGATCCCTATTCATGTTACCGTCCGCTACTCATTCC-3'	5' side ligation substrate
N.SUB2	5'-pCCGATCCCTCTTGCTGCCTACGCATGCTGTTACCGTCC-GCTACTCATTCC-3'	5' side ligation substrate
FOR	5'-AGCCTTTCTCGATCGGATCA -3'	Forward primer for amplification of ligation of 13ntT1(13ntT3) and SUB2 (N.SUB2)
FOR12	5'-CAAGCCTTCACAGCCTTCCTA-3'	Forward primer for amplification of ligation of SUB1 and SUB2 (N.SUB2)
REV	5'GGAATGAGTAGCGGACGGTAAC -3'	Reverse primer of all the ligations
BB probe	5'-FAM-CGATCCCTCTTGCTGCCTACGCA-TAMRA-3'	TaqMan probe for ligation product of N.SUB2
BB-MGB	5'-FAM -TGATCCGATCCCTATTCA -MGB-3'	TaqMan MGB probe for ligation product of SUB2

The schemes of ligations using 13ntT1 (three-piece) and 12p (four-piece) with new substrate oligonucleotides, are shown in Figure 4-6 and Figure 4-7, respectively. Both 13ntT1 (13ntT3) and 12p can form duplex with the anti-PDGF aptamer in the absence of PDGF. In the presence of PDGF and T4 DNA ligase, 13ntT1 or 13ntT3 is ligated to either SUB2 or N. SUB2 and SUB1 is ligated to either SUB2 or N. SUB2 using 12p as a splint.

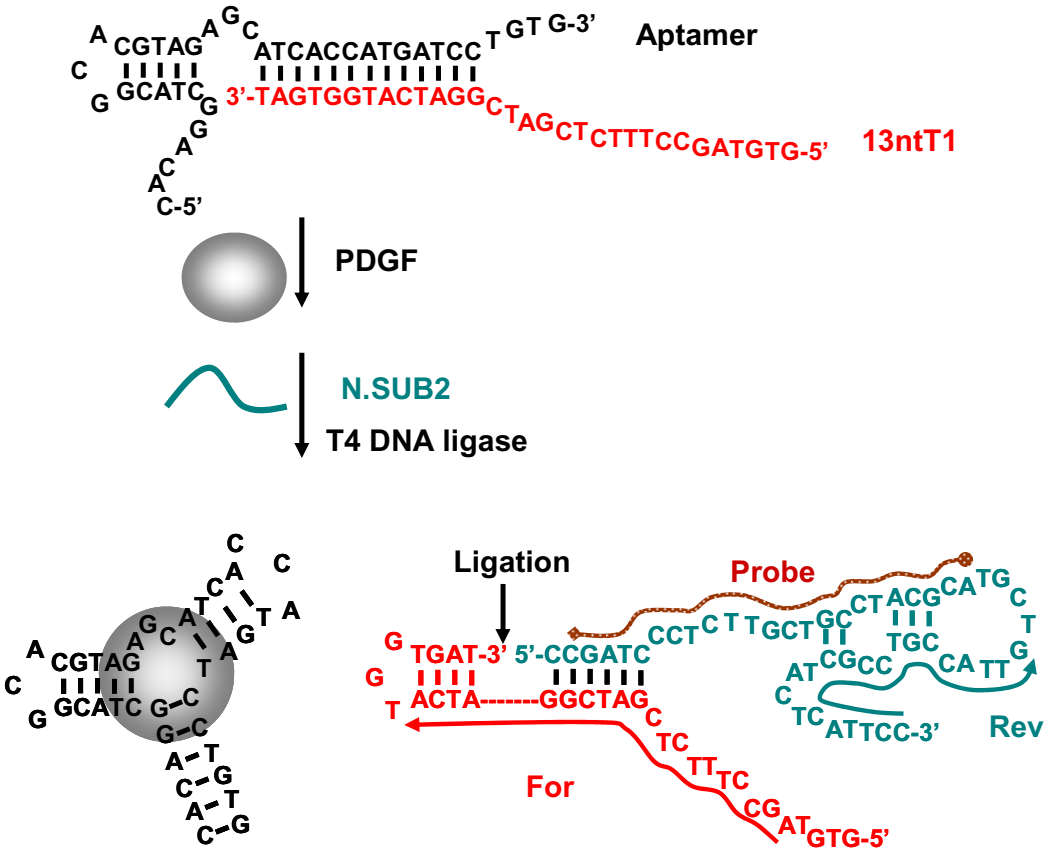

Figure 4-6. Design of 13ntT1 mediated three-piece ligation system followed by real-time PCR. 13ntT1 (red) and N. SUB2 (blue) are derived from 13p and 5'SUB, respectively. 13ntT1 forms duplex with the anti-PDGF aptamer. PDGF binding to the aptamer displaces 13ntT1, which then forms into a small hairpin to bind to N.SUB2. These oligonucleotides contain forward primer (For), reverse primer (Rev) and probe (Probe) sequences. Only ligated product can be amplified by real-time PCR.

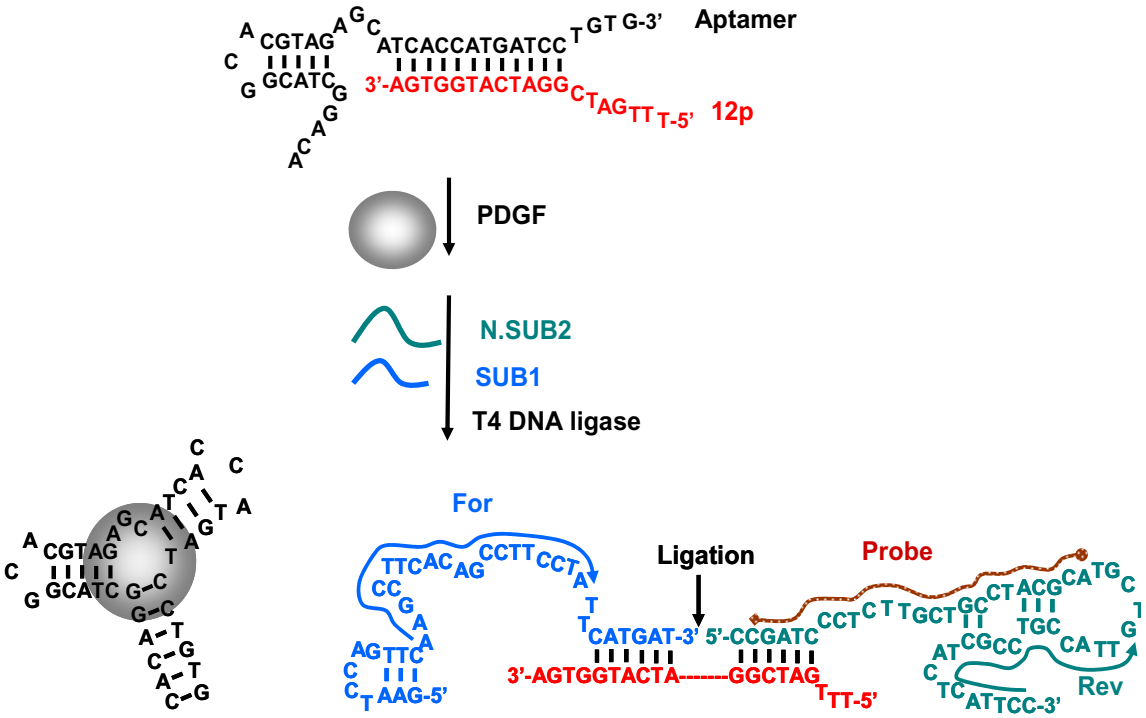

Figure 4-7. Example of four-piece ligation followed by real-time PCR. 12p forms duplex with the anti-PDGF aptamer. PDGF binding to the aptamer displaces 12p, which then bind to both SUB1 and N.SUB2. Ligated product is subsequently amplified by real-time PCR. For, Rev and Probe indicate forward primer, reverse primer and probe sequences, respectively.

Optimization of ligation time and oligonucleotide concentrations

To couple ligation with real-time PCR assays, there are several parameters to be considered for gaining the highest signal-to-background ratios (deta Ct). We tested different oligonucleotide concentrations, ligation timeperiods, and ratios of aptamer: antisense in the three-piece ligation system. For the oligonucleotide concentrations, we tested a series of concentrations of 13ntT1. To ensure 13ntT1 totally bound to aptamer, more aptamers than 13ntT1 were used for ligation and three aptamer : 13ntT1 ratios

([aptamer]: [13ntT1] = 3:1, 10:1 or 20:1) were tested. And the ratio of substrate (N.SUB2) : antisense (13ntT1) was always kept to be 2.5:1. For ligation timeperiods, four endpoints were chosen within 40 hours (Figure 4-8). A fraction of ligation reactions terminated at different timepoints was then used to seed a real-time PCR. As a control, a reaction without PDGF (but still containing BSA) was performed. Real-time PCR were carried out for 50 cycles and the delta Ct values were calculated by subtracting the Ct value for a reaction with PDGF from the Ct value for the reaction without PDGF.

As shown in Figure 4-8, amplified ligation activities varied at different oligonucleotide concentrations and aptamer : antisense(13ntT1) ratios. When 13ntT1 was 4 nM, delta Ct values obtained from the same aptamer : antisense ratios were irrespective of the lengths of ligation timeperiods (Figure 4-8A). However, when 13ntT1 concentration was 0.4 nM or 0.04 nM, big deviations of ligation activities were observed at different ligation timepoints (Figure 4-8B and C). The greatest Ct in the regard of shortest ligation time and lowest oligonucleotide ratio was obtained using 4 nM 13ntT1 at 10:1 aptamer : 13ntT1 ratio for an 8-hour ligation (Figure 4-8A). Because of this, we carried out both four- and three-piece ligations followed by real-time PCR using these above optimized conditions.

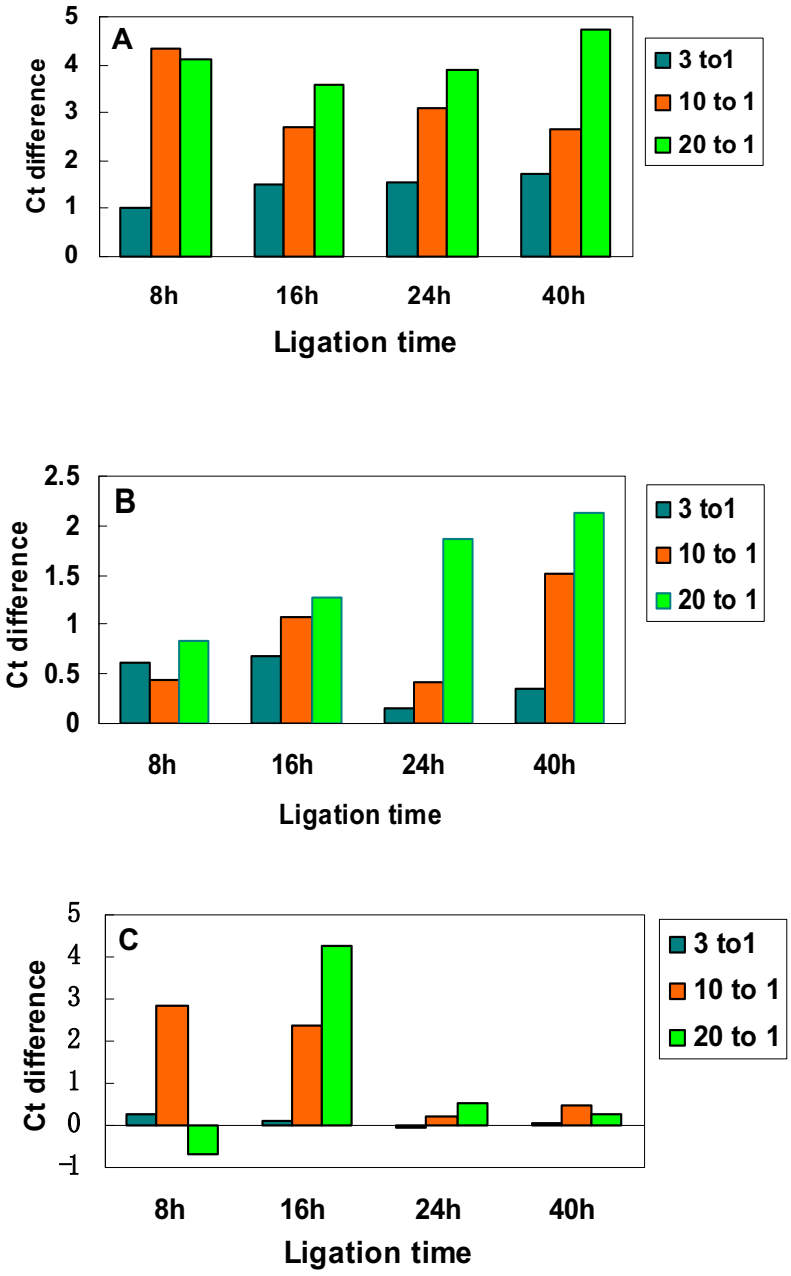

Figure 4-8. Optimization of detection. 4 nM (A), 0.4 nM (B) and 0.04 nM (C) 13ntT1 were mixed with aptamers at different ratios (1:3, 1:10 and 1:20). Ligation reactions were carried out in the presence or absence of 40 nM PDGF-BB and then detected via real-time PCR.

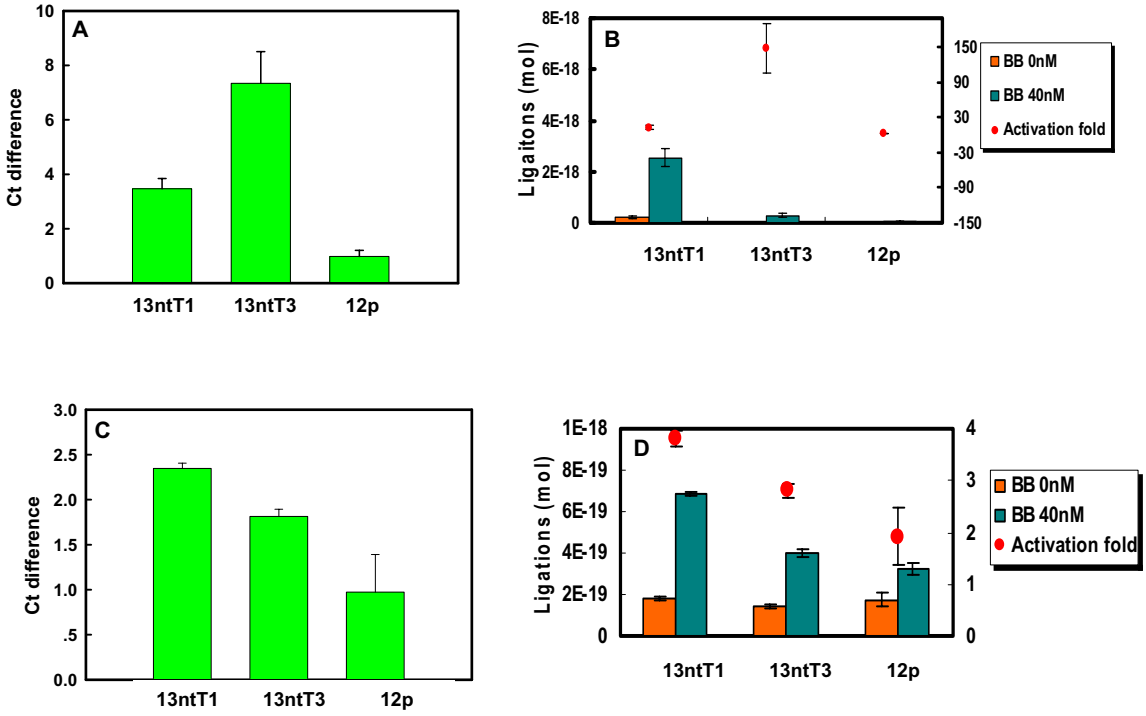

Figure 4-9. Amplified PDGF-activated ligation activities. Ligations were carried out using aptamer, one of the antisense oligonucleoties (13ntT1, 13ntT3 and 12p) and substrate oligonucleotide either N.SUB2 (A and B) or SUB2 (C and D). In the 12p involved four-piece ligation system, N. SUB2 or SUB2 is ligated to SUB1. Either Ct differences (A and C) or the amount of ligations (B and D) were analyzed for ligation activation.

Real-time amplification of PDGF-activated ligations

Using the optimized conditions, all the possible combinations of antisense and substrate oligonucleotides were examined in ligations followed by real-time PCR. In the three-piece ligations, both antisense strands (13ntT1 and 13ntT3) together with two substrate oligonucleotides (N.SUB2 and SUB2) were tested, respectively. In the four-piece ligations, 12p, SUB1 and either N.SUB2 or SUB2 were assayed. A FAM-TAMRA

probe was designed to detect ligations by N.SUB2 and a FAM-MGB probe was used to detect ligations by SUB2. To find out the best combination of these oligonucleotides for highest signal-to-background ratio, we carried out ligations in the presence of either 40 nM or 0 nM PDGF-BB. By comparing the obtained Ct differences shown in Figure 4-9A and C, ligations using N.SUB2 revealed better PDGF activation than that using SUB2 in both three- and four-piece assays.

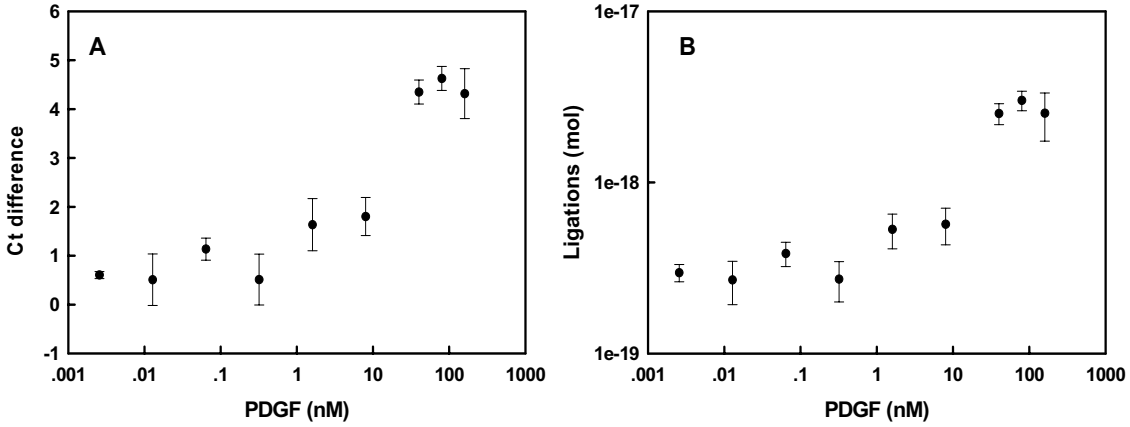

Figure 4-10. Dose-response for real-time PCR. Ligations were carried out using 13ntT1, aptamer and N.SUB2 at 25 ^{o}C for 8 h in the presence of a series of PDGF concentrations. 2 μL aliquot of ligation mixture was subject to a 30-μL PCR reaction for 50 cycles. Amplified ligation signals were determined as a function of PDGF concentrations based on either (A) Ct differences or (B) the amount of ligations.

However, compared to N.SUB2, the background ligation using SUB2 was higher as less Ct differences were observed. Since ligation was sequence dependent, the secondary structure and base pairs in the splint and substrates all played important roles in the determination of ligation activation and efficiency. Therefore it was not surprising that using different ligation strategies (four- or three-piece), ligation activations and ligation efficiencies were varied. In comparison to the three-piece ligation, less PDGF

activation was obtained using four-piece ligations. In addition, the two antisense strands (13ntT1 and 13ntT3) revealed different ligation activations in the three-piece ligations. For instance, by ligation with N.SUB2, the Ct difference using 13ntT3 was more than 7 while that using 13ntT1 was below 4 (Figure 4-9A). Moreover, the amount of ligated product was calculated and again activation folds were obtained (Figure 4-9 B and D). The highest activation (~150 fold) was observed with the combination of 13ntT3 and N. SUB2 (Figure 4-9B).

We proposed that the sensitivities of each assay were related to the PDGF activation levels. In another word, the assay with the highest PDGF activation level might also be the most sensitive one. To determine the sensitivity of the detection, we carried out three-piece ligations followed by real-time PCR in the presence of a series of PDGF concentrations. Amplified ligation activations as a function of PDGF concentrations using 13ntT1 and 13ntT3 are shown in Figure 4-10 and Figure 4-11, respectively. As expected, ligations using 13ntT3 demonstrated sharp signal increase over all the PDGF concentrations tested. However, ligations using 13ntT1 revealed good response only when PDGF concentration was above 8 nM. These results were consistent with the previous phenomena observed during optimization that detection using 13ntT3 should be more sensitive than that using 13ntT1. Based on these, we may also conclude that the sensitivity using 12p mediated four-piece ligations should be even lower than that obtained using 13ntT1.

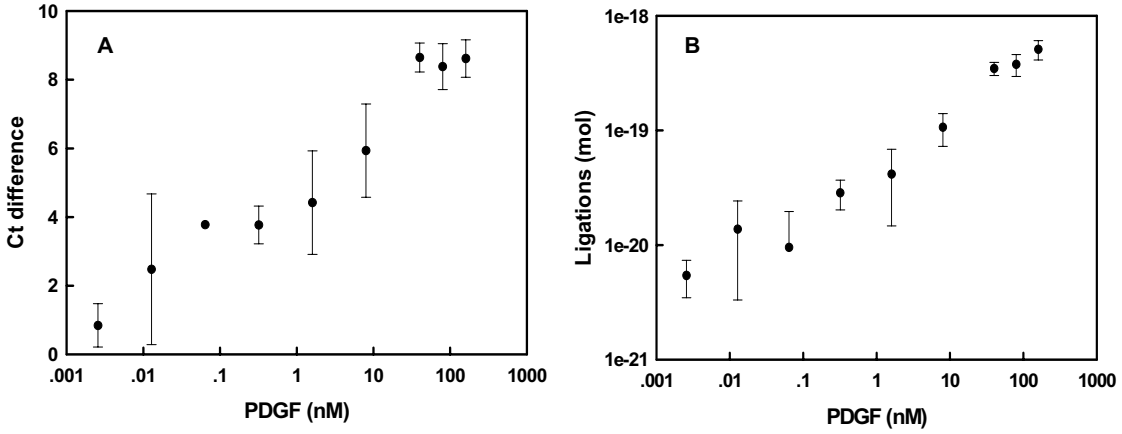

Figure 4-11. Amplified ligation activities over a series of PDGF-BB concentrations. Ligations using 13ntT3, SUB1 and N.SUB2 were carried out as described in Figure 4-10. Amplified ligation signals were determined as a function of PDGF concentrations based on either (A) Ct differences or (B) the amount of ligation product.

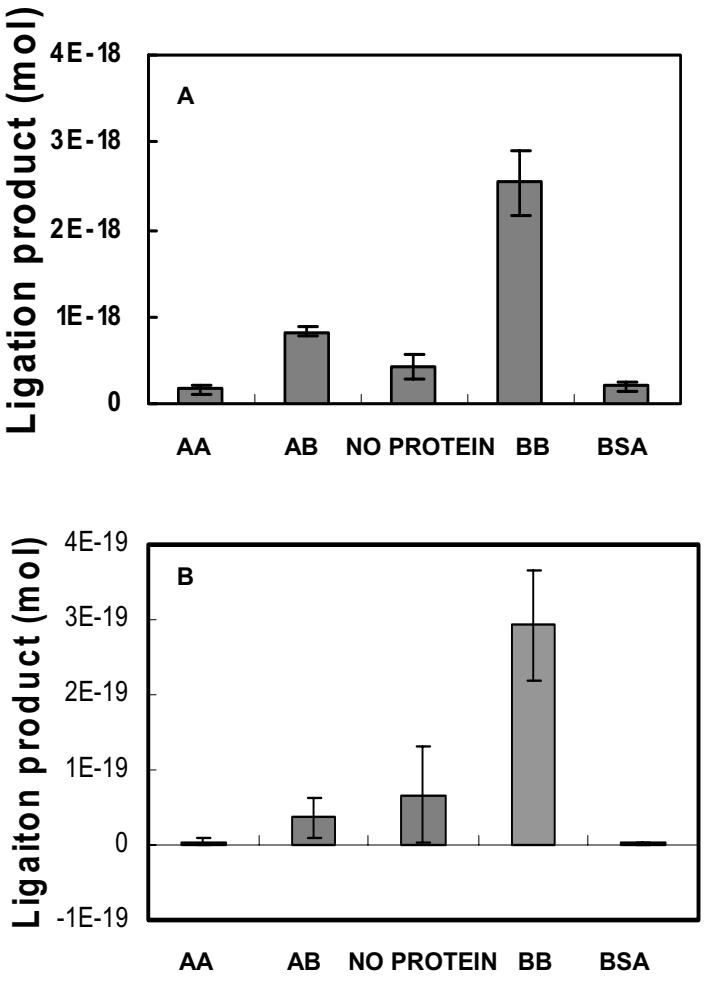

Figure 4-12. Specificities of response. Reactions were carried out using either 13ntT1 (A) or 13ntT3 (B). Ligations were carried out in the presence of 40 nM PDGF-AA, -AB or -BB. Negative controls were performed in the absence of protein or in the presence of BSA.

The specificity of the designed aptamer biosensor was also examined in the presence of different dimeric isoforms of PDGF: PDGF-AB, AA and BB (Figure 4-12). The presence of both PDGF-BB and PDGF-AB demonstrated 13ntT1 or 13ntT3 activated

ligation signals given that the aptamer was originally selected to bind to the B-chain (Green, Jellinek et al. 1996). The signal with PDGF-BB was greater than the signal with PDGF-AB probably because there were more B-chains in BB than that in AB. However, in the presence of PDGF-AA or BSA, the amplified ligation signals were even lower than controls without any protein. The suppression of the background ligation by either PDGF-AA or BSA may caused by their competing with DNA ligases for nonspecific binding to the aptamer.

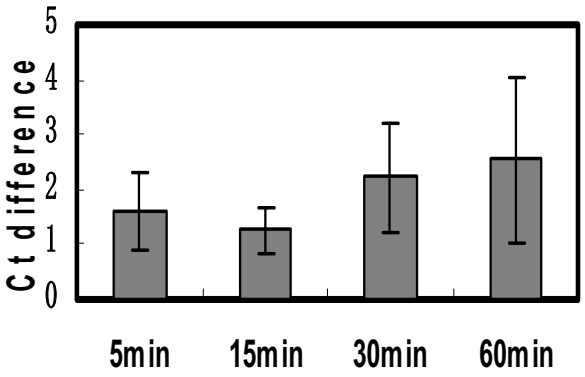

Figure 4-13. Amplification of ligation reactions performed at 25 ^{o}C within 1 hour. Ligations and real-time PCR were carried out using 13ntT3 as described previously except ligations were terminated at different timepoints within 1 hour.

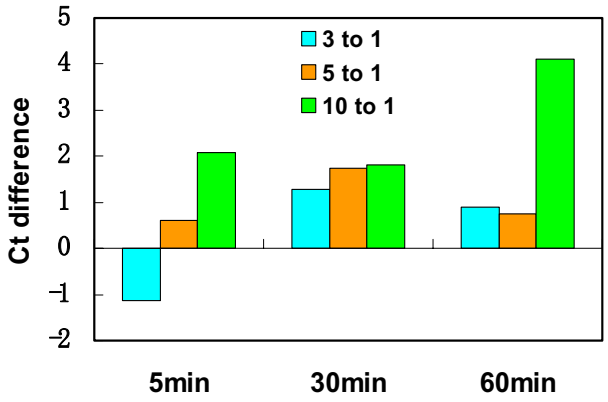

Figure 4-14. Amplification of ligation reactions performed at 37 °C within 1 hour. Ligations and real-time PCR were carried out using 13ntT3. In addition, different aptamer : 13ntT3 ratios were tested.

Detections in shorter ligation timeperiods

In order to find out the feasibility of detection using shorter ligation timeperiods, ligations were carried out within one hour followed by real-time PCR. As shown in Figure 14-13, the PDGF dependent ligation activations were less than those generated by 8 h ligations. Even ligations were carried out at elevated temperature (37 °C) (Figure 4-14); the highest Ct difference was around 4, which was about half reduction of that obtained from 8 h ligations. In addition, these results were consistent with the PAGE results (Figure 4-4 and Figure 4-5) which demonstrated that there were few ligated products in short timeperiods. Because the highest Ct difference was about 4, like the 13ntT1 detection, better sensitivity using shorter ligation time was not expected.

The advantages and problems of our design

One advantage of our structure-switching aptamer detection strategy is that it can be generalized to other aptamer based detections. Like fluorescent structure-switching

aptamers, antisense strand binding to any aptamer can be designed without knowing the secondary or tertiary structures of the aptamers. In addition, the use of a four-basepair hairpin which could serve as a half of the ligation junction allow the feasibility of short ligation junctions, facilitating the design of more stable aptamer-antisense duplex.

However, our design also has a couple of disadvantages. One is that ligation took 8 hours, which is impractical for sensing. Even though a series of oligonucleotide concentrations and elevated temperature have been tested, ligation rates are still very low. And sensitive detections were hard to be accomplished in a short time period such as 1 hour. The other disadvantage is that hybridization between aptamer and the antisense strands were not efficient. The 10:1 (aptamer : antisense) ratio suggested that large amount of aptamers were required to denature all the antisense strands. Similarly, the blocking oligonucleotides need to be in a 200-fold molar excess over the proximity probes in PLA (Schallmeiner, Oksanen et al. 2007). However higher concentration of aptamer would sacrifice more PDGF proteins, most of which may not be detected.

CONCLUSIONS

Our designed structure-switching aptamers demonstrated their feasibilities for signal amplifications. The detection also demonstrated high specificity with PDGF-BB. Furthermore, this was the first example to combine structure-switching aptamers with real-time PCR detections. Our results suggested that the stability of the duplex formed by aptamer and the antisense strand, sequences and secondary structures of the designed oligonucleotides all play important roles determining detection sensitivities and efficiencies.

FUTURE PLANS

In the future development, the ligation system should be improved for shorter ligation timeperiods and more efficient binding between aptamer and the antisense strands. Conditions such as hybridization time and temperature prior to ligation may be optimized to enhance DNA association. In addition, the lengths and sequences at the ligation junction may also be altered to speed up ligation rate. More importantly, intramolecular distance would be much closer than that of intermolecular distance. The shortened distance between aptamer and antisense molecules would facilitate the interaction among them. Therefore, combining the antisense strand and the aptamer into one molecule might improve detection simplicity and sensitivity.

MATERIALS AND METHODS

Materials

All the oligonucleotides except the TaqMan MGB probe were purchased from IDT (Coralville, IA). The TaqMan MGB probe was purchased from Applied Biosystems (Forster City, CA). Two amplicons N. Amplicon12 (5'-GAATCCAGTTCAAGCCTTCACAGCCTTCCTATTCATGATCCGATCCCTCTTGCTGCCTACGCATGCTGTTACCGTCCGCTACTCATTCC) and N. Amplicon13 (5'-GTGTAGCCTTTCTCGATCGGATCATGGTGATCCGATCCCTCTTGCTGCCTACGCATGCTGTTACCGTCCGCTACTCATTCC) were used to generate standard curved for the quantitation of ligations. The sequences of oligonucleotides used in ligation and PCR are shown in tables 4-1 and 4-2. PDGF-BB, AB and AA were purchased from R&D Systems (Minneapolis, MN). PDGF proteins were reconstituted in 4 mM HCL with 0.2 % BSA (Invitrogen, Carlsbad, CA) as suggested by the manufactures' instruction.

General method for ligation using short oligonucleotides

2 μL of 4 μM anti-PDGF aptamer and 2 μL of 2 μM antisense oligonucleotides were mixed in 1x ligation buffer (137 mM NaCl, 10.1 mM Na_2HPO_4, 1.8 mM KH_2PO_4, pH 7.4, 2.7 mM KCl, 10 mM Tris-Cl, pH 7.4, and 2.5 mM $MgCl_2$), then denatured at 70 ^oC for 3 min before cooling to room temperature. Then 4 μL of 2 μM PDGF-BB was added to the pre-ligation mixture. After incubation at room temperature for 60 min, 5 μL of 2 μM substrate oligonucleotides, 1.5 μL of T4 DNA ligase (2 U/μL, Epicentre, Madison, WI) and 1.5 μL of 25 mM ATP were added. Ligation reactions were carried out at room temperature for various time periods and stopped by addition of 95 % formamide gel-loading buffer and heating at 95 ^oC for 10 min. Ligated and unligated species were separated on denaturing 8-10 % polyacrylamide gels containing 7 M urea, stained with SYBR Gold (Molecular probe, Eugene, OR).

General method for ligation followed by real-time PCR

Pre-ligation mixtures were prepared similarly as described above except that the final concentrations of the antisense oligonucleotide and aptamer were 4 nM and 40 nM, respectively. Then 2 μL of 20 nM substrates, 1.5 μL T4 DNA ligase (2 U/μL, Epicentre) and 1.5 μL of 25 mM ATP were added after incubation with various concentration of BB for 1 h. 2 μL aliquot of the terminated ligaiton reaction, 15 μL of 2x TaqMan Universal PCR Master Mix (Applied Biosystems ABI, Foster City, CA), 0.5 μL of 10 μM forward primer, 0.5 μL of 10 μM reverse primer, 0.5 μL of 10 μM MGB probe and 11.5 μL H_2O were mixed to make a total volume of 30 μL. Real-time PCR was carried out in a 96-well PCR plate (ABI), covered with strip caps (ABI). The thermal cycling regime was: initial denaturation for 10 min at 95 ^oC, and then cycling for 15 s at 95 ^oC and 60 s at 60 ^oC, repeated 50 times on an ABI HT7900 real-time PCR machine.

Chapter 5: Real-time PCR detection of protein analytes with conformation-switching aptamers

INTRODUCTION

In chapter 4, we detected PDGF-BB using structure-switching aptamers coupled with ligation and real-time PCR. Similar to the design of other conformation-switching aptamers (Nutiu and Li 2003; Bayer and Smolke 2005; Liu and Lu 2005), in our method, antisense oligonucleotides bind to aptamer to promote the formation of a non-binding conformation. In the presence of analyte, the binding conformation is more favored, and the displaced antisense oligonucleotide forms into a short hairpin which hybridizes to a substrate oligonucleotide for subsequent ligation into an amplicon. Additional sequences added to either end of the antisense and substrate oligonucleotides served as primer- and probe-binding sites for real-time PCR.

However, the above ligation reaction required 8 hours to reach maximum analyte dependent activations. Such long time incubation is time-consuming for sensing in complex background such as serum and cellular lysate because proteases and nucleases may degrade oligonucleotides and analytes. In addition, the amount of aptamer needed to be ten times of that of the antisense oligonculeotides in order to totally occupy the antisense oligonucleotides. As a result, the sensitivity may be lowered by the free aptamers, which may take up to 90 % of the input protein analytes (Figure 5-1). When analyte concentration is lower than that of the aptamer low ligation rate may occur because either the antisense oligonucleotide is not displaced or the displaced antisense oligonucleotides form duplexes with other free aptamers but not the substrates for ligation (Figure 5-1). On the other hand, the additional primer sequence appended to the antisense oligonucleotide may interfere with aptamer or substrate binding, resulting in

difficult ligation. Therefore, we decided to increase the stability and efficiency of the hybridization between aptamer and the antisense by linking the antisense oligonucleotide to the 3' end of the aptamer. In this way, each aptamer could be denatured by hybridization with an antisense sequence *in cis*. And by the interaction with analyte, the number of displaced antisense tails would reflect the exact number of analyte binding.

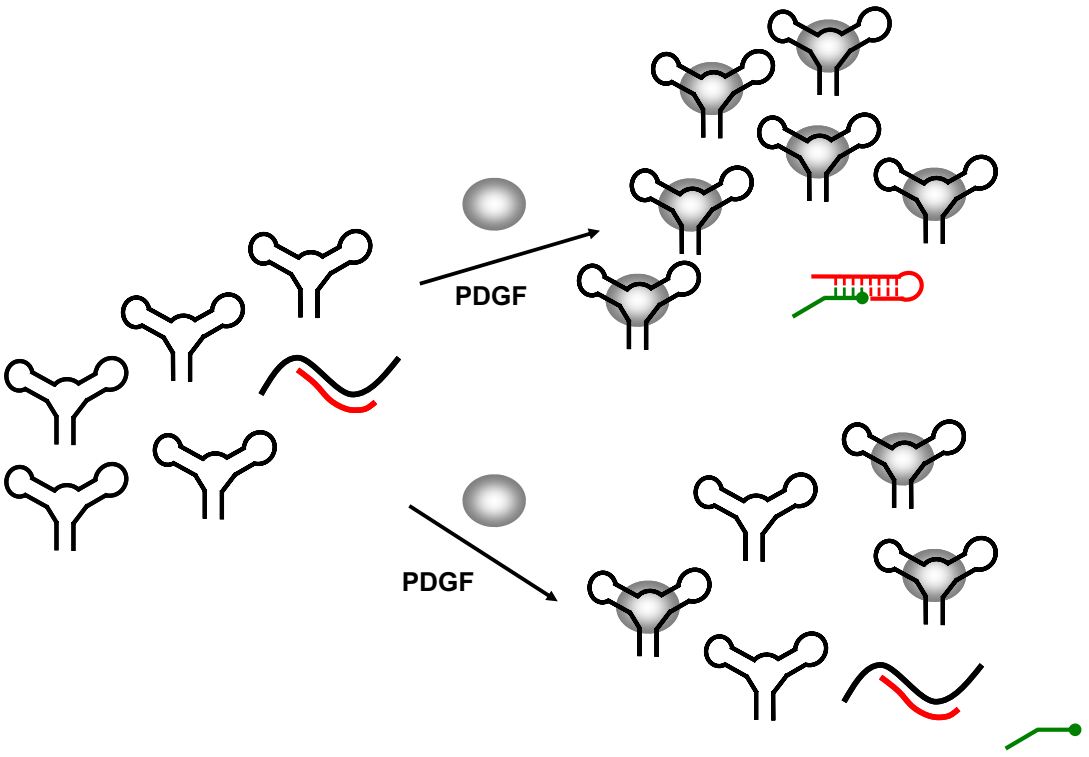

Figure 5-1. Schematic diagram of the explanation of low ligation rate observed in the three-piece ligations. Under optimized ligation conditions, the ratio of aptamer (black) to antisense oligonucleotide (red) is 10:1. When analyte (PDGF) concentration is more than that of the aptamer, all aptamers bind to analyte and the antisense oligonucleotides are ligated to the substrates (green). When analyte concentration is below that of the aptamer, aptamers can not be totally bound. Therefore, the antisense oligonucleotides may not be displaced or free antisense oligonucleotides may bind to other aptamers instead of the substrate oligonucleotides.

Moreover, primer sequences can be designed from the atpamer alone or the extension added on to the aptamer. Some secondary structures can be eliminated from the linker regions connecting aptamer and the antisense domain because the design of the linker region will be flexible. Therefore, the resultant two-piece ligation should be more suitable for real-time PCR detections.

In this chapter, we have extended the design in Chapter 4 to a two-piece ligation followed by real-time PCR for PDGF detection. Following this, the method was generalized to another anti-thrombin aptamer. Series of optimizations of oligonucleotide lengths and sequences were carried out to accomplish best sensitivity. Finally, the two-piece ligation was adapted to the design of antiswitches for the detection of PDGF and IgE.

RESULTS AND DISCUSSION

Two-piece ligation strategy

In order to shorten ligation time and increase detection sensitivity, we carried out the design of the two-piece ligations by attaching the antisense sequence to the 3' end of the aptamer. We have designed two different conformation-switching aptamers, one that binds PDGF and one that binds thrombin to show the generality of the method (Figures 5-2 and 5-3, respectively). In our method, the antisense sequences (blue, in Figures 5-2 and 5-3) were appended to 3' end of the aptamers (red) via linker regions. The combination of aptamer and antisense oligonucleotide into one piece would ensure that each aptamer forms a non-binding conformation (Figures 5-2A, 5-3A). In the presence of analyte, the aptamer sequence formed the binding conformation, and its 3' tail formed into a short hairpin for hybridization to an oligonucleotide substrate for subsequent

ligation (Figures 5-2B, 5-3B). The differences between the two designs was that the antisense sequence for the anti-PDGF aptamer could form a short hairpin stem itself while the 3' tail of the designed anti-thrombin aptamer forms into a short hairpin by the assistance of additional sequence at the 3' end of the aptamer. Additional sequences on either end of the aptamer served as primer- and probe-binding sites for real-time PCR. It should be noted that while one inhibitory conformation is indicated in Figure 5-3 two different, non-binding secondary structures are possible, similar to conformation-switching aptamers previously designed by Xiao *el al.* (Xiao, Piorek et al. 2005). While both conformation-switching aptamers employ the same basic design, different optimization methods were explored with the two aptamers, and assay results with PDGF and thrombin will be described separately. In addition, we extended our design to the construction of antiswitches for the detection of PDGF and IgE, which will be described later in this chapter.

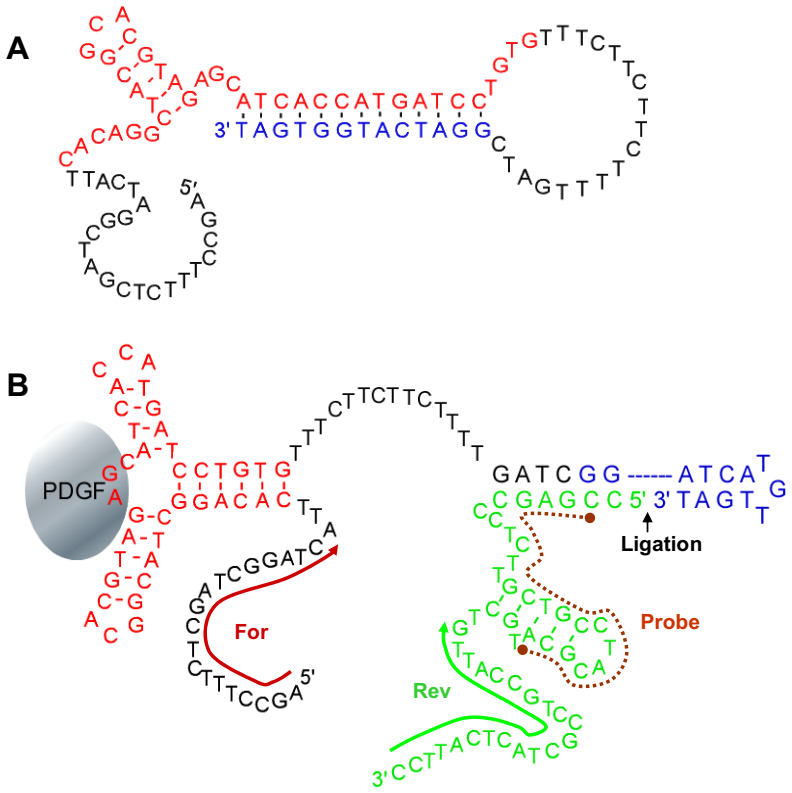

Figure 5-2. Sequence and secondary structure of a designed conformation-switching anti-PDGF aptamer. (A) Inactive conformation in the absence of PDGF. The 3' end of the aptamer has been extended with an antisense sequence (blue) in order to promote the formation of duplex structure and denaturation of the aptamer. (B)Active conformation in the presence of PDGF. Formation of a three-way junction and binding to PDGF stabilizes a structure in which the extended 3' end (blue) forms a short hairpin structure that can hybridize to a substrate oligonucleotide (green) to form a ligation junction. Following ligation with T4 DNA ligase, the ligated aptamer and substrate can be amplified by PCR using indicated forward (For) and reverse (Rev) primers. The position of the TaqMan probe (Probe) used during real-time PCR amplification is indicated by a dashed brown line.

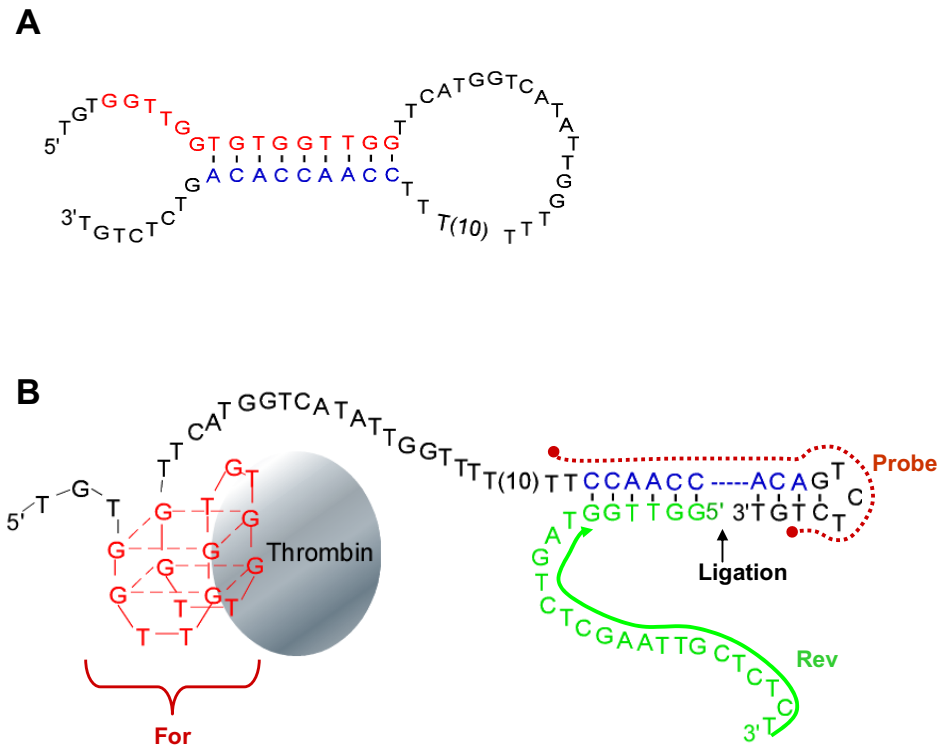

Figure 5-3. Sequence and secondary structure of a designed conformation-switching anti-thrombin aptamer. (A) Inactive conformation in the absence of thrombin. (B) Active conformation in the presence of thrombin. The active conformation of the anti-thrombin aptamer is a quadruplex. Features of the design are as in Figure 5-2.

PDGF mediated ligation followed by real-time PCR

As originally described in Figure 5-2, a conformation-switching aptamer was generated by appending a 13 nt antisense sequence to the 3' end of the anti-PDGF aptamer via an 18 nt linker. Therefore, the aptamer should form a hairpin in the non-binding conformation (Figure 5-2A), and assume its native binding structure in the presence of PDGF (Figure 5-2B). We used the same substrate oligonucleotide N.SUB2 as that used in Chapter 4 for ligation with the aptamer. N.SUB2 forms 6 basepairs at the

ligation junction. The same forward primer sequence (see Chapter 4) was appended to the 5' end of the anti-PDGF aptamer to enable real-time PCR. The probe binding site for real-time PCR was embedded in the substrate oligonucleotide sequence to allow real-time detection of amplification.

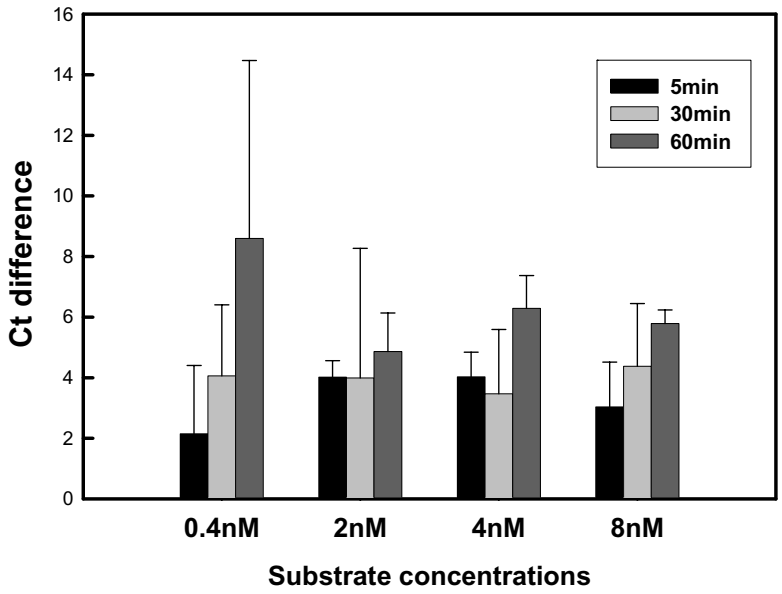

Figure 5-4. Optimization of two-piece ligation followed by real-time PCR for PDGF detection. Ligations were carried out for different time periods with different substrate (N.SUB2) concentrations. Ct differences were calculated based on the amplification of the sample with 40 nM PDGF and the control without PDGF.

This initial conformation-switching anti-PDGF aptamers worked well enough for immediate use in real-time PCR, without further sequence optimization. Optimization of oligonucleotide substrate (N.SUB2) concentration and ligation time prior to real-time PCR revealed that using 8 nM substrate at 60 minutes gave the greatest Ct with the least variance (Figure 5-4). Using an 8 nM substrate concentration and a ligation time of 60

min, real-time PCR was performed using a series of PDGF-BB concentrations. Delta-Ct represented as a function of PDGF-BB concentration is shown in Figure 5-5A. The lowest concentration that could be reliably detected was 0.32 nM, and the dynamic range of the assay extended to 40 nM.

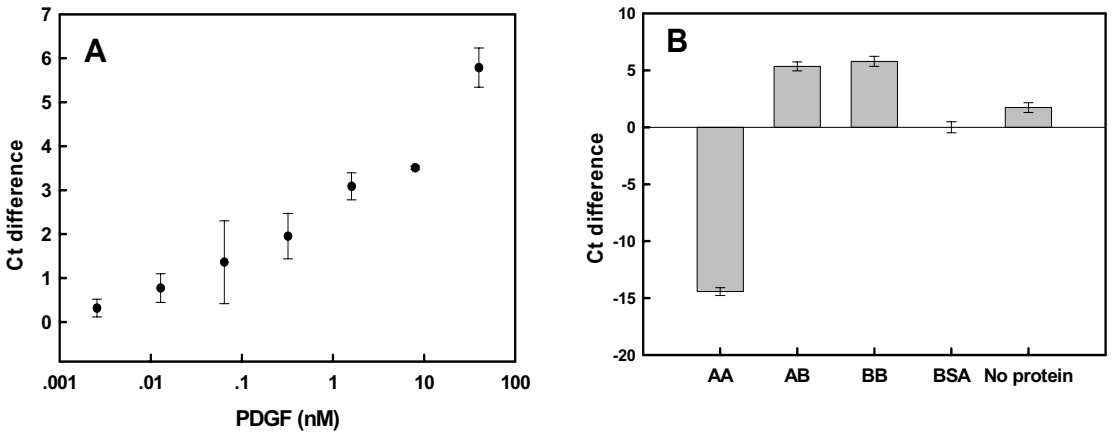

Figure 5-5. Real-time PCR amplification of PDGF-dependent ligation activities. (A) Signals were determined as a function of a range of PDGF concentrations. Ct differences were calculated relative to BSA alone (0.004 % final). (B) Specificity of response. Ligation reactions were carried out in the presence of 40 nM PDGF isoforms, respectively. Either BSA or no protein controls were also carried out.

The detections described here are consistent with the adaptation of this assay to clinical samples. PDGF levels in human serum have been found to be 14.4-24.8 ng/mL, or 0.56-1.12 nM (Singh, Chaikin, et al., 1982; Bowen-Pope, Malpass, et al., 1984). The sensitivities observed with our method are within these physiological levels. In addition, serum PDGF levels have been reported to be elevated in many diseased tissues.

These results compare well with most other analytical methods that utilize the same anti-PDGF aptamer. Low nanomolar detection limits have previously been observed with an aptamer beacon developed by Tan's group (Fang, Sen et al. 2003), with

an aptamer-based fluorescence anisotropy assay (Fang, Cao et al. 2001), with a colorimetric determination technique using aptamer-modified gold nanoparticles (Huang, Huang et al. 2005), with a luminescence detection strategy (Jiang, Fang et al. 2004), and with an exciton detection strategy (Yang, Jockusch et al. 2005). It should be noted, though, that proximity ligation coupled with real-time PCR could detect zeptomole amounts of PDGF (Fredriksson, Gullberg et al. 2002). However, the proximity ligation assay (PLA) requires two probes, rather than one, to achieve detection, and thus is not as generally applicable as the method we describe.

The specificity of detection was examined by determining the Delta Ct values with PDGF-AA, AB, BB and no protein at all (Figure 5-5B). In the presence of PDGF-AA, the amplified signal was much lower than the background level, while the signal in the presence of both PDGF-AB and -BB was significantly higher than background. These results accord with what is known of the anti-PDGF aptamer, as it binds to the B-chain of the protein and has roughly equal affinity for both PDGF-AB and-BB (Green, Jellinek et al. 1996). As we previously observed with the conformation-switching aptamers (Yang, Fung et al. 2007), protein interferents (either BSA or PDGF-AA) appeared to actually decrease the amplified signal relative to no protein controls, perhaps because non-specific interactions prevented conformational changes that might normally have occurred in solution.

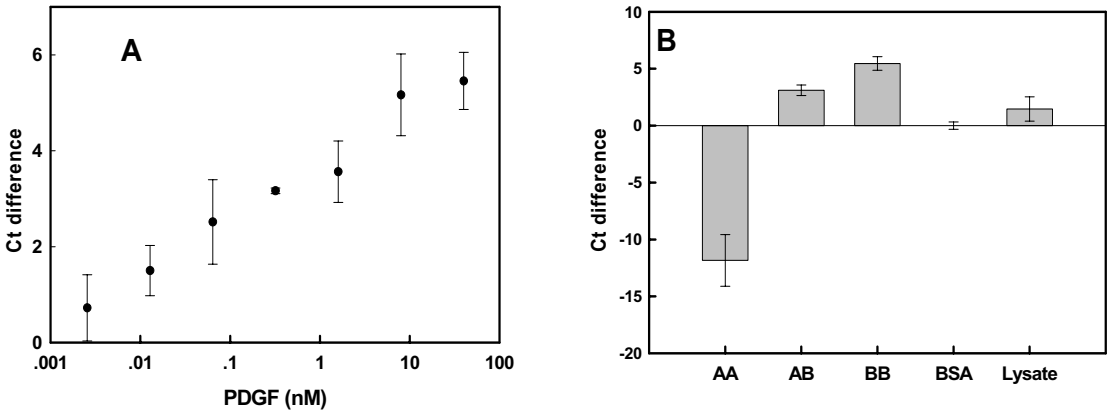

Figure 5-6. PDGF detection against a background of cell lysate. (A) Ct differences as a function of added PDGF concentration. Signal was determined as in Figure 5-5, except that ligation reactions were carried out in 1 μg/mL 293T fibroblast cell lysate. (B) Specificity of response in a background of cellular lysate. Negative controls included either lysate with no additions ("lysate") or lysate + 0.004 % BSA ("BSA").

The sensitivity, specificity, and resilience to interferences all suggested that the conformation-switching anti-PDGF aptamer should also function in the presence of cell lysates. Figure 5-6A and 5-6B summarize the dose response and selectivity of PDGF detection in cell lysate. The LOD was 12.8 pM and the Ct difference with the logarithm of PDGF concentrations was linear within the range of 12.8 pM-8 nM. These results again demonstrate that our conformation-switching aptamer technology in concert with real-time PCR should allow the sensitive quantitation of PDGF in clinical samples.

From the results above we can see that the two-piece ligation is faster than the three-piece ligation. The former takes only 1 h while the latter needs 8 h. More importantly, two-piece ligation can detect as low as 12.8 pM PDGF even against a background of cell lysate. Though similar sensitivity (64 pM) was observed for the

13ntT3 mediated three-piece ligation followed by amplification, the ligation assay was simply done in solution. If the three-piece ligation needed to be carried out in cell lysate for 8 h at room temperature prior to amplification, protease, nuclease and other enzymes in the lysate might interfere with the ligation signals.

Designing thrombin-sensing conformation-switching aptamers

In order to find out the generalizability of our design, we extended the strategy using the anti-thrombin aptamer. In PDGF sensing, the 13 nt antisense oligonucleotide folded into a short hairpin, which could form the ligation junction with the substrate oligoncucleotide. The reason for this was because it was complementary to one of the hairpins of the anti-PDGF aptamer. However, unlike the anti-PDGF aptamer, the anti-thrombin aptamer forms a free coil structure in the absence of thrombin. And it also folds into a quadruplex binding structure in the presence of thrombin. Therefore, no hairpin sequence is available from the anti-thrombin aptamer. To generate a hairpin, we first linked an antisense domain to the 3' end of the anti-thrombin aptamer (Figure 5-3, blue sequence). Then additional sequence was added following the antisense domain. This sequence was designed in order to form a short stem with a portion of the antisense domain (Figure 5-3B).

We also noted that in addition to adding a ligation junction and sequences for real-time PCR amplification to the aptamers, it was important to include spacer regions in order to allow both proteins (the analyte and the T4 DNA ligase) to simultaneously interact with the DNA. This can be seen by looking at results with a series of conformation-switching anti-thrombin aptamers (Figure 5-7). In initial designs, several different spacer lengths were used to separate the aptamer and antisense sequences. The spacer sequence was chosen by using the program Mfold

(http://www.bioinfo.rpi.edu/applications/mfold/dna/form1.cgi) to evaluate a variety of designs. A pyrimidine-rich spacer was found to minimize the formation of alternative secondary structures so that only the designed antisense sequences would pair with the aptamers. With the shortest spacer (21 residues; Thr9) no thrombin-dependent ligation was observed. When an additional T10 spacer was added (31 residues; Thr7), though, ligation was only observed in the presence of thrombin. When this spacer was extended to 20 residues (41 residues; Thr8), background ligation in the absence of thrombin increased. The longer spacer formed a longer loop structure that destabilized the interactions between the aptamer and the antisense sequence, promoting the non-binding conformation.

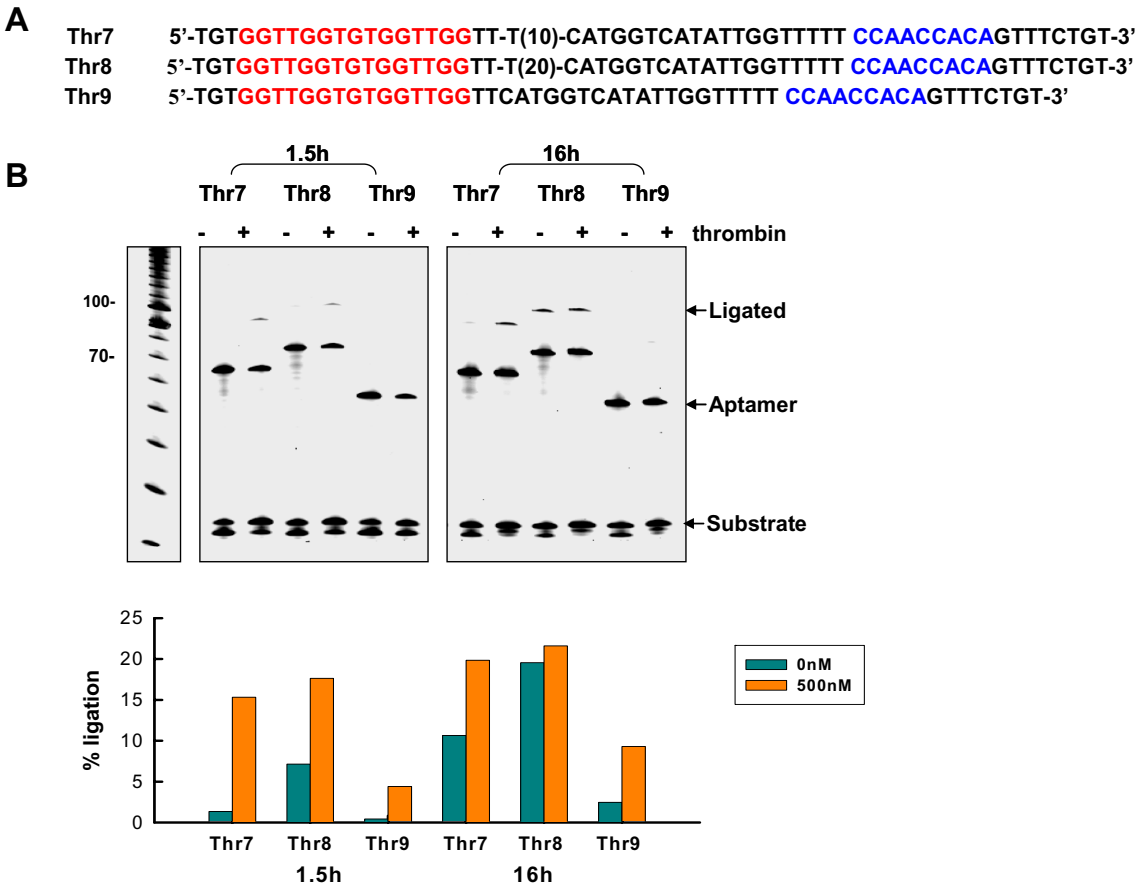

Figure 5-7. Effect of spacer length on thrombin-dependent ligation. (A) Sequences of thrombin-sensing structure-switching aptamers that have different spacer lengths connecting the antisense sequence (blue) and the aptamer (red). (B) Activation of ligation in the presence of thrombin. Ligation reactions were carried out for 1.5 or 16 hrs. Ligated and unligated species were visualized on 8 % PAGE gels stained with SYBR Gold. The percentage of ligation in the absence and presence of 500 nM thrombin was calculated by quantifying the amount of nucleic acid in each band using a QuantityOne software (BioRad Laboratories, Hercules, CA).

To further probe the relationship between sequence, conformation-switching, and ligation, a slightly different series of conformation-switching aptamers was synthesized and assayed (Figure 5-8). In this series, the T10 spacer has been repositioned within the

aptamer, closer to the 3' end. In addition, since it is likely that most optimizations of structure-switching aptamers will center on changing the number and types of basepairs between the aptamer and the added antisense sequences, we increased the designed basepairing from 9 bp (Thr7) to 10 bp (ThrX3), 11 bp (ThrX2), and 12 bp (ThrX1). Analyte-dependent ligation could be observed in ThrX3, but not in the two other constructs. The longer stems could no longer be readily displaced by thrombin. This was especially interesting because the 12 bp stem in ThrX1 was identical to that found in other conformation-switching anti-thrombin aptamer constructs (Nutiu and Li, 2003; Levy, Cater, et al., 2005). However, in these previous constructs basepairing was with an antisense oligonucleotide in *trans*, not an antisense sequence in *cis*, and thus the number of designed base pairs had to be shortened to accommodate the decreased entropy of structural rearrangement. The fact that the position of the spacer and the number of designed basepairs (9 in Thr7 and 10 in ThrX3) can be changed while structure-switching is retained indicates the robustness of this design approach.

These results indicated that both the Thr7 (9 bp hairpin) and ThrX3 (10 bp hairpin) conformation-switching aptamers were energetically poised to switch upon interaction with thrombin. This is important, since analyte responsivity should be highest when the free energy of interaction between the protein and the binding conformation of the aptamer is just slightly larger than the difference between the free energies of folding between the binding and non-binding conformations.

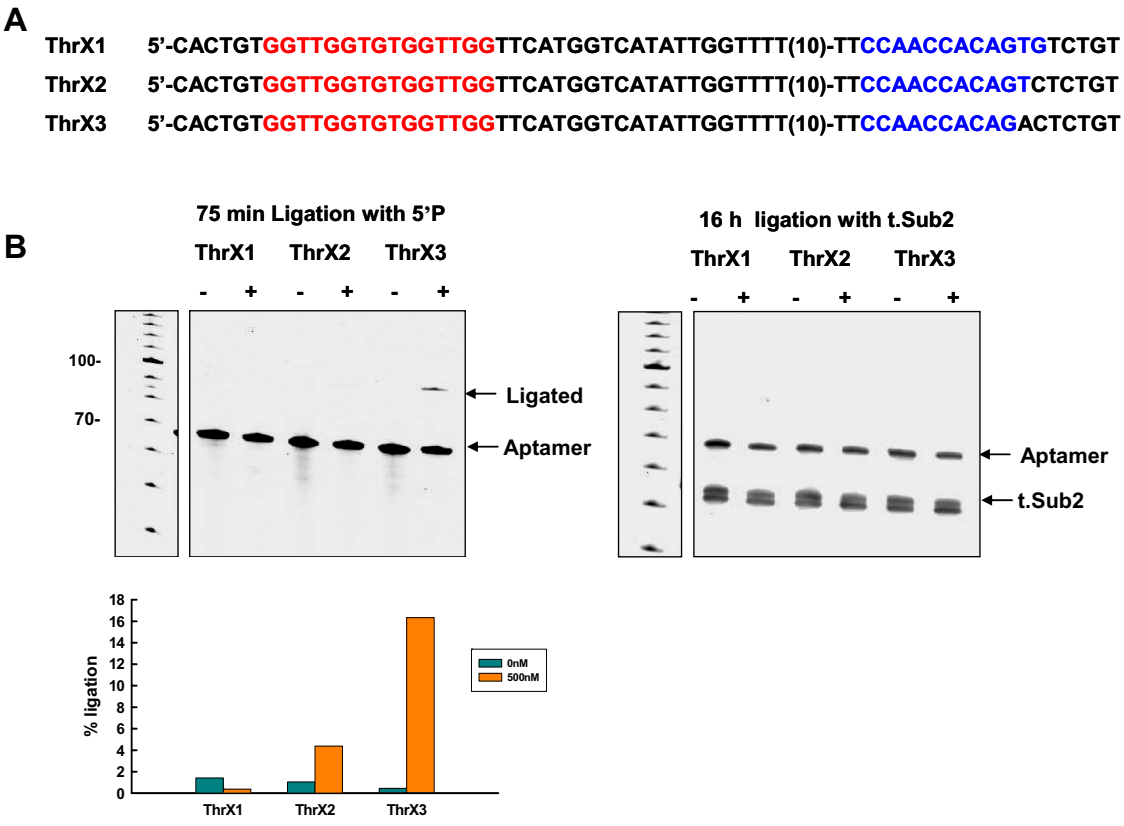

Figure 5-8. Effect of antisense sequence on thrombin-dependent ligation. (A) Sequences of the designed constructs. (B) Ligation assays using substrates 5'P and t.Sub2, respectively. (+) and (-) indicate the presence and absence of 500 nM thrombin. No ligation signals were observed using t.Sub2 even after overnight incubation.

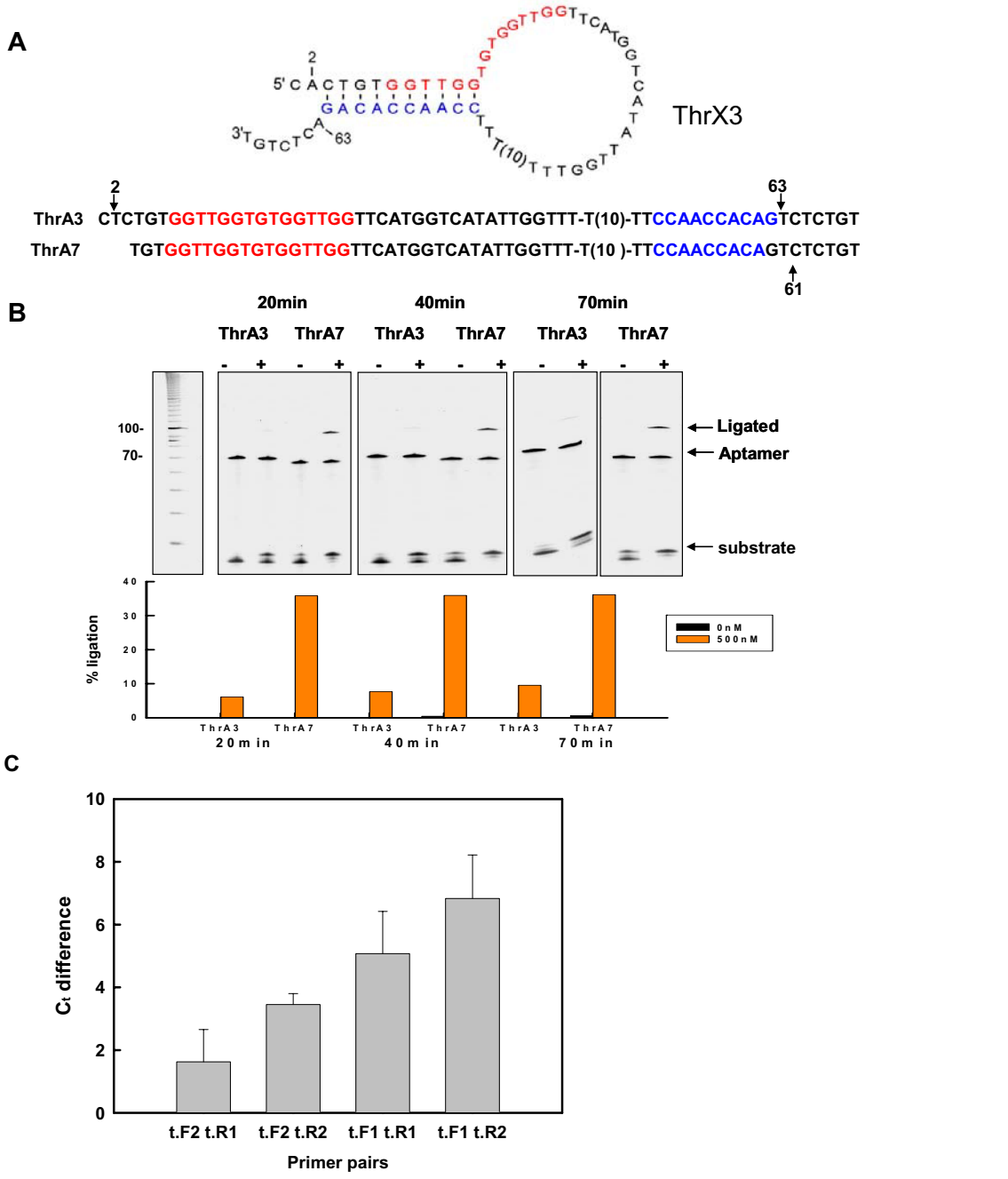

Figure 5-9. Two new constructs based on the design of ThrX3 and Thr7. (A) ThrA3 and ThrA7 were designed based on ThrX3 and Thr7, respectively. Arrows indicate the changes from the previous constructs. (B) Ligation assays and analyses of these two aptamers. (C) Amplified ligation signals using 4 sets of primers. Ligations were carried out in the presence or absence of thrombin using ThrA7 at room temperature for 20 min. Then, 2 μL aliquot of ligation reaction was used for real-time PCR.

The ThrX3 conformation-switching aptamer was further optimized for real-time PCR by changing the sequences of the probes, primers, and their complementary binding sites. Primer Express Software from Applied Biosystems was used for probe design, but initially did not identify a good probe for aptamer ThrX3. Therefore, we introduced slight sequence changes into ThrX3 in order to derive and utilize a better probe (and corresponding probe-binding site). This resulted in the production of the conformation-switching anti-thrombin aptamer ThrA3 (Figure 5-9A) which contained a T to A change in the probe-binding site (underlined in Figure 5-9A) at position 63 and that could therefore utilize a predicted 17 nt real-time PCR probe (5'-TTCCAACCACAGTCTCT; this probe was obtained from ABI and was also conjugated to a minor-groove binding compound, as detailed in Materials and Methods). Since position 63 was also involved in the formation of the hairpin stem in the non-binding conformation, position 2 had to be correspondingly changed from A to T, in order to avoid extending the helix.

Since the conformation-switching anti-thrombin aptamer Thr7 had also demonstrated excellent thrombin responsivity, we also attempted to adapt this aptamer to real-time PCR. The T10 spacer was again repositioned to be at the 3' end of the aptamer (as with ThrX1-ThrX3) and a mutation was introduced (T61 to C61) in order to create a probe-binding site (underlined in Figure 5-9A) that could utilize the same 17 nt predicted probe sequence described above for ThrX3, ultimately creating aptamer ThrA7.

Both new aptamers, ThrA3 and ThrA7 were assayed for their ability to ligate in the presence of 500 nM thrombin (Figure 5-9B; see also the following section for real-time PCR assay development). Both aptamers retained thrombin-dependence, although ThrA7 gives a higher signal than ThrA3. Again, the ability to readily manipulate the sequences of the conformation-switching aptamers without losing thrombin-dependence indicates the robustness of these constructs and of the design process in general.

In order to facilitate real-time PCR, several different primer sequences were assayed (Figure 5-9C). Two different forward primers and two different reverse primers were designed, each of which had a predicted T_m near 60 ^oC. Real-time PCRs were carried out with the four possible combinations of forward and reverse primers. The best pair of primers proved to be t.F1 and t.R2, which generated a Ct difference in the presence of saturating thrombin concentrations (500 nM) of 7, which is much higher than is typically observed for the determination of statistically significant changes in mRNA expression by real-time PCR. For example, delta Ct values in the range of -0.9 to 3 were considered significant for quantitating diagnostically important alterations in hemoglobin-alpha mRNA expression levels (Nussbaumer, Gharehbaghi-Schnell et al. 2006). Similarly, delta Ct values as low as 0.15 to 0.37 for κ and λ immunoglobulin light chain mRNA expression levels have been considered legitimate for determining B-lymphocyte monoclonality (Stahlberg, Aman et al. 2003). Hundley *et al.* (2006) have shown that a delta Ct of less than 2 represents at least a 3.2-fold difference in the expression of myosin binding protein H mRNAs (Hundley, Yuan et al. 2006).

Thrombin mediated ligation followed by real-time PCR

The optimized conformation-switching aptamers ThrA3 and ThrA7 and the primer set t.F1 and t.R2 were used in real-time PCR assays for the sensitive detection of thrombin. In these assays, protein-dependent ligation was first carried out, followed by real-time amplification and detection of the ligated products. Thrombin (with BSA as a carrier protein) was first incubated with the aptamers for 30 minutes, and T4 DNA ligase and reaction components were then added. Ligation was allowed to proceed for 5-40 minutes and stopped by heat denaturation. A fraction of the ligation reaction was then used to seed a real-time PCR plate. As a control, a reaction without thrombin (but still

containing BSA) was carried out. Delta Ct values were calculated by subtracting the Ct value for a reaction with thrombin (cycle threshold should be reached earlier) from the Ct value for the reaction without thrombin (cycle threshold should be reached later).

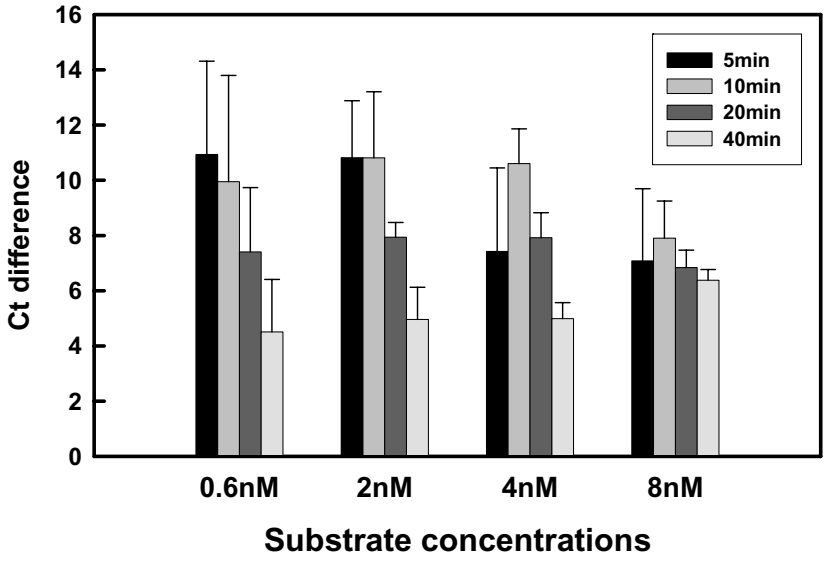

Figure 5-10. Optimization of thrombin-dependent ligation followed by real-time PCR. Thrombin-dependent ligations were carried out using 0.4 nM ThrA7 and different concentrations of substrate (t.5'P). Ligation reactions were terminated at different timepoints and then amplified by real-time PCR. The Ct difference between amplification in the presence and absence of thrombin is indicated

As can be seen in Figure 5-10, positive delta Ct values were obtained at a variety of oligonucleotide (t.5'P) substrate concentrations irrespective of the length of ligation time, although shorter ligation times tended to provide larger signals. However, when we repeated the experiments, there was larger variance in Ct values at ligation times shorter than 20 min. Because of this, all subsequent assays incorporated a ligation time of 20 min.

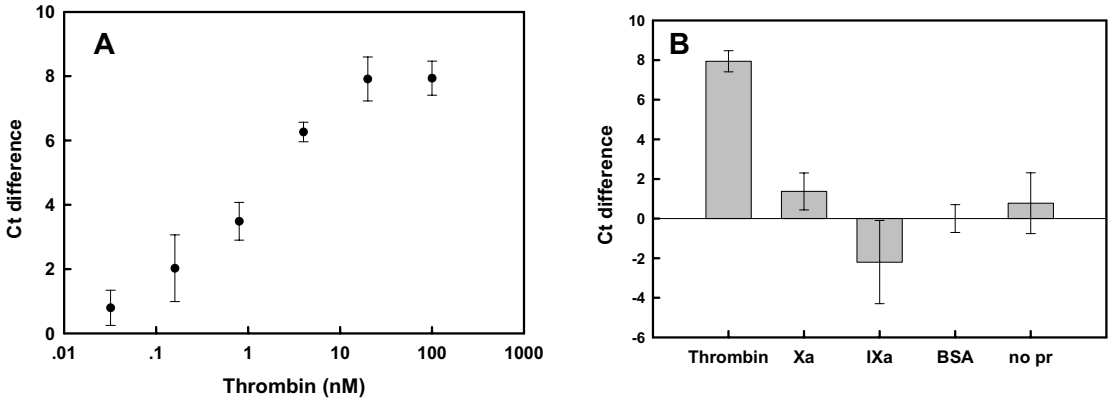

Figure 5-11. Real-time PCR amplification of thrombin-dependent ligation reactions. (A) Ct differences as a function of thrombin concentration. Ct differences were calculated relative to BSA alone (0.002 % final). (B) Specificity of response. Ligation reactions were carried out in the presence of either 100 nM thrombin or similar proteases, such as factor Xa and IXa. Either BSA or no protein controls were also carried out.

In order to determine the sensitivity of the method, ligation and real-time PCR assays were performed at a series of thrombin concentrations. Delta Ct values as a function of thrombin concentration are shown in Figure 5-11A. The variances of the delta Ct values were quite low; the limit of detection (a signal three times the standard deviation of the background) could be detected with as little as 0.8 nM thrombin. Moreover, the concentration of thrombin correlated well with the real-time PCR signal between 0.1 and 20 nM thrombin.

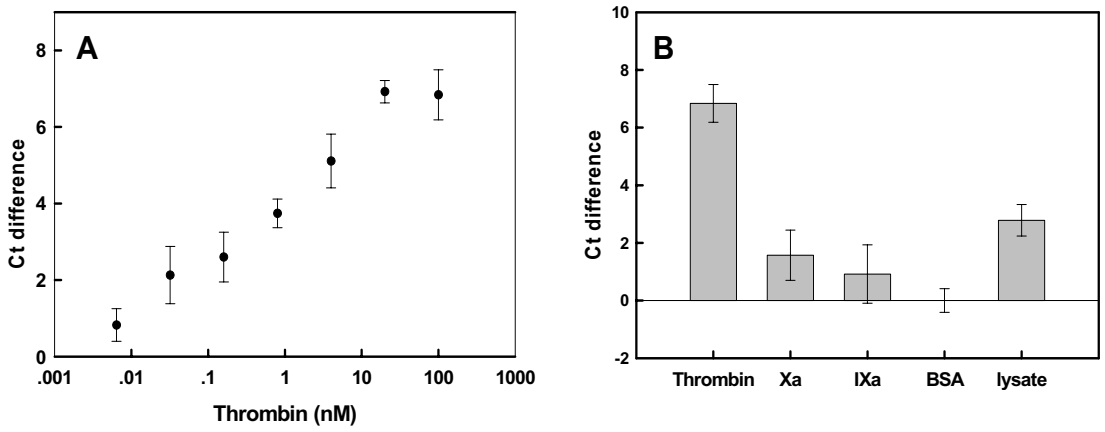

Figure 5-12. Thrombin detection against a background of cell lysate. (A) Signal was determined as in Figure 5-11, except that ligation reactions were carried out in 1 μg/mL 293T fibroblast cell lysate. (B) Specificity of response in a background of cell lysate. Negative controls included lysate with no additions ("lysate") or lysate + 0.004 % BSA ("BSA").

The thrombin concentration range in blood plasma is 5-500 NIH units/mL, where 1NIH Unit=0.324+/-0.073 μg (Aronson, Stevan et al. 1977; Fenton 1986). Therefore, the lowest physiologically relevant thrombin concentration would be nanomolar to low micromolar concentrations (Lee and Walt 2000; Spiridonova and Kopylov 2002), well within the range of our assay.

Our results compare quite favorably with previous aptamer-based thrombin assays. The observed detection limits using the anti-thrombin aptamer and optical biosensors varied between 1 nM (Spiridonova and Kopylov, 2002; fiber optic biosensor with labeled thrombin); 373±30 pM (aptamer beacon that dequenched; Li, Fang, et al., 2002); and 429±63 pM (aptamer beacon that yielded changes in FRET; Li, Fang, et al., 2002). For electronic biosensors the values were 2-3 nM (Radi, Acero Sanchez et al.

2005; Xiao, Lubin et al. 2005; Xiao, Piorek et al. 2005). Using capillary electrophoresis with laser-induced fluorescence detection (CE_LIF) detection limit was 40 nM and K_d value was about 450 nM (German, Buchanan et al. 1998). When the anti-thrombin aptamer was adapted to the equivalent of an ELISA the limit of detection was <1 nM (Baldrich, Restrepo et al. 2004). The best results have been garnered by other real-time methods: a detection limit of 30 pM by proximity rolling circle amplification (Di Giusto, Wlassoff, et al., 2005), and down to several hundred of molecules by exonuclease protection coupled with real-time PCR (Wang, Li, et al., 2005).

The specificity of detection was examined by substituting thrombin with other proteases from the clotting cascade, Factors IXa and Xa (Figure 5-11B). In the absence of protein or in the presence of carrier BSA, Factor IXa, Factor Xa, or in the absence of protein, the delta Ct signal was very small relative to the value obtained with thrombin. The amplified signal in the absence of any protein is again higher than that in the presence of BSA.

Taken together, these results suggest that assays with physiological samples should also yield sensitive and specific detection, especially given that our limits of detection seem to be within the same range as thrombin concentrations found in physiological samples, as described above. In order to test this possibility, we carried out assays with thrombin in human 293T fibroblast cell lysates (Figures 5-12A and 5-12B). Despite the fact that lysate was in weight excess (for example, if thrombin concentration is 32 pM, lysate amount is about 845-fold of that of thrombin), the detection of thrombin in cell lysate was specific and sensitive as in the absence of lysate. Even though the signal of protein and no protein controls were somewhat higher than those in solution, the detection limit (a signal three times the standard deviation of the background) was 32 pM, even lower than that in the absence of lysate (800 pM).

Table 5-1. Summary of the sensing of PDGF and thrombin.

	PDGF	Thrombin
Aptamer	0.4 nM	0.4 nM
Antisense length	13 nt	9 nt
3' hairpin stem	Formed by the antisense sequence	Formed by antisense and additional sequences
Substrate	8 nM	2 nM
Ligation time	60 min	20 min
K_d of the selected aptamer	0.1 nM	2.68-200 nM
Detection limit	12.8 pM	32 pM

Table 5-1 summarized the sensing of PDGF and thrombin using the two-piece ligations followed by real-time PCR. First of all, our designed demonstrated its ability for protein analyte detections. The detection limits achieved by our methods are much lower than the K_d values of the selected anti-PDGF and anti-thrombin aptamers.

In addition, our methods also demonstrate the generalizability to any aptamer. Presumably, any DNA aptamer can be designed using our strategies. We also noted that for each analyte detection reaction, optimizations are usually necessary for more sensitive, faster and simpler detections. This is because currently there is no prefect prediction of conformational changes available. So the sequences and the lengths of the designed oligoncleotides need to be fine tuned based on the feedback of the ligation data. In addition, ligation time, oligonucleotide concentrations and ratios are also parameters under concern. As shown in Table 5-1, ligation time for the detection of PDGF is 60 min, while that for detection of thrombin is only 20 min. Though the same aptamer

concentrations were used in both assays, substrate concentrations are varied (8 nM vs. 2 nM). These differences may be caused by the different affinity of the aptamer and hybridization abilities of the oligonucleotides.

Coupling antiswitches for signal amplification

In order to find out the applicability of our method for other designs, we have attempted to fit our antisense-ligation strategy into the concept of antiswitch. Antiswitch (RNA) contains an aptamer domain and an antisense domain. The former binds to a small molecule analyte and the latter is a *trans*-acting antisense RNA which targets the 5' end of mRNA in order to control gene expression at the translational level (Figure 5-13A). The interaction (nucleic acid hybridization) between both domains is controlled by analyte binding. For the "off-switch", the antisense domain folds into a hairpin with a portion of the aptamer domain in the absence of analyte. Upon binding to analyte, the stem of the antisense domain is separated and becomes single stranded RNA, which then hybridizes to the target mRNA and blocks translation. For the "on-switch" the antisense domain is free to bind to target mRNA and suppress gene expression in the absence of analyte. Small molecule binding promotes to binding of the aptamer domain and the antisense domain, resulting in gene expression.

One difference between antiswitch and our design is that the antisense strand in antiswitch is complementary to one end of the aptamer while in our design the antisense strand could be complementary to any portion of the aptamer. Therefore, we should be able to use antiswitch to carry out analyte-dependent ligations. Similar to the design of the thrombin-sensing structure-switching aptamer, additional sequences were added to the antisense strands via a linker sequence in order to generate a short hairpin to bind to

substrate oligonucleotide for ligation (Figure 5-13B). We have carried out the design of antiswitch coupled with ligation for the sensing of PDGF and IgE, respectively.

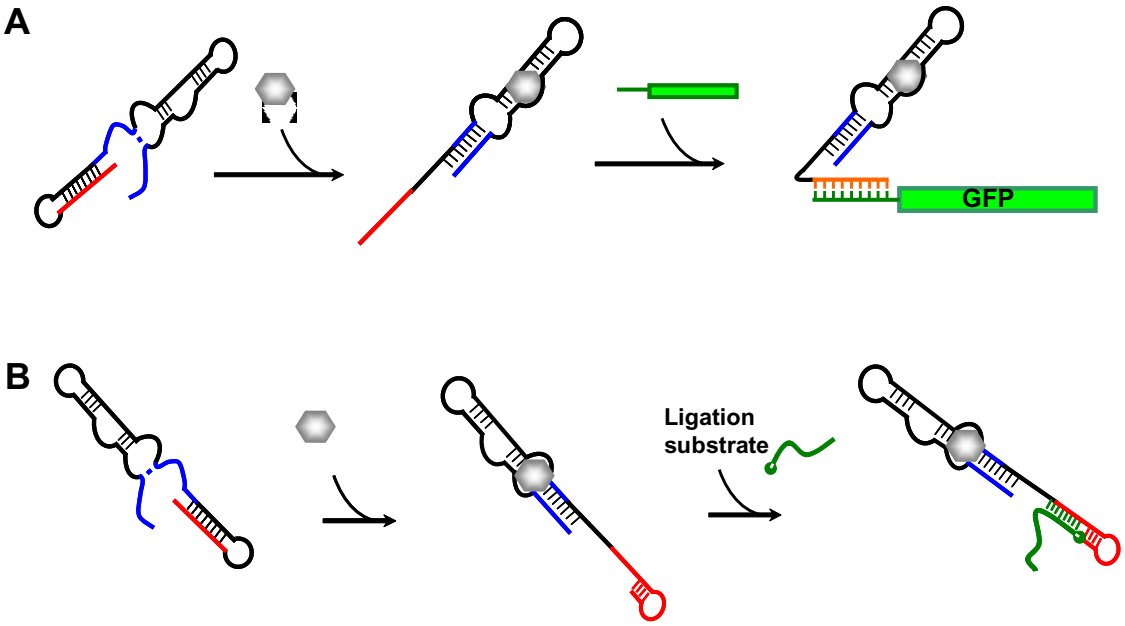

Figure 5-13. Coupling antiswitch with ligation. (A) The design of antiswitch for the control of GFP expression. In the absence of analyte, the antisense targeting the 5' end UTR of GFP mRNA, forms hairpin with the aptamer. Analyte binding displaces the antisense strand, which then hybridizes to the mRNA and blocks GFP translation. (B) Design scheme of coupling antiswitch with ligation. Additional sequence is added to the 3' end of the antisense domain in order to form a short hairpin in the presence of analyte. This hairpin structure can hybridize with a substrate oligonucleotide to form a ligation junction to be closed by T4 DNA ligase.

Designing antiswitch coupled with ligation for the detection of PDGF

Based on antiswitch (Figure 5-13A), the conformational switches are between the aptamer folding structure and the hairpin formed by the aptamer and the antisense. To create the structure switches, the aptamer's folding conformation should be less stable than the aptamer-antisense duplex (inactive conformer). And in the presence of PDGF, the binding energy would lower the folding energy, resulting in switching to aptamer

binding conformation. Therefore, aptamers with truncated stem were constructed (Figure 5-14). However, the aptamer stem should also be kept at a certain length to ensure correct folding. In order to find out the optimal stem lengths, we tested aptamers with stem lengths varying from 5 bp to 7 bp (Figure 5-14). The antisense strand in each of them could form 10 bp duplex with the aptamer. The difference between construct BB1 and BB4 was that the G in the linker of BB1 was T in that of BB4. Therefore, the secondary structure formed by the linker regions in BB1 and BB4 might be different due to the stability of a GC pair. Ligations were carried out in the either presence or absence of PDGF using these designed constructs and two substrate oligonucleotides, respectively. These two substrate oligonucleotides (PDGF.6p and PDGF.8p) could hybridize with either 6 bases or 8 bases in the ligation junction.

As can be seen in Figure 5-15, no ligation signals were detected using substrate PDGF.6p, suggesting that the hybridization between the PDGF.6p and the displaced strand was so weak that there was no ligation junction formed in the presence of PDGF. On the contrary, the binding of PDGF.8p and the displaced strand allowed ligation to occur. Antiswitch BB1, BB3 and BB4 demonstrated PDGF activated ligaiton signals. In addition, the ligation signal generated by BB3 was stronger than that generated by BB2. This might indicate that the longer the aptamer stem, the easier the ligation junction is formed. The ligation activation using BB4 was more significant than that using BB1 probably due to less secondary structure in the linker region of BB4.

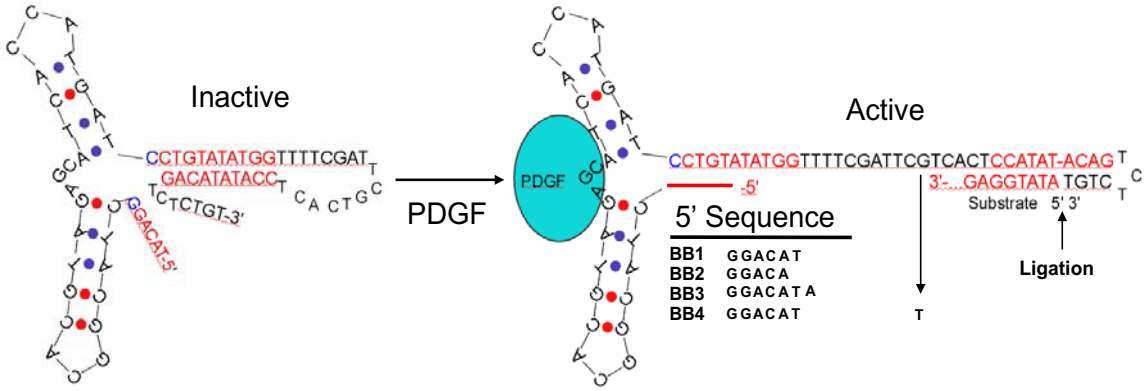

Figure 5-14. Coupling PDGF-sensing antiswitch with ligation. Antisense sequence complementary to the anti-PDGF aptamer is appended to the 3' end of the aptamer via a linker sequence so that the end sequence of the aptamer binds to the antisense sequence instead of the 5' end sequence of the aptamer. Therefore the binding conformation of the aptamer is disrupted. Additional sequence is also added to the 3' end of the antisense strand to help generate a short hairpin structure with the antisense in the presence of PDGF. Hybridization-switching regions are highlighted in red. A GC pair remained in the aptamer stem is highlighted in blue. Antiswitch constructs (BB1-3) have different lengths at their 5' stems. The difference between BB1 and BB4 is that a G in the linker of BB1 is replaced by a T in that of BB4. This G to T change is to reduce possible secondary structure in the linker.

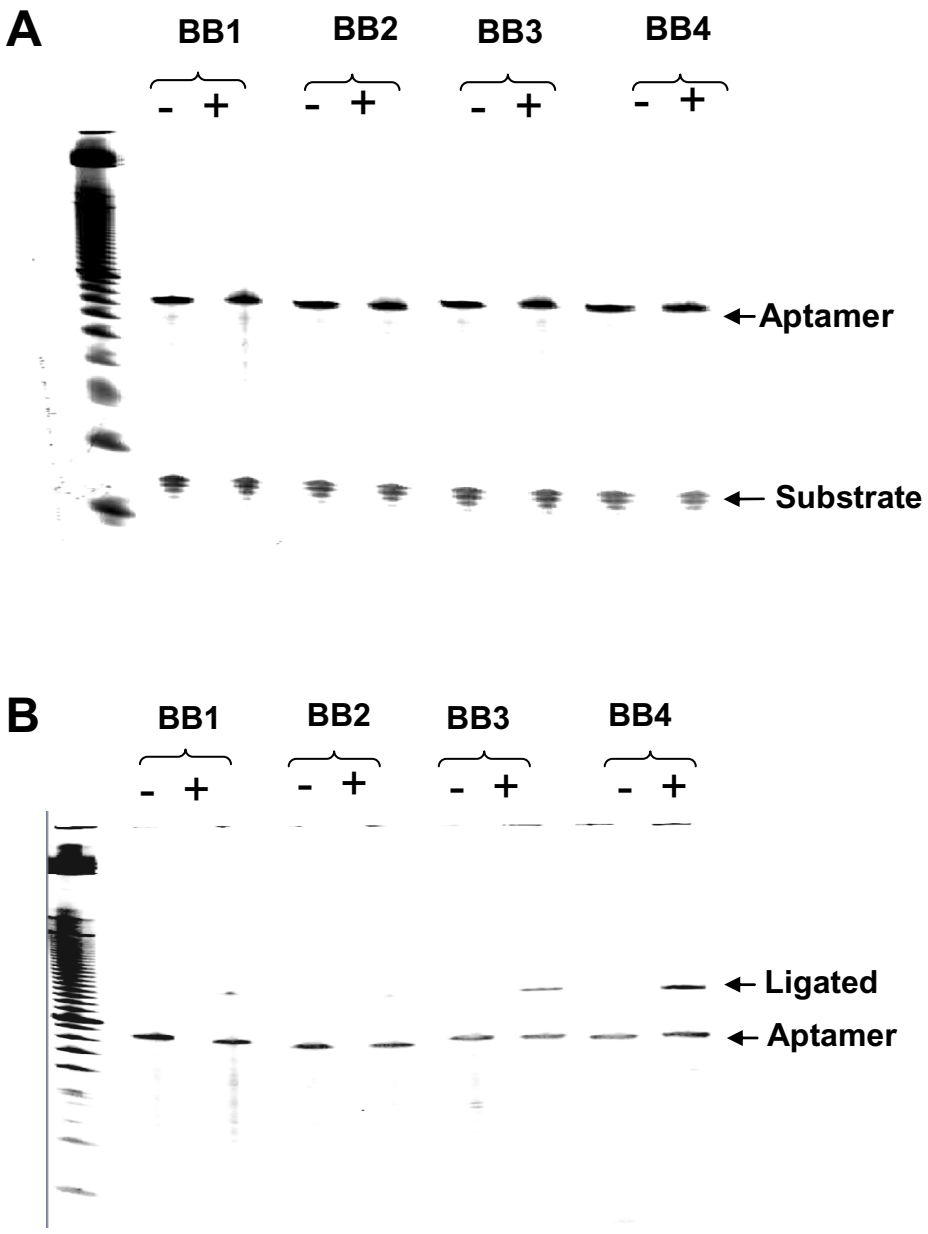

Figure 5-15. Ligation assays for PDGF activation. Ligations were carried out using all the designed constructs (BB1-4) for 2 hours in the presence (+) or absence (-) of 40 nM PDGF. M represents the 10-bp ladder. (A) Ligation with substrate oligonucleotide (PDGF.6p) which forms 6 bp stem at the ligation junction. (B) Ligation with substrate oligonucleotide (PDGF.8p) which forms 8 basepairs at the ligation junction.

Design of antiswitch coupled with ligation for the detection of IgE

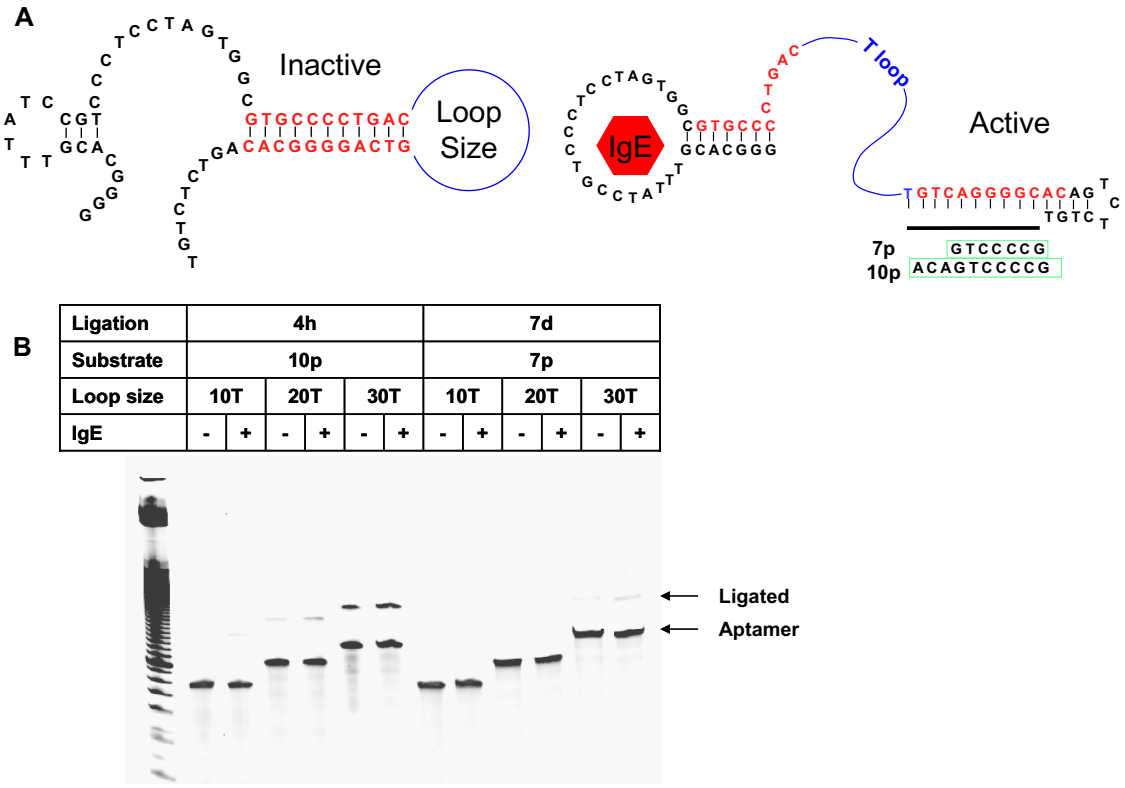

Figure 5-16. Optimization of the lengths of the spacers of the IgE-sensing antiswitch. (A) Ligation scheme for the detection of IgE. The linker region is shown as a T-loop (blue). Complementary regions on the substrate oligonucleotides are framed in green boxes. The antisense and the complementary region in the aptamer are highlighted in red. (B) Ligation assays using aptamers with varied linker lengths. Aptamers with linker lengths varying from 10T to 30T were assayed with substrate IgE.7p and IgE.10p, respectively. (-) and (+) indicate the absence and presence of 90 nM IgE.

In order to show the genralizability of the design, we have also carried out the adaption of the anti-IgE aptamer (Wiegand, Williams et al. 1996) to antiswitche coupled with ligation. To find out the length of the spacer separating IgE binding domain and the

ligation junction, a series of IgE-sensing antiswitches were designed to have different lengths at their linker regions. To prevent any secondary structure formed by the spacer, these linkers were designed containing multiple T residues. In addition, to test the feasibility of ligation, two substrate oligonucleotides (IgE.7p and IgE.10p) with different lengths in the binding regions were also constructed. Our results showed that it took 7 days to detect ligation signals produced by substrate IgE.7p, while using the other substrate IgE.10p, ligation signals could be detected as soon as 4h. However, neither ligation assays demonstrated significant IgE-activated ligation signals. These results might suggest that either aptamer stem was too stable or ligation junction was too stable that one conformer was always dominant.

To optimize the lengths of the substrate binding sites, we created another two substrate oligonucleotides (IgE.8p and IgE.9p) which can form 8 basepairs and 9 basepairs with the IgE-sensing antiswitch, respectively. In addition, since there was no significant IgE-activated ligation observed previously, the binding conformation of the aptamer might be more stable than the antisense-aptamer duplex. Therefore, we designed antiswithes with truncated stems. Antiswitches IgE4-8 could form 3-7 basepairs by both their two termini in the active conformer. Figure 5-17 shows the ligation results using these antiswitches. Apparently, IgE activations using substrate IgE.8p were more significant than those using IgE.9p (Figure 5-17B and C). Antiswitches IgE4-7 demonstrated significant IgE activation by ligation with IgE.8p. Furthermore, such activations were accomplished as soon as 1.5 h.

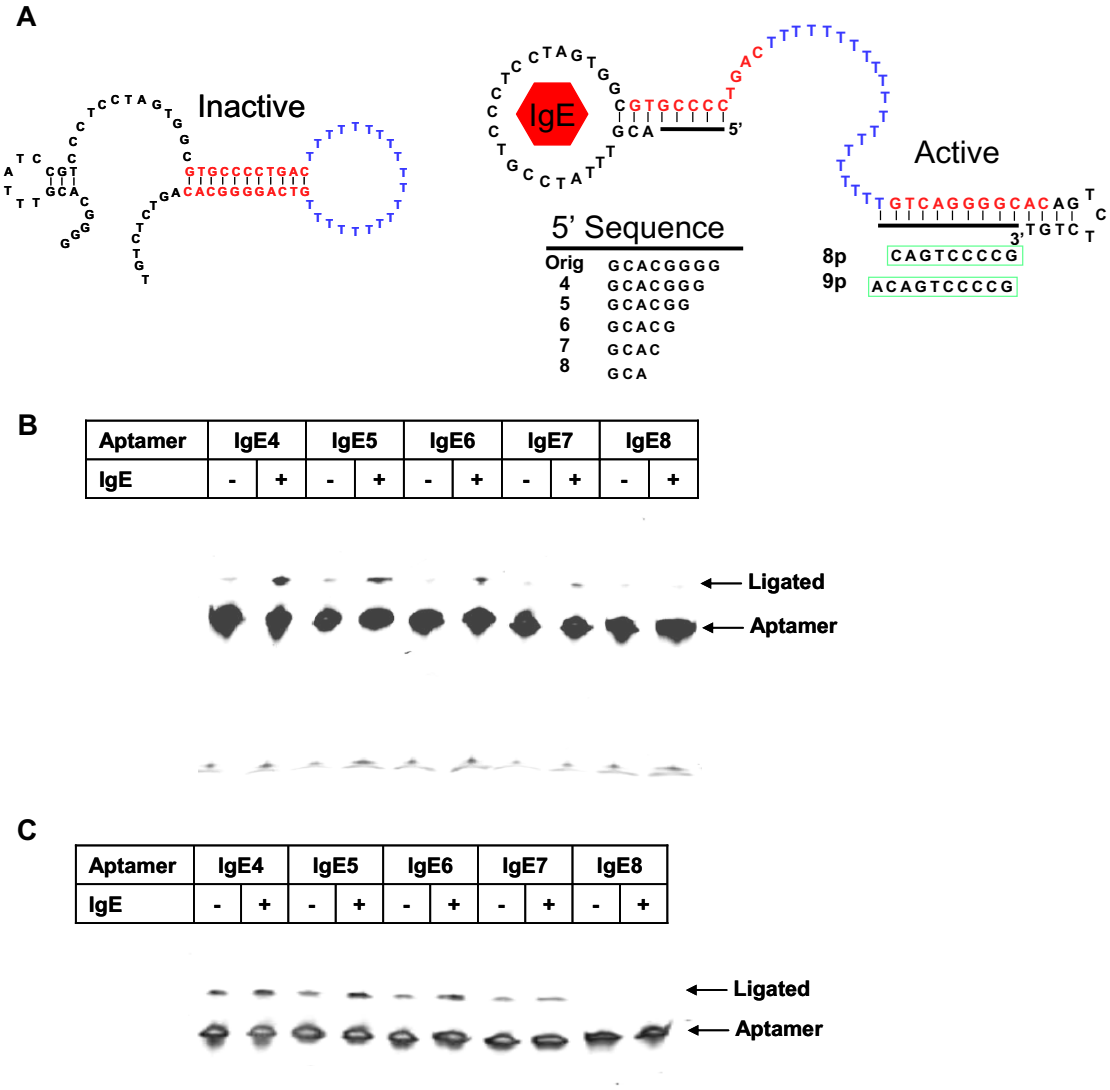

Figure 5-17. Optimization of both substrate binding sites and aptamer stem. (A) Conformational changes of the designed IgE-sensing antiswitches. The 5' end sequences of the antiswitches IgE4-8 are indicated as well as that of the original sequence of the aptamer. Ligation assays using designed aptamer and either IgE.8p (A) or IgE.9p (B) in the presence (+) or absence (-) of 170 nM IgE.

In summary, after series of optimization, we have successfully adapted our method to antiswitch coupled ligation. Both PDGF and IgE antiswitches demonstrated significant analyte-dependent ligations. In addition, ligations could be finished within a couple of hours. Amrita Singh will carry out the real-time PCR assays using these designed antiswitches. Again, like real-time PCR detection of PDGF and thrombin described previously, series of optimizations of the ligation time periods, oligonucleotide concentrations and ratios will be performed and the detection specificity and sensitivity will be evaluated.

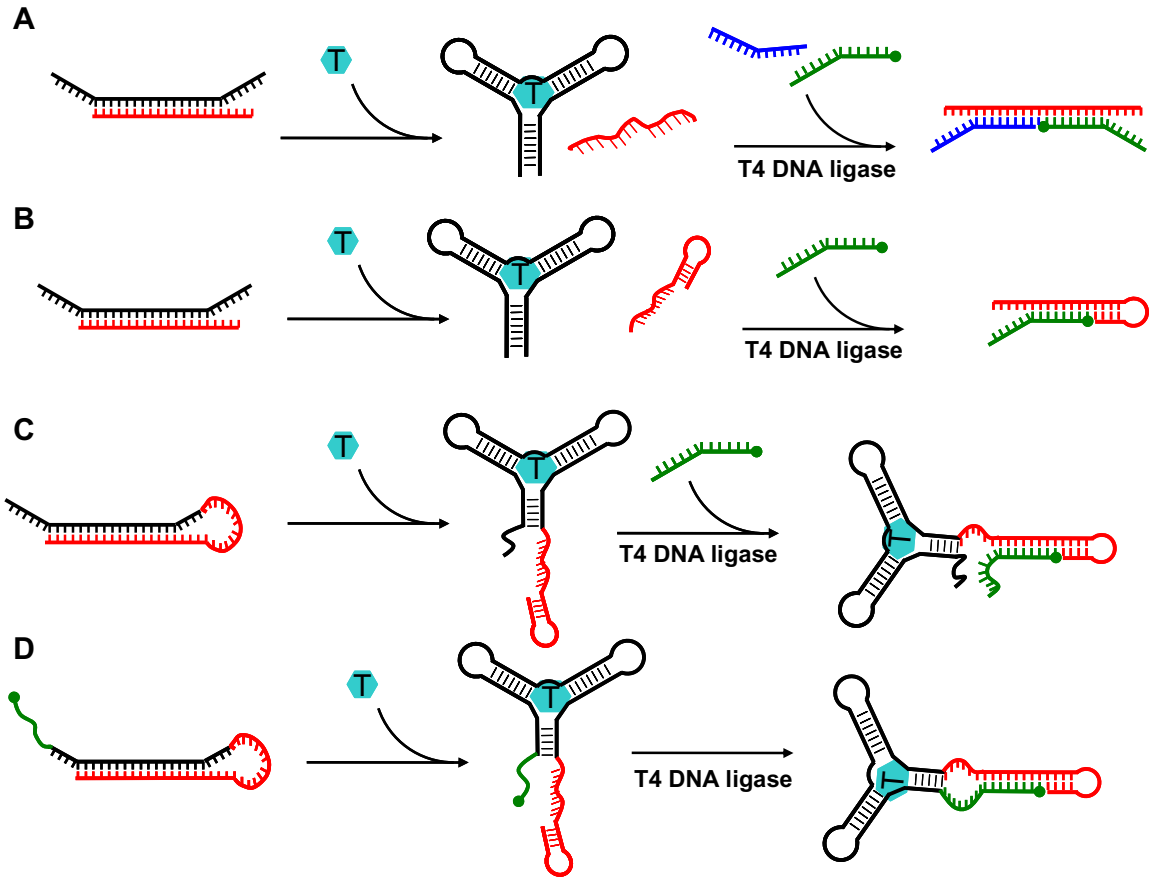

Figure 5-18. Summary of all the ligation strategies. In these strategies the formation of non-binding conformation relies on aptamer (black) hybridization with the antisense sequence (red). In the presence of analyte (T), the antisense sequence is displaced. In the four-piece ligation (A), displaced antisense strand forms ligation junction with a pair of substrate oligonucleotides (blue and green) for subquent ligation. In the three-piece ligation, antisense strand forms a short hairpin stem, which serves as half of the ligation junction. And only one substrate oligonucleotide (blue) is required for ligation. In two- and one-piece ligations the antisense sequence is attached to the 3' end of the aptamer. Upon interaction with the analyte, aptamer folds into binding strcutre, resulting in the displaced antisense strand binding to either a substrate oligonucleotide (C) or substrate attached on the 5' end of the aptamer (D).

CONCLUSIONS

Taken together with the assays from Chapter 3 through Chapter 5, we have tested four strategies for analyte-dependent ligations (Figure 5-18). Among these four strategies, both the four-piece (Figure 5-18A) and three-piece (Figure 5-18B) ligations take long time to reach maximum activation. And the detection by the four-piece ligation is the least sensitive. Two-piece (Figure 5-18C) and one-piece (Figure 5-18D) ligations demonstrated shorter ligation time, more sensitivity and simpler operation in comparison to the three- and four-piece ligations. And they should be more suitable to be applied to sensing other analytes.

FUTURE PLANS

The future development of such ligatable structure-switching aptamer biosensors can be the improvement of the sensitivities of current detections. As we described previously, the limitation of our method lies on the design of structure-switching aptamer. Because part of the analyte binding energy is used to drive the aptamer's conformational change, structure-switching aptamers usually have reduced affinity with their analytes. Therefore, amplification techniques are necessarily to be used for magnifying the analyte-binding. Further development of our detections might be the improvement of such affinity reductions. Since the short hairpin formed by the antisense domain is essential for the formation of a ligation junction, the sequence and the length of the hairpin stem can also potentially be rationally manipulated in order to further poise the aptamer between binding and non-binding conformations. Also base numbers and sequences at the other side of the ligation junction would be optimized to improve the detection. Both computational design and *in vitro* selections can be carried out to identify optimal

constructs for folding transitions and amplification, thus further increase the sensitivity of the assay.

In addition, in principle RNA aptamers could also be adapted to our method as in the analyte-dependent ligation a modified RNA aptamer could be linked to either a RNA or a DNA substrate oligonucleotide. T4 RNA ligase 2 instead of T4 DNA ligase might be employed for such ligation because it catalyzes ligation of 3' RNA strand to either DNA or RNA also in a template dependent manner. The ligated product could be amplified and analyzed by RT-PCR or transcription-mediated amplification (TMA) in real time. Currently, more RNA aptamers have been selected than DNA ones. The feasibility of this method applied for RNA aptamers would allow the more sensitive detections in the future.

MATERIALS AND METHODS

Materials

The sequences of the conformation-switching aptamers for the detection of PDGF were: p.3_13 (5'-AGCCTTTCTCGATCGGATCATTCACAGGCTACGGCACGTAGAGCATCACCATGATCCTGTGTTTCTTCTTCTTTTGATCGGATCATGGTGAT). The substrate for ligation was N.SUB2 (5'-pCCGATCCCTCTTGCTGCCTACGCATGCTGTTACCGTCCGCTACTCATTCC), where p denotes a phosphate. Primers for PCR were p.F (5'-AGCCTTTCTCGATCGGATCA) and p.R (5'-GGAATGAGTAGCGGACGGTAAC). The TaqMan probe used for real-time PCR was BB-PROBE-12 (5'-FAM-CGATCCCTCTTGCTGCCTACGCA-TAMRA-3'). All oligonucleotides were purchased

from IDT (Coralville, IA). PDGF-BB, -AA, and -AB were purchased from R&D Systems (Minneapolis, MN). The PDGF proteins were reconstituted in 4 mM HCl with 0.2% BSA (Invitrogen, Carlsbad, CA), as suggested by the supplier.

The sequences of the conformation-switching aptamers for the detection of thrombin are shown in the figures presented in this chapter. The substrates for ligation were t.Sub2 (5'-pGGTTGGCGATCCCTCTTGCTGCCTACGCATGCTGTTACCGTCCGCTACTCATTCC) and t.5'P (5'-pGGTTGGTAGTCTCGAATTGCTCTCT). Primers for PCR were t.F1 (5'-TGTGGTTGGTGTGGTTGGTT), t.F2 (5'-GGTTGGTTCATGGTCATATTGGT), t.R1 (5'-GAGAGCAATTCGAGACTACCAACC) and t.R2 (5'-AGAGAGCAATTCGAGACTACC). All oligonucleotides except MGB probes were purchased from IDT (Coralville, IA).

The MGB probe used for real-time PCR was t.MGB17 (5'-FAM-TTCCAACCACAGTCTCT-MGB-3') and it was obtained from Applied Biosystems ABI (Foster City, CA). The advantage of the MGB (minor groove binding) probe is that the 3' adduct can form extremely stable duplexes with single-stranded DNA targets, leading to higher melting temperature and increased specificity compared with unmodified DNA (Afonina, Zivarts et al. 1997; Kutyavin, Afonina et al. 2000). In addition, the 3' adduct acts as a quencher, leading to lower background. MGB probes can be as short as 13 nucleotides, compared with 18-22 nt for normal TaqMan probes. MGB probes have been widely used for real-time PCR assays and for quantitation (Decaro, Elia et al. 2006; Hoehne and Schreier 2006; Lole and Arankalle 2006).

Human α-thrombin, human Factor IXa, and human Factor Xa were purchased form Haematologic Technologies Inc. (Essex Junction, VT).

Detection of PDGF by ligation and real-time PCR

Pre-ligation mixtures contained 5 μL of 10x PDGF binding buffer (1.37 M NaCl, 101 mM Na_2HPO_4, 18 mM KH_2PO_4 pH 7.4, 27 mM KCl, 100 mM Tris.Cl, pH 7.4, and 25 mM $MgCl_2$) and 1 μL of 20 nM conformation-switching aptamer p.3_13 and were denatured at 70 ^oC for 3min prior to cooling to room temperature. The reaction mixture was incubated with PDGF-BB for 30min, and then 1.5 μL of 25mM ATP (final concentration of 0.75 mM), and 1, 5, 10, or 20 μL of 20nM oligonucleotide substrate (N.Sub2, denatured prior to use) and 1 μL T4 DNA ligase (2 U/μL, Epicentre, Madison, WI) were added separately to make a final reaction volume of 50 μL. The final concentration of BSA in ligation reactions with PDGF was always 0.004 %. Ligation was allowed to proceed for 5 min, 30 min, or 60 min at room temperature, and was terminated by heating the reaction to 95 ^oC for 15 min. A 2 μL aliquot of terminated ligation reaction was introduced into 1x TaqMan Universal Master Mix (ABI) containing 167 nM p.F, 167 nM p.R and 334 nM BB-PROBE-12. Real-time PCR was carried out in a 96-well PCR plate (ABI), covered with strip caps (ABI). The thermal cycling regime was: initial denaturation for 10min at 95 ^oC, and then cycling for 15 s at 95 ^oC and 60 s at 60 ^oC, repeated 50 times on an ABI HT7900 real-time PCR machine.

Assaying conformation-switching aptamers

In order to test the structure-switching abilities of the designed constructs, ligation was assayed by gel electrophoresis. Pre-ligation mixtures (45 μL) contained 5 μL of 10x binding buffer (50 mM KCl, 10 mM $MgCl_2$, and 20 mM Tris.Cl, pH 7.4), 1 μL of 10 μM designed conformation-switching anti-thrombin aptamer and 39 μL H_2O were denatured at 70 ^oC for 3min and cooled to room temperature. The reaction mixture was incubated with or without thrombin for 30 min, and then 1.5 μL of 25 mM ATP, 1.5 μL of 10 μM

substrate (denatured prior to use) and 1 μL T4 DNA ligase (2 U/μL, Epicentre, Madison, WI) were added separately. The final concentration of ATP in the 50 μL ligation mixture was 0.75 mM, and substrate oligonucleotide was 0.3 μM. Ligation reactions were carried out at room temperature for various times and were terminated by heating to 95 ^{o}C for 15min. Ligated and unligated species were separated on denaturing (7 M urea) 8 % polyacrylamide gels and stained with SYBR Gold (Molecular Probes, Eugene, OR) for visibility. Aptamer concentrations for ligation assays were 200 nM, higher than that used in real-time PCR assays (0.4 nM) in order to be visible by staining.

Detection of thrombin by ligation and real-time PCR

Ligaiton reactions were first carried out and then subjected to real-time PCR. The ligation reactions were similar to those described above except that the final concentration of ThrA7 was 0.4 nM and 0.002 % BSA was present. The reaction mixture was incubated with thrombin for 30 min, and then ATP, various amounts of substrate oligonucleotide (t.5'P) and 1 μL T4 DNA ligase were added separately. Ligation proceeded at room temperature for 20min, and was terminated by heating at 95 ^{o}C for 15min. A 2 μL aliquot of the terminated ligaiton reaction, 15 μL 2xTaqMan Universal PCR Master Mix (Applied Biosystems ABI, Foster City, CA), 0.5 μL of 10 μM forward primer, 0.5 μL of 10μM reverse primer, 0.5 μL of 10 μM MGB probe and 11.5 μL H_2O were mixed to make a total volume of 30 μL. The final PCR mixture contained 167 nM t.F1, 167 nM t.R2, and 167nM t.MGB17 in 1x TaqMan Universal PCR Master Mix. And real-time PCR was carried out as detailed for thrombin detection, above.

Ligation in cell lysate

To prepare lysate, approximately $1x10^7$ human 293T fibroblast cells (ATCC, Manassas, VA) were collected. Cells were treated with 4 mL M-PER mammalian protein extraction reagent (Pierce Biotechnology, Rockford, IL) and shaken at room temperature for 10 min. After centrifugation at 10,000 rpm at 4 ^oC for 25 min, pellets containing cell membranes and hydrophobic membrane proteins were removed and the supernatant consisting of intracellular proteins and nucleic acids was collected and frozen at -80 ^oC. Total protein in lysate aliquots was quantitated using a bicinchoninic acid total protein assay kit (Pierce Biotechnology, Rockford, IL). The final concentration of lysate proteins in each 50 μL ligation reaction mixture was 1 μg/mL. Protein analytes at different concentrations were added to the lysate and ligation and real-time PCR were carried out as above. PDGF samples were always in 0.004 % BSA (final concentration in 50 μL ligation reaction) and thrombin samples were always in 0.002 % BSA (final concentration in 50 μL ligation reaction).

Ligation assays using designed antiswitches

The ligation reaction for the detection of PDGF was similar to the above description except the final concentrations were 0.4 μM for antiswitch constructs (BB1-4) and 0.8 μM for the substrate oligonucleotide (BB.6p and BB.8p).

Ligation with IgE-sensing antiswitches were carried out as following: 0.4 μM IgE1-8 was incubated with or without 170 nM IgE in 1x PBSM buffer (137 mM NaCl, 3 mM KCl, 8 mM Na_2HPO_4, 1.5 mM KH_2PO_4, 1 mM $CaCl_2$, and 5.5 mM $MgCl_2$) prior to ligation. After incubation at 25 ^oC for 30 min, 2 μL of 25 mM ATP, 6 μL of 10 μM substrate (denatured prior to use) IgE.7-10p and 2 μL T4 DNA ligase (2 U/μL, Epicentre, Madison, WI) were added separately. The final concentration of ATP in the 50 μL ligation

mixture was 1 mM, and substrate oligonucleotide was 1.2 μM. Ligation reactions were carried out at room temperature for various times and were terminated by heating to 95 ^{o}C for 15min. Ligated and unligated species were separated on denaturing (7 M urea) 8 % polyacrylamide gels and stained with SYBR Gold (Molecular Probes, Eugene, OR).

References

Adler, M. (2005). "Immuno-PCR as a clinical laboratory tool." Adv Clin Chem **39**: 239-92.

Afonina, I., M. Zivarts, et al. (1997). "Efficient priming of PCR with short oligonucleotides conjugated to a minor groove binder." Nucleic Acids Res **25**(13): 2657-60.

Araki, M., Y. Okuno, et al. (1998). "Allosteric regulation of a ribozyme activity through ligand-induced conformational change." Nucleic Acids Res **26**(14): 3379-84.

Aronson, D. L., L. Stevan, et al. (1977). "Generation of the combined prothrombin activation peptide (F1-2) during the clotting of blood and plasma." J Clin Invest **60**(6): 1410-8.

Baldrich, E., J. L. Acero, et al. (2005). "Displacement enzyme linked aptamer assay." Anal Chem **77**(15): 4774-84.

Baldrich, E., A. Restrepo, et al. (2004). "Aptasensor development: elucidation of critical parameters for optimal aptamer performance." Anal Chem **76**(23): 7053-63.

Baner, J., M. Nilsson, et al. (1998). "Signal amplification of padlock probes by rolling circle replication." Nucleic Acids Res **26**(22): 5073-8.

Barletta, J. (2006). "Applications of real-time immuno-polymerase chain reaction (rt-IPCR) for the rapid diagnoses of viral antigens and pathologic proteins." Mol Aspects Med **27**(2-3): 224-53.

Bayer, T. S. and C. D. Smolke (2005). "Programmable ligand-controlled riboregulators of eukaryotic gene expression." Nat Biotechnol **23**(3): 337-43.

Bock, L. C., L. C. Griffin, et al. (1992). "Selection of single-stranded DNA molecules that bind and inhibit human thrombin." Nature **355**(6360): 564-6.

Bowen-Pope, D. F., T. W. Malpass, et al. (1984). "Platelet-derived growth factor in vivo: levels, activity, and rate of clearance." Blood **64**(2): 458-69.

Bunka, D. H. and P. G. Stockley (2006). "Aptamers come of age - at last." Nat Rev Microbiol **4**(8): 588-96.

Cho, E. J., M. Rajendran, et al. (2005). Aptamers as Emerging Probes for Macromolecular Sensing Topics in Fluorescence Spectroscopy (Advanced Concepts in Fluorescence Sensing, Part B). J. R. Lakowicz. New York, Plenum Press. **10** 127-155.

Cho, E. J., L. Yang, et al. (2005). "Using a deoxyribozyme ligase and rolling circle amplification to detect a non-nucleic acid analyte, ATP." J Am Chem Soc **127**(7): 2022-3.

Christian, A. T., M. S. Pattee, et al. (2001). "Detection of DNA point mutations and mRNA expression levels by rolling circle amplification in individual cells." Proc Natl Acad Sci U S A **98**(25): 14238-43.

Conrad, R. and A. D. Ellington (1996). "Detecting immobilized protein kinase C isozymes with RNA aptamers." Anal Biochem **242**(2): 261-5.

Daubendiek, S. L. and E. T. Kool (1997). "Generation of catalytic RNAs by rolling transcription of synthetic DNA nanocircles." Nat Biotechnol **15**(3): 273-7.

Davis, K. A., B. Abrams, et al. (1996). "Use of a high affinity DNA ligand in flow cytometry." Nucleic Acids Res **24**(4): 702-6.

Davis, K. A., Y. Lin, et al. (1998). "Staining of cell surface human CD4 with 2'-F-pyrimidine-containing RNA aptamers for flow cytometry." Nucleic Acids Res **26**(17): 3915-24.

Decaro, N., G. Elia, et al. (2006). "A minor groove binder probe real-time PCR assay for discrimination between type 2-based vaccines and field strains of canine parvovirus." J Virol Methods **136**(1-2): 65-70.

Di Giusto, D. A., W. A. Wlassoff, et al. (2005). "Proximity extension of circular DNA aptamers with real-time protein detection." Nucleic Acids Res **33**(6): e64.

Dirks, R. M. and N. A. Pierce (2004). "Triggered amplification by hybridization chain reaction." Proc Natl Acad Sci U S A **101**(43): 15275-8.

Drolet, D. W., L. Moon-McDermott, et al. (1996). "An enzyme-linked oligonucleotide assay." Nat Biotechnol **14**(8): 1021-5.

Ellington, A. D. and J. W. Szostak (1990). "In vitro selection of RNA molecules that bind specific ligands." Nature **346**(6287): 818-22.

Espy, M. J., J. R. Uhl, et al. (2006). "Real-time PCR in clinical microbiology: applications for routine laboratory testing." Clin Microbiol Rev **19**(1): 165-256.

Fang, X., Z. Cao, et al. (2001). "Molecular aptamer for real-time oncoprotein platelet-derived growth factor monitoring by fluorescence anisotropy." Anal Chem **73**(23): 5752-7.

Fang, X., A. Sen, et al. (2003). "Synthetic DNA aptamers to detect protein molecular variants in a high-throughput fluorescence quenching assay." Chembiochem **4**(9): 829-34.

Faruqi, A. F., S. Hosono, et al. (2001). "High-throughput genotyping of single nucleotide polymorphisms with rolling circle amplification." BMC Genomics **2**(1): 4.

Fenton, J. W., 2nd (1986). "Thrombin." Ann N Y Acad Sci **485**: 5-15.

Ferguson, A., R. M. Boomer, et al. (2004). "A novel strategy for selection of allosteric ribozymes yields RiboReporter sensors for caffeine and aspartame." Nucleic Acids Res **32**(5): 1756-66.

Fredriksson, S., M. Gullberg, et al. (2002). "Protein detection using proximity-dependent DNA ligation assays." Nat Biotechnol **20**(5): 473-7.

German, I., D. D. Buchanan, et al. (1998). "Aptamers as ligands in affinity probe capillary electrophoresis." Anal Chem **70**(21): 4540-5.

Green, L. S., D. Jellinek, et al. (1996). "Inhibitory DNA ligands to platelet-derived growth factor B-chain." Biochemistry **35**(45): 14413-24.

Guerrier-Takada, C., K. Gardiner, et al. (1983). "The RNA moiety of ribonuclease P is the catalytic subunit of the enzyme." Cell **35**(3 Pt 2): 849-57.

Gullberg, M., S. M. Gustafsdottir, et al. (2004). "Cytokine detection by antibody-based proximity ligation." Proc Natl Acad Sci U S A **101**(22): 8420-4.

Gustafsdottir, S. M., A. Nordengrahn, et al. (2006). "Detection of individual microbial pathogens by proximity ligation." Clin Chem **52**(6): 1152-60.

Gustafsdottir, S. M., E. Schallmeiner, et al. (2005). "Proximity ligation assays for sensitive and specific protein analyses." Anal Biochem **345**(1): 2-9.

Hamaguchi, N., A. Ellington, et al. (2001). "Aptamer beacons for the direct detection of proteins." Anal Biochem **294**(2): 126-31.

Harvey, J. J., S. P. Lee, et al. (2004). "Characterization and applications of CataCleave probe in real-time detection assays." Anal Biochem **333**(2): 246-55.

Hatch, A., T. Sano, et al. (1999). "Rolling circle amplification of DNA immobilized on solid surfaces and its application to multiplex mutation detection." Genet Anal **15**(2): 35-40.

Hesselberth, J. R., M. P. Robertson, et al. (2003). "Simultaneous detection of diverse analytes with an aptazyme ligase array." Anal Biochem **312**(2): 106-12.

Heyduk, E. and T. Heyduk (2005). "Nucleic acid-based fluorescence sensors for detecting proteins." Anal Chem **77**(4): 1147-56.

Ho, H. A. and M. Leclerc (2004). "Optical sensors based on hybrid aptamer/conjugated polymer complexes." J Am Chem Soc **126**(5): 1384-7.

Hoehne, M. and E. Schreier (2006). "Detection of Norovirus genogroup I and II by multiplex real-time RT- PCR using a 3'-minor groove binder-DNA probe." BMC Infect Dis **6**: 69.

Huang, C. C., Z. Cao, et al. (2004). "Protein-protein interaction studies based on molecular aptamers by affinity capillary electrophoresis." Anal Chem **76**(23): 6973-81.

Huang, C. C., Y. F. Huang, et al. (2005). "Aptamer-modified gold nanoparticles for colorimetric determination of platelet-derived growth factors and their receptors." Anal Chem **77**(17): 5735-41.

Hundley, A. F., L. Yuan, et al. (2006). "Skeletal muscle heavy-chain polypeptide 3 and myosin binding protein H in the pubococcygeus muscle in patients with and without pelvic organ prolapse." Am J Obstet Gynecol **194**(5): 1404-10.

Jayasena, S. D. (1999). "Aptamers: an emerging class of molecules that rival antibodies in diagnostics." Clin Chem **45**(9): 1628-50.

Jiang, Y., X. Fang, et al. (2004). "Signaling aptamer/protein binding by a molecular light switch complex." Anal Chem **76**(17): 5230-5.

Jonstrup, S. P., J. Koch, et al. (2006). "A microRNA detection system based on padlock probes and rolling circle amplification." Rna **12**(9): 1747-52.

Jose, A. M., G. A. Soukup, et al. (2001). "Cooperative binding of effectors by an allosteric ribozyme." Nucleic Acids Res **29**(7): 1631-7.

Joyce, G. F. (2004). "Directed evolution of nucleic acid enzymes." Annu Rev Biochem **73**: 791-836.

Kertsburg, A. and G. A. Soukup (2002). "A versatile communication module for controlling RNA folding and catalysis." Nucleic Acids Res **30**(21): 4599-606.

Kingsmore, S. F. and D. D. Patel (2003). "Multiplexed protein profiling on antibody-based microarrays by rolling circle amplification." Curr Opin Biotechnol **14**(1): 74-81.

Kirby, R., E. J. Cho, et al. (2004). "Aptamer-based sensor arrays for the detection and quantitation of proteins." Anal Chem **76**(14): 4066-75.

Koizumi, M., G. A. Soukup, et al. (1999). "Allosteric selection of ribozymes that respond to the second messengers cGMP and cAMP." Nat Struct Biol **6**(11): 1062-71.

Kool, E. T. (1996). "Circular oligonucleotides: new concepts in oligonucleotide design." Annu Rev Biophys Biomol Struct **25**: 1-28.

Kotia, R. B., L. Li, et al. (2000). "Separation of nontarget compounds by DNA aptamers." Anal Chem **72**(4): 827-31.

Kruger, K., P. J. Grabowski, et al. (1982). "Self-splicing RNA: autoexcision and autocyclization of the ribosomal RNA intervening sequence of Tetrahymena." Cell **31**(1): 147-57.

Kutyavin, I. V., I. A. Afonina, et al. (2000). "3'-minor groove binder-DNA probes increase sequence specificity at PCR extension temperatures." Nucleic Acids Res **28**(2): 655-61.

Lee, J. F., G. M. Stovall, et al. (2006). "Aptamer therapeutics advance." Curr Opin Chem Biol **10**(3): 282-9.

Lee, M. and D. R. Walt (2000). "A fiber-optic microarray biosensor using aptamers as receptors." Anal Biochem **282**(1): 142-6.

Levy, M. (2003). Design and evolution of functional nucleic acids. Biochemistry. Austin, The University of Texas at Austin. **Ph.D.:** 21.

Levy, M., S. F. Cater, et al. (2005). "Quantum-dot aptamer beacons for the detection of proteins." Chembiochem **6**(12): 2163-6.

Levy, M. and A. D. Ellington (2002). "ATP-dependent allosteric DNA enzymes." Chem Biol **9**(4): 417-26.

Li, J. J., X. Fang, et al. (2002). "Molecular aptamer beacons for real-time protein recognition." Biochem Biophys Res Commun **292**(1): 31-40.

Liss, M., B. Petersen, et al. (2002). "An aptamer-based quartz crystal protein biosensor." Anal Chem **74**(17): 4488-95.

Liu, J. and Y. Lu (2005). "Fast colorimetric sensing of adenosine and cocaine based on a general sensor design involving aptamers and nanoparticles." Angew Chem Int Ed Engl **45**(1): 90-4.

Lizardi, P. M., X. Huang, et al. (1998). "Mutation detection and single-molecule counting using isothermal rolling-circle amplification." Nat Genet **19**(3): 225-32.

Lole, K. S. and V. A. Arankalle (2006). "Quantitation of hepatitis B virus DNA by real-time PCR using internal amplification control and dual TaqMan MGB probes." J Virol Methods **135**(1): 83-90.

Najafi-Shoushtari, S. H. and M. Famulok (2005). "Competitive regulation of modular allosteric aptazymes by a small molecule and oligonucleotide effector." Rna **11**(10): 1514-20.

Nallur, G., C. Luo, et al. (2001). "Signal amplification by rolling circle amplification on DNA microarrays." Nucleic Acids Res **29**(23): E118.

Niemeyer, C. M., M. Adler, et al. (2005). "Immuno-PCR: high sensitivity detection of proteins by nucleic acid amplification." Trends Biotechnol **23**(4): 208-16.

Nilsson, M., M. Gullberg, et al. (2002). "Real-time monitoring of rolling-circle amplification using a modified molecular beacon design." Nucleic Acids Res **30**(14): e66.

Nussbaumer, C., E. Gharehbaghi-Schnell, et al. (2006). "Messenger RNA profiling: a novel method for body fluid identification by real-time PCR." Forensic Sci Int **157**(2-3): 181-6.

Nutiu, R. and Y. Li (2003). "Structure-switching signaling aptamers." J Am Chem Soc **125**(16): 4771-8.

Nutiu, R. and Y. Li (2004). "Structure-switching signaling aptamers: transducing molecular recognition into fluorescence signaling." Chemistry **10**(8): 1868-76.

Nutiu, R. and Y. Li (2005). "In vitro selection of structure-switching signaling aptamers." Angew Chem Int Ed Engl **44**(7): 1061-5.

Nutiu, R., J. M. Yu, et al. (2004). "Signaling aptamers for monitoring enzymatic activity and for inhibitor screening." Chembiochem **5**(8): 1139-44.

Pai, S., A. D. Ellington, et al. (2005). "Proximity ligation assays with peptide conjugate 'burrs' for the sensitive detection of spores." Nucleic Acids Res **33**(18): e162.

Piganeau, N., A. Jenne, et al. (2001). "An Allosteric Ribozyme Regulated by Doxycyline This work was supported by Aventis Gencell and by a grant from the Volkswagen Foundation (Priority program "conformational control") to M.F. We thank M. Blind, G. Mayer, D. Proske, and G. Sengle (Universitat Bonn) for helpful discussions as well as J. Crouzet, J. F. Mayaux, and M. Finer (Aventis Gencell) for support." Angew Chem Int Ed Engl **40**(19): 3503.

Piganeau, N., V. Thuillier, et al. (2001). "In vitro selection of allosteric ribozymes: theory and experimental validation." J Mol Biol **312**(5): 1177-90.

Potyrailo, R. A., R. C. Conrad, et al. (1998). "Adapting selected nucleic acid ligands (aptamers) to biosensors." Anal Chem **70**(16): 3419-25.

Proske, D., M. Blank, et al. (2005). "Aptamers--basic research, drug development, and clinical applications." Appl Microbiol Biotechnol **69**(4): 367-74.

Qi, X., S. Bakht, et al. (2001). "L-RCA (ligation-rolling circle amplification): a general method for genotyping of single nucleotide polymorphisms (SNPs)." Nucleic Acids Res **29**(22): E116.

Radi, A. E., J. L. Acero Sanchez, et al. (2005). "Reusable impedimetric aptasensor." Anal Chem **77**(19): 6320-3.

Rajendran, M. and A. D. Ellington (2002). Nucleic acids for reagentless biosensors. Optical Biosensors. F. S. Ligler and C. A. R. Taitt. Amsterdan, Neth, Elsevier Science B. V.**:** 369-396.

Rector, A., R. Tachezy, et al. (2004). "A sequence-independent strategy for detection and cloning of circular DNA virus genomes by using multiply primed rolling-circle amplification." J Virol **78**(10): 4993-8.

Rehder, M. A. and L. B. McGown (2001). "Open-tubular capillary electrochromatography of bovine beta-lactoglobulin variants A and B using an aptamer stationary phase." Electrophoresis **22**(17): 3759-64.

Robertson, M. P. and A. D. Ellington (1999). "In vitro selection of an allosteric ribozyme that transduces analytes to amplicons." Nat Biotechnol **17**(1): 62-6.

Robertson, M. P. and A. D. Ellington (2000). "Design and optimization of effector-activated ribozyme ligases." Nucleic Acids Res **28**(8): 1751-9.

Robertson, M. P. and A. D. Ellington (2001). "In vitro selection of nucleoprotein enzymes." Nat Biotechnol **19**(7): 650-5.

Robertson, M. P., S. M. Knudsen, et al. (2004). "In vitro selection of ribozymes dependent on peptides for activity." Rna **10**(1): 114-27.

Romig, T. S., C. Bell, et al. (1999). "Aptamer affinity chromatography: combinatorial chemistry applied to protein purification." J Chromatogr B Biomed Sci Appl **731**(2): 275-84.

Rye, P. D. and K. Nustad (2001). "Immunomagnetic DNA aptamer assay." Biotechniques **30**(2): 290-2, 294-5.

Schallmeiner, E., E. Oksanen, et al. (2007). "Sensitive protein detection via triple-binder proximity ligation assays." Nat Methods **4**(2): 135-7.

Schweitzer, B., S. Roberts, et al. (2002). "Multiplexed protein profiling on microarrays by rolling-circle amplification." Nat Biotechnol **20**(4): 359-65.

Schweitzer, B., S. Wiltshire, et al. (2000). "Inaugural article: immunoassays with rolling circle DNA amplification: a versatile platform for ultrasensitive antigen detection." Proc Natl Acad Sci U S A **97**(18): 10113-9.

Seetharaman, S., M. Zivarts, et al. (2001). "Immobilized RNA switches for the analysis of complex chemical and biological mixtures." Nat Biotechnol **19**(4): 336-41.

Singh, J. P., M. A. Chaikin, et al. (1982). "Phylogenetic analysis of platelet-derived growth factor by radio-receptor assay." J Cell Biol **95**(2 Pt 1): 667-71.

Smolina, I. V., V. V. Demidov, et al. (2004). "Real-time monitoring of branched rolling-circle DNA amplification with peptide nucleic acid beacon." Anal Biochem **335**(2): 326-9.

Soderberg, O., M. Gullberg, et al. (2006). "Direct observation of individual endogenous protein complexes in situ by proximity ligation." Nat Methods.

Soukup, G. A. and R. R. Breaker (1999). "Design of allosteric hammerhead ribozymes activated by ligand-induced structure stabilization." Structure **7**(7): 783-91.

Soukup, G. A. and R. R. Breaker (1999). "Engineering precision RNA molecular switches." Proc Natl Acad Sci U S A **96**(7): 3584-9.

Soukup, G. A., G. A. Emilsson, et al. (2000). "Altering molecular recognition of RNA aptamers by allosteric selection." J Mol Biol **298**(4): 623-32.

Spiridonova, V. A. and A. M. Kopylov (2002). "DNA aptamers as radically new recognition elements for biosensors." Biochemistry (Mosc) **67**(6): 706-9.

Stahlberg, A., P. Aman, et al. (2003). "Quantitative real-time PCR method for detection of B-lymphocyte monoclonality by comparison of kappa and lambda immunoglobulin light chain expression." Clin Chem **49**(1): 51-9.

Stojanovic, M. N., P. de Prada, et al. (2001). "Aptamer-based folding fluorescent sensor for cocaine." J Am Chem Soc **123**(21): 4928-31.

Stojanovic, M. N., P. d. Prada, et al. (2000). "Fluorescent Sensors Based on Aptamer Self-Assembly." J. Am. Chem. Soc. **122**: 11547-11548.

Tang, J. and R. R. Breaker (1997). "Rational design of allosteric ribozymes." Chem Biol **4**(6): 453-9.

Tang, J., J. Xie, et al. (2006). "The DNA aptamers that specifically recognize ricin toxin are selected by two in vitro selection methods." Electrophoresis **27**(7): 1303-11.

Tuerk, C. and L. Gold (1990). "Systematic evolution of ligands by exponential enrichment: RNA ligands to bacteriophage T4 DNA polymerase." Science **249**(4968): 505-10.

Vicens, M. C., A. Sen, et al. (2005). "Investigation of molecular beacon aptamer-based bioassay for platelet-derived growth factor detection." Chembiochem **6**(5): 900-7.

Wang, X. L., F. Li, et al. (2005). "Ultrasensitive detection of protein using an aptamer-based exonuclease protection assay." Anal Chem **77**(7): 2278.

Watzinger, F., K. Ebner, et al. (2006). "Detection and monitoring of virus infections by real-time PCR." Mol Aspects Med **27**(2-3): 254-98.

Wiegand, T. W., P. B. Williams, et al. (1996). "High-affinity oligonucleotide ligands to human IgE inhibit binding to Fc epsilon receptor I." J Immunol **157**(1): 221-30.

Wilson, D. S. and J. W. Szostak (1999). "In vitro selection of functional nucleic acids." Annu Rev Biochem **68**: 611-47.

Xiao, Y., A. A. Lubin, et al. (2005). "Label-free electronic detection of thrombin in blood serum by using an aptamer-based sensor." Angew Chem Int Ed Engl **44**(34): 5456-9.

Xiao, Y., B. D. Piorek, et al. (2005). "A Reagentless Signal-On Architecture for Electronic, Aptamer-Based Sensors via Target-Induced Strand Displacement." J Am Chem Soc **127**(51): 17990-1.

Yamamoto, R., T. Baba, et al. (2000). "Molecular beacon aptamer fluoresces in the presence of Tat protein of HIV-1." Genes Cells **5**(5): 389-96.

Yan, A. C., K. M. Bell, et al. (2005). "Aptamers: prospects in therapeutics and biomedicine." Front Biosci **10**: 1802-27.

Yang, C. J., S. Jockusch, et al. (2005). "Light-switching excimer probes for rapid protein monitoring in complex biological fluids." Proc Natl Acad Sci U S A **102**(48): 17278-83.

Yang, L. and A. D. Ellington (2006). Prospects for the de novo design of nucleic acid biosensors. . Fluorescence Sensors and Biosensors. R. B. Thompson. Boca Raton, CRC Press LLC**:** 5-43.

Yang, L., C. W. Fung, et al. (2007). "Real-Time Rolling Circle Amplification for Protein Detection." Anal Chem.

Yang, X., X. Li, et al. (2003). "Immunofluorescence assay and flow-cytometry selection of bead-bound aptamers." Nucleic Acids Res **31**(10): e54.

Yi, J., W. Zhang, et al. (2006). "Molecular Zipper: a fluorescent probe for real-time isothermal DNA amplification." Nucleic Acids Res **34**(11): e81.

Zhang, D. Y., W. Zhang, et al. (2001). "Detection of rare DNA targets by isothermal ramification amplification." Gene **274**(1-2): 209-16.

Zhou, C., Y. Jiang, et al. (2006). "Detection of oncoprotein platelet-derived growth factor using a fluorescent signaling complex of an aptamer and TOTO." Anal Bioanal Chem **384**(5): 1175-80.

Zhou, H., K. Bouwman, et al. (2004). "Two-color, rolling-circle amplification on antibody microarrays for sensitive, multiplexed serum-protein measurements." Genome Biol **5**(4): R28.

Zhou, Y., M. Calciano, et al. (2001). "In situ detection of messenger RNA using digoxigenin-labeled oligonucleotides and rolling circle amplification." Exp Mol Pathol **70**(3): 281-8.

Vita

Litao Yang was born in Handan, Hebei Province, China on August 31, 1976, the daughter of Fengqin Liu and Shushan Yang. After attending the No.1 High School of Handan, she entered Nankai University, Tianjin, China in 1994 and received her Bachelors in Science degree in Biology in 1998. Upon finish her B.S. she continued graduate studies in Nankai University under the instruction of Prof. Jianyu Zheng and received her Masters of Science in Biochemistry and Molecular Biology in 2001. She entered Graduate School at the University of Texas, Austin under the supervisions of Prof. Andrew D. Ellington and Prof. George Georgiou in 2001. Her publications include:

Litao Yang, Christine W. Fung, Eun Jeong Cho and Andrew D. Ellington (2007). Real-time Rolling Circle Amplification for Protein Detection. Ana Chem.

Litao Yang and Andrew D. Ellington (2006). Prospects for the De Novo Design of Nucleic Acid Biosensors, Fluorescence Sensors and Biosensors, R. B. Thompson. Boca Raton, CRC Press LLC: 5-43.

Eun Jeong Cho, Litao Yang, Matt Levy and Andrew Ellington. (2005) Using a deoxyribozyme ligase and rolling circle amplification to detect a non-nucleic acid analyte, ATP. J Am Chem Soc, 127(7): 2022-3

Permanent address: #18-2-9 Yongxinli, Lianfang Road, Handan, Hebei, PRC. 056004
This dissertation was typed by the author.